

**MANUFACTURING OF MICRO HOLES BY USING
MICRO ELECTRIC DISCHARGE MACHINING
(MICRO-EDM)**

**A MASTER'S THESIS
in
Mechatronics Engineering
Atılım University**

**by
TAHSİN TECELLİ ÖPÖZ**

JANUARY 2008

**MANUFACTURING OF MICRO HOLES BY USING
MICRO ELECTRIC DISCHARGE MACHINING
(MICRO-EDM)**

**A THESIS SUBMITTED TO
THE GRADUATE SCHOOL OF NATURAL AND APPLIED SCIENCES
OF
ATILIM UNIVERSITY**

**BY
TAHSİN TECELLİ ÖPÖZ**

**IN PARTIAL FULFILLMENT OF THE REQUIREMENTS FOR THE DEGREE
OF
MASTER OF SCIENCE
IN
THE DEPARTMENT OF MECHATRONICS ENGINEERING
JANUARY 2008**

I hereby declare that all information in this document has been obtained and presented in accordance with academic rules and ethical conduct. I also declare that, as required by these rules and conduct, I have fully cited and referenced all material and results that are not original to this work.

Name, Last Name: Tahsin Tecelli ÖPÖZ

Signature:

ABSTRACT

MANUFACTURING OF MICRO HOLES BY USING MICRO ELECTRIC DISCHARGE MACHINING (MICRO-EDM)

ÖPÖZ, Tahsin Tecelli

M.S. in Mechatronics Engineering

Supervisor: Prof. Dr. Abdulkadir ERDEN

January 2008, 122 pages

Rapidly developing technology aims to develop products in miniaturized compact volumes with more functions are embedded in the products and product components. This requires advancement of micro manufacturing processes, hence industrial research on micro-machining has become considerably important and widespread. Manufacturing of micro holes by using Micro Electric Discharge Machining (Micro-EDM) is one of the topics towards developing micro manufacturing technology. The topic is investigated experimentally and extensively in this work.

There are many electrical and technological parameters of Micro-EDM process which are decisive in the machining characteristics and affect geometrical shape and surface quality of the machined parts. In this study, geometrical shapes of micro-holes machined by micro-EDM with different machining parameters are investigated. End tip shape formation, hole size expansion and hole wall-side parallelism are examined in blind and through micro-hole manufacturing. Consequently, destructive range of parameters which lead to defect formation inside the hole are found to be due to long pulse duration (>500 ns) together with higher gain (>15). In addition, entrance and exit diameters of through micro-holes are also measured and experimental data are discussed. Conclusively over-travel of tool electrode or secondary machining with a new electrode is recommended to obtain

straighter walls and fine surface in micro-holes. Aspect ratios around 20 are obtained easily by using tool electrode with a diameter equal to or less than 100 μm in blind holes.

Progress of the machining is observed at the end tip of the tools and holes. Relation between machining time and expected hole depth is studied and found to be increasing with slowing rate. Another relation between machining time and hole expansion in radial direction is also found to be a linear relation within defined band width of 20 μm for hole diameter.

This thesis is aimed to contribute understanding of micro-EDM operating parameters which are affecting on geometrical shape formation of micro-hole machining. We may conclude that the hole manufacturer can predict the expected shape of micro-hole in advance and save waste of time for sacrificial experiments.

Keywords: Micro Electric Discharge Machining (Micro-EDM), Micromachining, Wire-Electric Discharge Grinding (WEDG), Micro-tool, Micro-hole, Electrode wear, Material removal rate.

ÖZ

MİKRO ELEKTRİKSEL AŞINDIRMA İLE İŞLEME KULLANARAK MİKRO DELİKLERİN ÜRETİMİ

ÖPÖZ, Tahsin Tecelli

Yüksek Lisans, Mekatronik Mühendisliği Bölümü

Tez Yöneticisi: Prof. Dr. Abdulkadir ERDEN

Ocak 2008, 122 sayfa

Hızla gelişen teknoloji, ürün ve parçaların daha fazla işlevsel fonksiyonlar ile bütünleştirilmiş, boyutları küçültülmüş kompakt hacimlerdeki parçaların ve aksamaların geliştirilmesini amaçlamaktadır. Bu hedef doğrultusunda mikro imalat yöntemlerinin geliştirilmesi gerekmektedir bundan dolayı mikro işleme üzerindeki endüstriyel araştırmalar oldukça önemli olmakta ve yaygınlaşmaktadır. Mikro elektriksel aşındırma ile mikro deliklerin üretimi mikro üretim teknolojisinin geliştirilmesine yönelik konulardan biridir. Bu konu bu çalışmada deneysel olarak geniş bir şekilde incelenmiştir.

Mikro elektriksel aşındırma ile işlemede, işlenen parçanın geometrik şeklini yüzey kalitesini etkileyen, işleme karakteristiğini belirleyen, birçok elektriksel ve teknolojik parametre bulunmaktadır. Bu çalışmada, mikro elektrik aşındırma ile işlenen mikro deliklerin geometrik şekilleri farklı işleme parametreleri kullanılarak incelenmiştir. Kör ve boydan delik delinmesinde, deliklerin son uç şekillerinin oluşumu, delik çapında meydana gelen genişlemeler ve delik duvarlarının paralelliği araştırılmıştır. Sonuç olarak, delik içinde geometrik bozulmalara uzun sinyal süreleri (>500 ns) ile birlikte yüksek kazanım değerlerinin (<15) neden olduğu saptanmıştır. Ek olarak, boydan mikro deliklerin giriş ve çıkış çapları ölçülmüş ve ölçüm verileri değerlendirilmiştir. Bu değerlendirme sonucunda, daha düzgün duvar kenarları ve daha az pürüzlü yüzey elde etmek için, deliğin açılmasından sonra elektrotun fazla

beslenmesi yada aşınmamış bir elektrot ile yeniden işleme tavsiye edilmiştir. Kör deliklerde 100 µm lik yada daha küçük çaplı elektrotlar kullanarak 20 boy/çap oranına erişilmiştir.

Elektrotlarda ve deliklerde oluşan uç şekil gelişimi gözlemlenmiştir. İşleme süresi ve bu işleme süresine karşılık delik derinliği arasındaki ilişkiyel bağ üzerinde çalışılmış ve işleme süresi arttıkça delik derinliğinde oransal azalma olduğu bulunmuştur. İşleme süresi ve deliğin radyal yönde genişlemesi arasındaki bir diğerk ilişki de delik çapı için 20 µm lik bir bant içerisinde doğrusal olarak değıştiğı bulunmuştur.

Bu tezde mikro elektriksel aşındırma ile mikro deliklerin işlenmesinde, işleme parametrelerinin mikro delik geometrisi üzerindeki etkilerinin anlaşılmasına katkıda bulunulması amaçlanmıştır. Böylelikle, elde edilen bulgularla, üreticiler mikro deliğin şeklini, birçok uzun ve maliyetli deneyler yapmadan, tahmin edebilecektir.

Anahtar Kelimeler: Mikro-Elektriksel Aşındırma ile İşleme (Mikro-EDM), Mikro-işleme, Tel Elektrik Aşındırma (WEDG), Mikro Elektrot, Mikro delik, Elektrot aşınması, Malzeme kaldırma hızı.

To My Parents

ACKNOWLEDGEMENTS

The author wishes to express his deepest gratitude to Prof. Dr. Abdulkadir ERDEN for his advice, criticism and encouragement during the investigation and fulfillment of this study.

The author also would like to thank Dr. Bülent EKMEKÇİ for his invaluable advice and criticism and also his great effort during the metallographic preparation of test specimen in Zonguldak Karaelmas University.

The author wishes to thank Dr. H. Selçuk HALKACI, Dr. Fuad ALİEW, Dr. Bülent İRFANOĞLU, Dr. Zuhal ERDEN, Inst. Kutluk Bilge ARIKAN and Inst. Aylin K. EROĞLU for their suggestions and comments.

Also, the author would like to thank Emrah DEMİRCİ, Alper GÜNER and M. Burcu BİLDİRGEN for their supports and friendship during my study.

I would like to offer my great thanks to my parents for their endless supports and patience.

This thesis is fulfilled within the context of the research project entitled “Development and implementation of micro machining (especially micro-EDM) methods to produce (design and manufacture) of mini/micro machines/robots”; funded by the State Planning Organization of Turkey (DPT). The author acknowledges the contributions of the main funding organization; State Planning Organization of Turkey (DPT) and the other supporting organization Atılım Univestiy.

TABLE OF CONTENTS

ABSTRACT	iv
ÖZ	vi
ACKNOWLEDGEMENT	ix
TABLE OF CONTENTS	x
LIST OF TABLES	xii
LIST OF FIGURES	xiii
LIST OF ABBREVIATIONS	xviii
CHAPTER	
1. INTRODUCTION	1
1.1. Background of Electrical Discharge Machining.....	2
1.2. Basic Principles of Micro Electrical Discharge Machining	4
1.3. Wire-Electric Discharge Grinding Process.....	6
1.4. Start-up micro-EDM Research Laboratory	8
1.5. Applications of micro-EDM	9
1.6. Scope of the Thesis.....	11
2. LITERATURE SURVEY	13
2.1 Existing Micro-EDM Systems.....	13
2.2 Material Removal of micro-EDM	15
2.3 Tool Electrode Manufacturing and Wear in micro-EDM....	17
2.4 2D&3D Machining by micro-EDM.....	21
2.5 Micro hole Machining by Varying micro-EDM Specifications.....	23

3.	EXPERIMENTAL SETUPS AND PROCEDURES	29
3.1.	Micro-EDM Tool and Its Peripherals	29
3.2.	Material used for Micro-Hole Machining.....	33
3.3.	Receiving Voltage and Current Pulse Shapes	35
3.4.	Taking Cross-Section of Micro-Holes.....	36
3.5.	Use of Microscope and Dimensional Measurement.....	40
4.	EXPERIMENTAL RESULTS AND DISCUSSIONS	41
4.1.	Hole Machining Considering Energy Parameter	42
4.2.	Hole Properties Versus Machining Time	55
4.3.	Hole Machining by Varying Width and Frequency	61
4.4.	Hole Machining by Varying Open Voltage and Gap Voltage.....	68
4.5.	Manufacturing of Micro-Holes by Using $\text{\O}100\ \mu\text{m}$ Tool Electrode	71
4.6.	Defect Formation Inside Machined Hole	75
4.7.	Preventive Machining Parameters from Defect Formation and Achievable Aspect Ratio by Smaller Tool Electrode.....	79
4.8.	Through Hole machining.....	83
5.	CONCLUSION AND FUTURE WORK.....	90
	REFERENCES.....	93
	APPENDICES	
A	HOLE SHAPES WITH VARYING MACHINING TIME	99
B	HOLE-SHAPES WITH VARYING TIME WIDTH.....	103
C	HOLE-SHAPES WITH VARYING FREQUENCY	107
D	HOLE AND PULSE SHAPES WITH VARYING OPEN VOLTAGE.....	109
E	MACHINING RESULTS FOR MICRO-HOLE DRILLING .. WITH $\text{\O}100\ \mu\text{m}$ TOOL ELECTRODE	117

LIST OF TABLES

TABLE

2.1	Commercially available micro-EDM system and their capabilities (Moylan et al., 2005).....	14
3.1	Tungsten Carbide (WC) Properties.....	35
3.2	Dielectric Oil Characteristics.....	35
4.1	Machining conditions for varying energy parameter.....	43
4.2	Description of energy parameters (Sarix operating manual version 1.20) ..	43
4.3	Hole diameter variation with energy type.....	51
4.4	Machining parameters for varying machining time.....	55
4.5	Machined hole data for hole wall-side straightness calculation	61
4.6	Machining parameters for varying width and frequency	62
4.7	Machining results with variant width	64
4.8	Machining parameters for hole machining by Ø100 µm electrode	72
4.9	Machining parameters for defected holes	75
4.10	Time depended machining table	76
4.11	Machining parameters (rough condition) for through hole drilling	84
4.12	Over-travel settings for each hole	84
4.13	Settings for hole machining with secondary electrode	87
D.1	Machining results for varying gap voltage	116
E.1	Machining results by using 100 µm diameter of electrode.....	117
E.2	Machining results with the corresponding parameters	119
E.3	Circularity degree of micro-holes	122

LIST OF FIGURES

FIGURES

1.1	The gap current and gap voltage for four types of discharges seen in the EDM process (Rajurkar, 1987)	3
1.2	Proposed model of breakdown phase. (a) Emission of prebreakdown current and heating at micro peaks. (b) Bubble nucleation at micro-peak. (c) Reaching electron impact criteria at bubble interface. (d) Bubble elongation towards anode. (e) Bubble abridged the interelectrode gap and fully developed plasma channel at the end of the breakdown phase (Dhanik and Joshi, 2005)	6
1.3	(a) Wire dressing unit photograph, (b) Schematic drawing of wire dressing unit (i) front view, (ii) top view	7
1.4	Micro-tool prepared by using wire dressing unit	7
1.5	An overall picture of the micro-EDM laboratory	8
1.6	Sample of micro-EDM products which are named as in (a) Nozzle for diesel injectors (b) Plastic gear for watches (c) Micro-gear die with outer diameter around 600 μm and depth of 100 μm (d) A letter of ‘mekatronik’ and ‘M’ are machined by contouring process, (e) Micro-channels with a depth of 1 mm by using 400 μm -diameter circular electrode, (f) Department of Mechatronics Engineering Logo machined on a metal plate with a depth of 100 μm . Products in c, d, e, and f are machined by using Sarix micro-EDM machine in Atılım University Laboratory	9
2.1	Single discharge RC-circuit of micro-EDM (Wong et al., 2003)	16
2.2	Principle of WEDG with one wire guide (Fleischer, 2004).....	18
2.3	Principle of obtaining micro-rod (Yamazaki et al., 2004)	18
2.4	(a) SEM image of a copper structure with a gear shape as a machining electrode, (b) SEM image of EDMed workpiece by the electrode shown in (a) (Takahata et al., 1999)	19
2.5	(a) Shape of micro-hole by tubular electrode (b) Shape of micro-hole by rod electrode (Pham et al., 2007)	20

2.6	(a) Cu electrode arrays with patterned interconnect fabricated by using LIGA technique with two-mask alignment sequence, (b) WC-Co super hard alloy gears cut from 70- μ m thick workpiece using electrode arrays of (a) (Takahata and Gianchandani, 2002).....	23
2.7	Section view of a single-notch electrode (Wansheng et al., 2002).....	25
2.8	Schematic diagrams of four methods micro-hole micro-EDM drilling (a) using cylinder electrode for micro-EDM, (b) using cylinder electrode for micro-EDM combined with ultrasonic vibration, (c) using a helical micro-tool electrode for micro-EDM and (d) using a helical micro-tool electrode for micro-EDM combined with ultrasonic vibration (Hung et al., 2006).....	26
2.9	(a) Triangular blind hole (b) square blind hole (c) pentagonal blind hole (Yu et al., 2002).	27
3.1	Schematic drawing of micro-EDM system.....	29
3.2	Micro-EDM machine.	31
3.3	Wire dressing unit and optical microscope with 125x magnification lens	31
3.4	Spark observation during machining	32
3.5	Electrode dressing by wire dressing unit	32
3.6	A sample of drilled micro-holes with a $\text{\O}100 \mu\text{m}$ tool electrode.....	33
3.7	Flowchart for the experimental processes.....	33
3.8	Sample of plastic mold steel (70x10x2) used for micro-EDM.....	34
3.9	Tool electrodes and low resistance resistor.....	34
3.10	Agilent 54621D Mixed Signal Oscilloscope 60MHz, 200Msa/sec.	36
3.11	Buehler precision isomet low speed saw.	37
3.12	Automatic hot mounting press	38
3.13	Grinding and Polishing machine.....	38
3.14	A sample of specimen.....	39
3.15	Overall pictures of metallographic machines used in the specimen preparation	39
3.16	Nikon microscope and digital camera.....	40
4.1	Voltage (upper case) and current (lower case) pulse form for energy level of 350 (a) two pulse (b) one pulse.....	44
4.2	Voltage (upper case) and current (lower case) pulse form for energy level of 305 (a) squashed time scale (b) extended time scale.....	45
4.3	Voltage (upper case) and current (lower case) pulse form for energy level of 250 (a) squashed time scale (b) extended time scale.....	46

4.4	Voltage (upper case) and current (lower case) pulse form for energy level of 205 (a) squashed time scale (b) extended time scale	47
4.5	Voltage (upper case) and current (lower case) pulse form for energy level of 114 (a) squashed time scale (b) extended time scale	48
4.6	Voltage (upper case) and current (lower case) pulse form for energy level of 14 (a) squashed time scale (b) extended time scale	49
4.7	Target hole depth and removed electrode length with energy parameter	52
4.8	Mean hole diameter and overcut versus energy parameter	52
4.9	Micro-hole diameter measurement from top view, diameter measurement shown on micro-hole sequenced regarding with the energy parameter	53
4.10	Micro-holes wall edge photographs with X1000 magnification with respect to energy level.....	53
4.11	Cross-sectional photographs of micro-holes machined with different energy level	54
4.12	Machined hole depth and electrode removal versus machining time	56
4.13	Relation between hole diameter and machining time	57
4.14	Cross-sectional geometry of machined holes with varying machining time .	58
4.15	A sample of geometrical shape analysis for 24 min.-machined hole.....	59
4.16	End tip shape variation of hole with increasing machining time	59
4.17	Measurement of 5% reduction of entry diameter.....	60
4.18	Graphical representation of machining time versus T.length / u.length ratio	61
4.19	The signal that generates the pulses	62
4.20	Cross-sectional view of machined holes with variant width	63
4.21	Block diagram representation of average target hole depth and electrode removal by variant width value.....	65
4.22	Graphical representation of target hole depth versus width.....	65
4.23	Shapes of the pulse form for different time width of 0.1, 0.5,1, 6, 8 μ s for the each row from top to bottom, respectively.....	66
4.24	Variation in micro hole geometry with varying frequency values.....	67
4.25	Cross-sectional views of machined holes by using varying open voltages ...	69
4.26	Cross-sectional view of machined holes by using variant gap voltage. Each machining were repeated three times and represented by 1, 2, and 3...	70
4.27	Cross-sectional view of holes machined by $\text{\O}100 \mu\text{m}$ electrode with a machining time of A) (a) and (b) 20 min. (c) 30 min., B) (a), (b) and (c) 40 min while energy parameter is set to 14.	72

4.28	Cross-sectional view of holes machined by Ø100 µm electrode with a machining time of 60 min. and energy parameter for a) 14, b) 105 and c) 114.....	74
4.29	Cross-sectional view of holes machined by Ø100 µm electrode with a machining time of 15 min. and energy parameter of 350 for a, b, and c.	74
4.30	A series of hole machining defectively (numbers assigned to each pictures are given considering total machined holes as given in Appendix F).....	76
4.31	Defective hole shape labeled with (4-1).....	77
4.32	SEM photographs of defective hole from top view	76
4.33	Recorded pulse forms of defective hole in Figure 4.31 with instant machining time shown under the captured pulse shapes.	77
4.34	Cross-sectional views of defective and smooth machined holes	80
4.35	Cross-sectional views of machined micro-holes.....	81
4.36	Micro-holes to show circularity, label in the bottom of each picture represent hole number, electrode size, machining time and microscopic magnification, respectively	82
4.37	Schematic views of (a) tapered shape hole and (b) exactly cylindrical shape hole (Hung et al., 2006).	83
4.38	Schematic illustration of electrode over-travel to avoid from tapered shape (a) Worn tip of rod electrode causes a narrower hole exit and (b) enlarged hole exit is generated due to the over-travel of rod electrode.....	84
4.39	Machined hole entrance and exit diameter pictures by applying electrode over-travel.	85
4.40	Entrance and exit diameter photos of holes machined by using two electrodes.	88
A.1	Micro-holes cross-sectional shape with different machining time from 1min. to 80 min. and constant machining parameters as given in Table 4.4.....	99
B.1	Micro-hole photographs from top view by using variant width time	103
B.2	Cross-sectional photographs of micro-holes by using variant width time.....	105
C.1	Micro hole photographs machined with different frequency values of 10 kHz, 25 kHz, 50 kHz, 100 kHz, and 150 kHz r for each row, respectively...	107
D.1	Machined hole photos by setting gap voltage 50 V and gradually increasing open voltage value as given beneath the related pictures. 1000x magnified pictures of each holes are also illustrated to discuss the quality of the hole wall surface with varying open voltage value.....	109
D.2	Captured Pulse form for different open voltage values	111

D.3 Machined hole pictures from top view and 1000x magnified edge view with different gap voltage value and constant open voltage at 100V. 113

D.4 Voltage and current pulse forms for different gap voltage while open voltage kept constant at 100V 114

E.1 Pulse shapes for 100 μm diameter of electrode by using energy parameter 350 and 14 118

E.2 Micro-hole pictures for determining circularity with the magnified view represented under each picture..... 120

LIST OF ABBREVIATIONS

EDM	Electric Discharge Machining
MEMS	Micro-Electro Mechanical Systems
EBM	Electron Beam Machining
ECM	Electro Chemical Machining
MUSM	Micro Ultrasonic Machining
LBM	Laser Beam Machining
WEDG	Wire-Electric Discharge Grinding
3D	Three-Dimensional
2D	Two-Dimensional
CAD	Computer-Aided Design
CAM	Computer-Aided Manufacturing
MRM	Material Removal Mechanism
PWM	Pulse-Width Modulation
MRR	Material Removal Rate
CNC	Computer Numerical Control
DVEE	Diameter Variations between Entrance and Exit
WC	Tungsten Carbide
GPIB	General Purpose Interface Bus
STD	Standard Deviation

CHAPTER 1

INTRODUCTION

Miniaturization of parts and components play an important role in the development of today's and future's sophisticated technology in various fields. With the increasing demand for micro parts and structures in many industries, and also with rapid developments in micro-electro-mechanical systems (MEMS), micro manufacturing techniques for producing these parts become increasingly important. Micro structures including micro holes, micro slots, micro shafts, and micro gears are mostly used micro products needed in industry. Especially micro holes are needed in optical devices, medical instruments and automobile engine parts (Masuzawa, 2000, Kim et al., 2006).

Currently micro holes are formed by different manufacturing methods including micro electrical discharge machining (micro-EDM), electron beam machining (EBM), laser machining, etching, electro chemical machining (ECM), micro-ultrasonic machining (MUSM), micro mechanical drilling, micro punching, (Masuzawa, 2000, Kim et al., 2006, Kaminski and Capuano, 2003, Takahata and Gianchandani, 2002, Her and Weng, 2001, Yu et al., 2002, Diver et al., 2004, Yan et al., 2002). The selection of appropriate micromachining technique mainly depends on the type of material, size and shape of feature, aspect ratios (in the case of micro hole), cost of process etc. For example, laser beam machining (LBM) can be used to drill a hole under diameter of $4\mu\text{m}$, however, it causes deterioration and micro cracks on the machined surface. ECM can improve the material removal rate to 1.5 mm/min and surface roughness to $0.008\ \mu\text{m}$, however, the walls of the micro-holes are over etched. Microelectronic processing technologies such as photolithography and etching are not suitable to machine micro features on metallic alloys.

Mechanical manufacturing methods such as drilling can be used to drill holes of 70 μm in diameter. Laser has the ability of drilling holes of 40 μm with the possible aspect ratios of around 10 for metallic materials (Yu et al., 2002). However, with these methods, besides cost aspect, it is very difficult to drill a high aspect ratio or a blind noncircular micro hole with sharp corners and edges with super alloys such as stainless steel and tungsten carbide. Among of these micromachining techniques, micro-EDM is mainly preferred where the high aspect ratio, high surface integrity and low cost are required on any conductive material regardless of its hardness. Micro-EDM has successfully been applied to machine micro-holes of 5 μm and also 3D complex cavities (Masuzawa, 2000).

1.1 Background of Electrical Discharge Machining

Electrical discharge machining (EDM) is a thermal material removal process by melting and, partially, vaporization of the workpiece material. Source of the energy used for melting and vaporization is found in the form of heat, generated by electrical discharges and sparks between two electrodes in close proximity. The electrodes (tool electrode and workpiece) are immersed in dielectric liquid or flowing pressurized dielectric medium. Electrical discharge occurs when the dielectric is broken down by the application of voltage pulse. Some of the released energy during discharge is transferred to the electrodes and results in the heating of highly localized regions of the electrodes. When the temperature of the heating region exceeds melting temperature of the electrodes, material removal starts in size of very small particles. Molten and/or vaporized particles (debris material) are washed away from the sparking area by the continuously flushing dielectric fluid. Flowing pressure of the dielectric fluid should be used in an appropriate value, high pressurized fluid result in vanishing the influence of electrical sparks, and removed together with debris particles, however, low pressure flow result in rising debris concentration in sparking area and cause secondary discharge, arc, and short circuit.

In EDM process, mechanical properties of the workpiece do not affect the machining process. Thermal properties such as melting point, boiling point, and electrical conductivity of workpiece materials affect the machining characteristics. The material removal rate of EDM process is primarily determined by the electrical conductivity and melting temperature of the workpiece material. A workpiece with higher electrical conductivity and lower melting temperature can be machined more efficiently (Qu, 2002).

Four possible discharge types occur in conventional EDM process (hereafter conventional EDM stands for ram type EDM or die-sinking EDM). They are illustrated and named in Figure 1.1. The first one is the open circuit state, actually it is not a discharge, but it is the prerequisite for 'spark' good discharge. The third and the last one, 'arc' and 'short' respectively, are undesired discharges, they adversely affect the machining efficiency and surface roughness. Type of pulses in micro-EDM is different from that of conventional EDM. This is caused mostly by the type of circuit used in pulse generator and its advance control mechanism, additional information about type of micro-EDM pulse is given in forthcoming chapters.

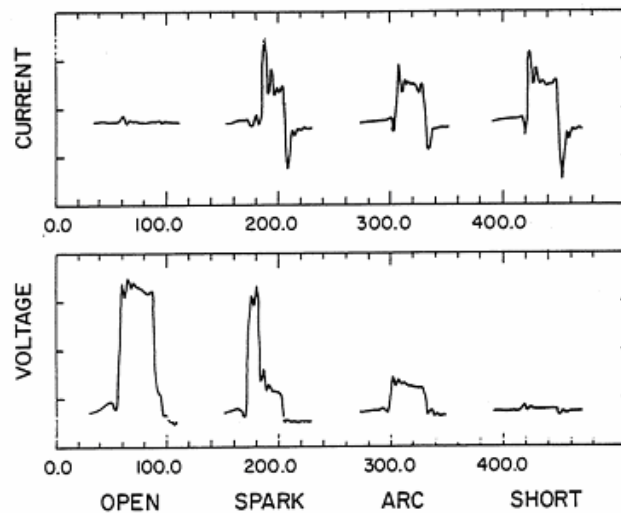


Figure 1.1 The gap current and gap voltage for the four types of discharges seen in the EDM process (Rajurkar, 1987).

1.2 Basic Principles of Micro Electrical Discharge Machining

Micro electrical discharge machining (micro-EDM) is a derived form of EDM, which is generally used to manufacture micro and miniature parts and components by using the conventional electrical discharge machining principles. Similar to conventional EDM, material is removed by a series of rapidly recurring electric spark discharges between the tool electrode and the workpiece in micro-EDM. Actually main differences of micro-EDM from conventional EDM are being in the type of pulse generator, the resolution of the X-, Y- and Z- axes movement, and the size of the tool used. In micro-EDM; pulse generator produces very small pulses within pulse duration of a few micro seconds or nano seconds. Because of this reason, micro-EDM utilizes low discharge energies ($\sim 10^{-9} - 10^{-5}$ joules) to remove small volumes ($\sim 0.05 - 500 \mu\text{m}^3$) of material (Moylan et al., 2005). The most important factor which makes micro-EDM very important in micromachining is its machining ability on any type of conductive and semi-conductive materials with high surface accuracy irrespective of material hardness. It is preferred especially for the machining of difficult-to-cut material due to its high efficiency and precision.

Small volumetric material removal of micro-EDM provides substantial opportunities for manufacturing of micro-dies and micro-structure such as micro holes, micro slot, and micro gears etc. The use of micro-EDM has many advantages in micro-parts, the main advantage is that it can machine complex shapes into any conductive material with very low forces. The forces are very small because the tool and the workpiece do not come into contact during the machining process. This property provides advantages to both the tool and the workpiece. For example, in EDM, a very thin tool can be used because it will not be bent by the machining force. The other advantages of micro-EDM include low set-up cost, high aspect ratio, enhanced precision and large design freedom. In addition, EDM does not make direct contact between the tool electrode and workpiece material, hence eliminating mechanical stress, chatter and vibration problems during machining. Therefore, relying on the above advantages, micro-EDM is very effective to

machine any kind of holes such as small diameter holes down to 10 μm and blind holes with 20 aspect ratio.

Although micro-EDM is a very efficient process in micro hole machining and having many advantages, it has also some disadvantages. One of them is that it is a rather slow machining process; the other is that while the workpiece electrode is being machined, the tool electrode also wears at a rather significant rate. This tool-wear leads to shape inaccuracies. Another drawback is the formation of a heat affected layer on the machined surface. Since it is impossible to remove all the molten part of the workpiece, a thin layer of molten material remains on the workpiece surface, which re-solidifies during cooling (Masuzawa, 2000).

The theoretical and physical model of conventional EDM with its basic elements were discussed and explored with all details in PhD thesis (Erden, 1977 and Ekmekçi, 2004). Physical model developed for micro-EDM is slightly different from that of conventional EDM. The use of resistance capacitance pulse generator, an advanced controller for machining in smaller interelectrode gaps and with lower discharge energies than in EDM, makes the material removal characteristics of a single discharge in micro-EDM different from that of the EDM (Dhanik and Joshi, 2005). In Figure 1.2, breakdown phase of single discharge model in micro-EDM is demonstrated. In EDM, breakdown of liquid dielectric leads to the formation of a plasma channel between the electrodes. The plasma expands and interacts with electrodes to effect the material removal from the respective electrodes.

Another significant point of micro-EDM is the inverted polarity of the tool electrode. Due to polarity effect in conventional EDM with long pulse duration, the tool electrode is usually charged as anode to increase material removal rate and to reduce electrode wear. At short pulse durations as used in micro-EDM, this effect is reversed. Therefore, in micro-EDM, the tool electrode is usually charged as cathode (Uhlmann et al., 2005).

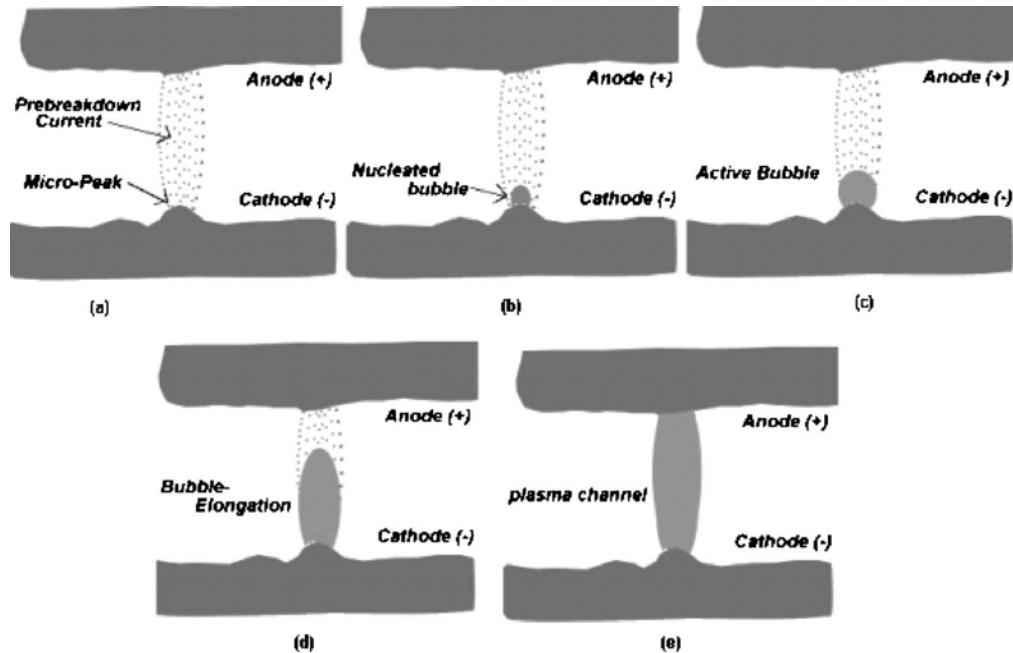


Figure 1.2 Proposed model of breakdown phase. (a) Emission of prebreakdown current and heating at micro peaks. (b) Bubble nucleation at micro-peak. (c) Reaching electron impact criteria at bubble interface. (d) Bubble elongation towards anode. (e) Bubble abridged the interelectrode gap and fully developed plasma channel at the end of the breakdown phase (Dhanik and Joshi, 2005).

Micro-EDM can be used as variant machining processes; they are micro-ED drilling, micro-ED milling, micro-ED die sinking, micro-ED contouring, micro-ED dressing, and micro wire electrical discharge grinding (micro-WEDG). All of these processes are integrated in a today's sophisticated micro-EDM machines.

1.3 Wire-Electric Discharge Grinding Process

Wire-Electric Discharge Grinding (WEDG) (Masuzawa et al., 1985) is a prerequisite machining for drilling micro-holes and milling micro-cavities with micro-EDM technology. WEDG is used to prepare smaller size tool down to $\text{Ø}10 \mu\text{m}$ by using electrical discharge machining principle with reverse polarity. Smaller size tool is prepared from larger tools. This process can be divided into two steps. At first step, the diameter of larger tool is reduced to nearly the desired smaller diameter by rough

machining. At second step, the roughly machined tool diameter is reduced to the desired diameter by using finish machining parameters.

This process is performed by wire dressing unit (Figure 1.3) in Sarix micro-EDM machine. It is placed to the work-table on micro-EDM machine, in order to avoid from misalignment and increase repetition accuracy during machining. A sample of micro-tool produced by using wire dressing unit is shown in Figure 1.4.

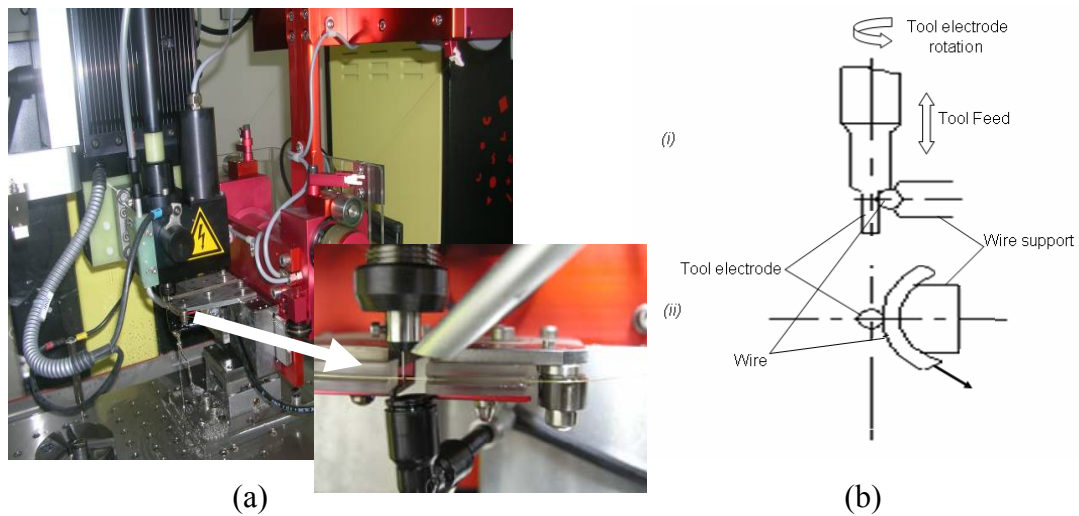
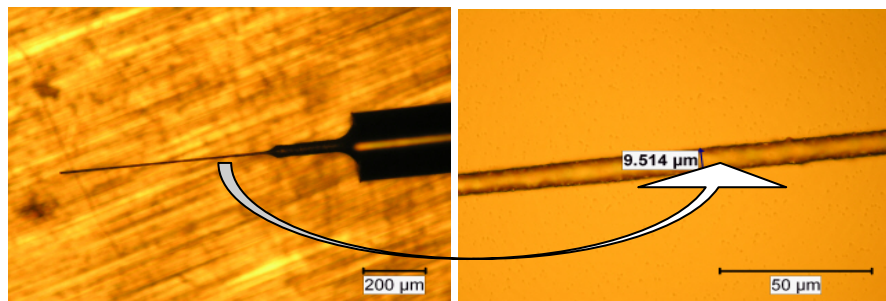


Figure 1.3 (a) Wire dressing unit photograph. (b) Schematic drawing of wire dressing unit, (i) front view, (ii) top view



(a) magnification 50x

(b) magnification 500x

Figure 1.4 Micro-tool prepared by using wire dressing unit.

1.4 Start-up micro-EDM Research Laboratory

Micro-EDM research laboratory was started to develop in January, 2006 at The Department of Mechatronics Engineering in Atılım University. This Laboratory is equipped with some recent technological machines, devices and equipments. The Laboratory is fully funded by the research project entitled “Development and implementation of micro machining (especially micro-EDM) methods to produce (design and manufacture) of mini/micro machines/robots”; funded by the State Planning Organization of Turkey (DPT). A swiss made four axis movement high precision micro-EDM (SX-100, Sarix) machine was purchased from Sarix company with all necessary equipments. A Nikon optical microscope and digital camera with clemex image analysis software were purchased and installed to the laboratory. A hot mounting press and a precision cutter were purchased from Metkon Instruments Ltd. for specimen preparation. An overall picture from the micro-EDM laboratory is given in Figure 1.5.



Figure 1.5 An overall picture of the micro-EDM laboratory

1.5 Applications of micro-EDM

Machining capability of micro-EDM, in conductive materials with high precision regardless of material hardness, create a wide range of application area with the increasing demand for miniaturized parts and components such as holes, nozzles, and gears. Produced micro parts by micro-EDM are widely used in micro-electro-mechanical systems (MEMS), biomedical applications, automotive industry, and defense industry.

Several typical components are manufactured using micro-EDM. Although the main research is going on micro-hole manufacturing, different shape of three-dimensional (3D) and two-dimensional (2D) cavities are also machined to demonstrate the machining capability of micro-EDM. A CAD/CAM system is used to generate tool paths of 3D and 2D micro-parts. Commercially available Catia V5 and Esprit CAM software are used to meet this requirement. Sample of micro-EDM products are demonstrated in Figure 1.6.

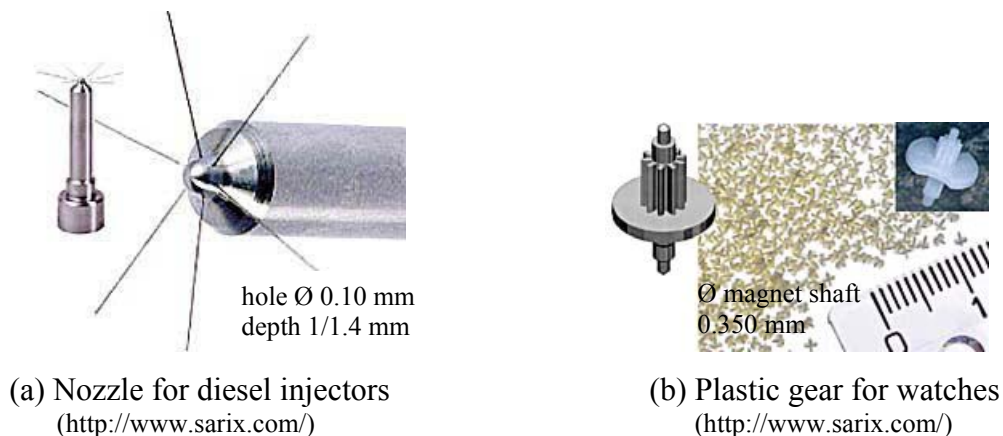
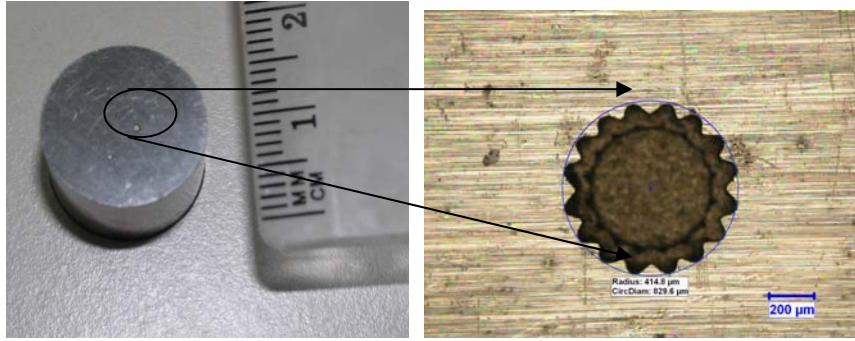
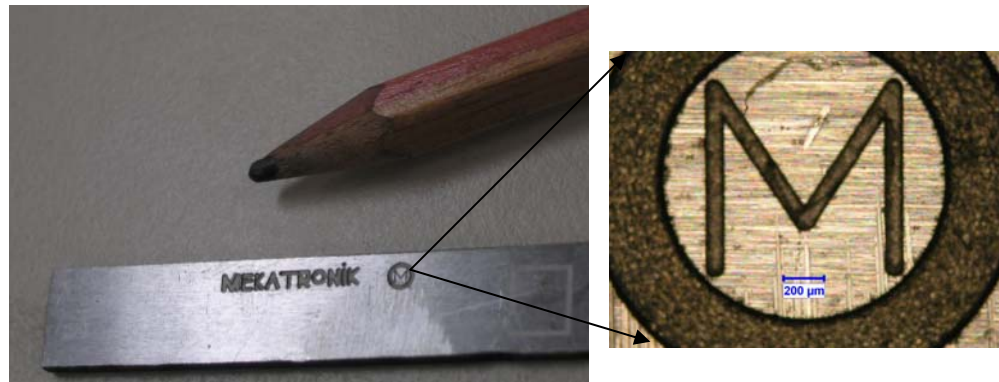


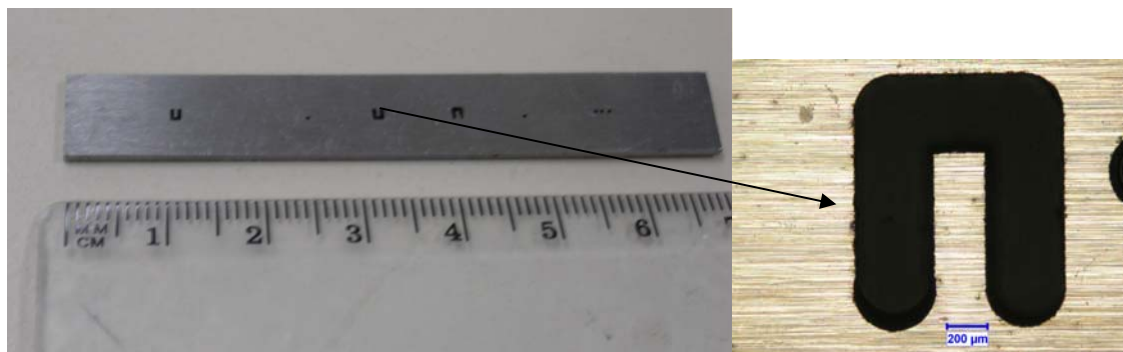
Figure 1.6 Sample of micro-EDM products which are named as in a, b, c, d, e, and f. Products in c, d, e, and f are machined by using Sarix micro-EDM machine in Atılım University Laboratory (cont.).



(c) Micro-gear die with outer diameter around 600 μm and depth of 100 μm .

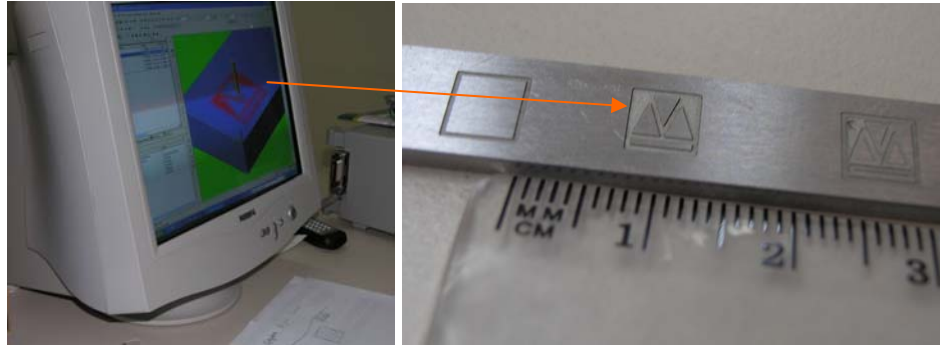


(d) A letter of 'mekatronik' and 'M' shape are machined by contouring process.



(e) Micro-channels with a depth of 1mm by using 400 μm -diameter circular electrode.

Figure 1.6 (cont) Sample of micro-EDM products which are named as in a, b, c, d, e, and f. Products in c, d, e, and f are machined by using Sarix micro-EDM machine in Atılım University Laboratory.



(f) Department of Mechatronics Engineering Logo machined on a metal plate with a depth of 100 μm .

Figure 1.6 (cont) Sample of micro-EDM products which are named as in a, b, c, d, e, and f. Products in c, d, e, and f are machined by using Sarix micro-EDM machine in Atılım University Laboratory.

1.6 Scope of the Thesis

In micro-EDM, machining characteristics primarily based on electrical and technological parameters such as current, voltage, pulse duration, pulse width, frequency, etc and material properties such as electrical conductivity, melting point, heat capacitance, etc. Especially electrical parameters play an important role in determining the machining accuracy, surface precision, and surface finish.

In this thesis, geometrical shape formations of micro-holes by varying machining parameters of micro-EDM are investigated. Influences of machining parameters and tool electrode size on the shape formation of micro-hole are reported. Moreover, achievable aspect ratios, straightness of hole wall-side, electrode wear, and material removal rate are also investigated and discussed. Therefore, optimal parameters to drill micro-holes in desired shape is investigated by considering several micro-hole machining experiments.

With the result of this study, obtained geometrical shape of micro holes, aspect ratios, side wall straightness, depth/machining time demonstrate the achievable machining limit using state-of-the-art micro-EDM technology. Micro-EDM user can predict the

geometry and size of micro-holes machined by using micro-EDM when the recommended machining parameters and materials are used.

Besides chapter 1, in chapter 2, a literature survey on micro-holes machined by micro-EDM process is presented. Additional systems and mechanisms integrated to the micro-EDM to increase machining quality and to obtain higher aspect ratios are also presented. In chapter 3, experimental set-ups and procedure is given. Micro-EDM peripherals for safe and reliable manufacturing procedure, and also data acquisition and measurement systems are described. In chapter 4, experimental results of micro-hole machining obtained with using different machining parameters and machining time are given and also overall discussion is made on experimental results and micro-EDM technology. In final chapter, chapter 5, concluded remarks from the thesis are presented and possible future works are recommended.

CHAPTER 2

LITERATURE SURVEY

Most of the published papers on micro-EDM are about the applications with micro-EDM to meet the needs for industrial applications. Many of them generally mention about technology, significant machining parameters such as voltage, current, etc., affecting the machining qualities, its machining ability on different type materials, material removal rate of workpiece and wear ratios of tool electrode and so on. Advantages and disadvantages of micro-EDM as a micromachining technique are also generally reported in several published papers. Micro-hole machining by micro-EDM is the dominant subject for this thesis. This is because literature is reviewed mostly regarding the micro-hole machining parameters, geometry of micro-hole, aspect ratios, tool wear and material removal with respect to machining time. However, additional configurations on micro-EDM machine for enhancing machining quality, 3D micro-parts machining, and comparison of micromachining systems are also studied for contributing to understand the micro-EDM phenomena easily.

2.1 Existing Micro-EDM Systems

Micro-EDM systems started to develop with an attempt to produce small size holes. Development of the micro-EDM systems has gained acceleration with the invention of wire-electro discharge grinding (WEDG). The latest model of micro-EDM systems can produce their own tool electrodes directly on the machine utilizing the WEDG

process. Today, there are only three micro-EDM manufacturer, they are Panasonic Factory Automation (Illinois, USA, www.panasonicfa.com), Sarix SA (Losone, Switzerland, www.sarixsa.com), and Pacific Controls Inc. (California, USA, www.pasificcontrols.com). Moreover, Agie SA (Losone, Switzerland, www.agieus.com) manufactures micro-wire EDM (Moylan et al., 2005). Table 2.1 summarizes the existing micro-EDM systems with their important specifications.

Table 2.1 Commercially available micro-EDM systems and their capabilities
(Moylan et al., 2005)

Machine	Power Supply	Motion Control	Electrode Size	User Applications
Panasonic	Relaxation Generator (RC circuit) 10 nsec pulse-width	0.1 μm resolution 1 μm positioning accuracy	Holes as small as 5 μm , WEDG makes electrodes on machine	Three axis machining and shafts, etc as well as holes and complex cavities. Real 3D shapes.
Sarix	Undisclosed 50 nsec pulse-width 0.05-40 Amp	1 μm resolution 1 μm positioning accuracy	Electrodes as small as 12 μm diameter (Purchased)	Holes, Shaped electrodes make shaped holes, Machining in 3 axes possible, but not demonstrated.
Pacific Controls	555 multi-shot (dual gap voltage 2. μsec pulse width 0.002-100 amp)	Monitored to 0.5 μm	Electrodes as small as 2.5 μm diameter (purchased)	Holes only, no mention of shaped electrodes. Machining only in z-axis.
Agie	Undisclosed	0.1 μm resolution 1 μm positioning accuracy	Wire as small as 25 μm diameter	Any type of 2-D part. Machining in x- and y- axes only. Wire tilt not available With 25 μm wire.

2.2 Material Removal of Micro-EDM

Material removal mechanism (MRM) in micro-EDM is similar to the conventional EDM, spark discharge between the workpiece and tool electrode in the dielectric medium release intense energy in the form of heat. This released energy removes a droplet material from the workpiece and tool electrode by melting and vaporization phenomena. Another typical examples of removal by this type physical phenomenon are LBM (laser beam machining), and EBM (electron beam machining) (Masuzawa, 2000). The molten part is removed from the discharge area by the pressurized dielectric fluid. The types of workpiece and mate tool electrode together with the used dielectric fluid affect the MRM depending on the change in sparking conditions, which is altering the three sparking phase called as breakdown, discharge and erosion (Ho and Newman, 2003). Additionally, reversing the polarity of sparking alters the material removal phenomenon with an appreciable amount of electrode material depositing on the workpiece surface (Ganhaddar et al., 1992).

The scientists have continually tried to get more efficient material removal mechanism in EDM systems, mostly researchers have worked on the type of circuit used for pulse generation, and they have used different circuit mechanism to obtain efficient material removal in micro-EDM. Han et al. (2006) have developed a new transistor-type isopulse generator for micro-EDM. Their experiments showed the machining characteristics proved that the transistor type isopulse generator is suitable for micro-EDM. Their experimental results reveal that the transistor-type pulse train generator is unsuitable for micro-EDM due to its low removal rate. The removal rate of the transistor-type isopulse generator is two or three times higher than that of the traditional RC pulse generator. Wong et al. (2003) investigated the micro-EDM material removal characteristics using single RC-pulse discharges. It was reported that the estimated erosion efficiency of material removal at low-energy ($<50\mu\text{J}$) discharges is found to be seven to eight times higher than that at higher-energy discharges. They observed that the volume and size of the microcraters are more consistent at lower energy discharge than at higher energy discharges. A single-discharge erosion RC circuit with dc voltage power supply

(0-300V), shown in Figure 2.1, was developed. Kim et al. (2006) has studied the characteristic of micro EDM process and application on micro holes machining. They have built PWM circuit into RC circuit to control pulse width of 200 ns per each step. Because arc discharge can occur and result in unstable machining in RC circuit type micro-EDM process.

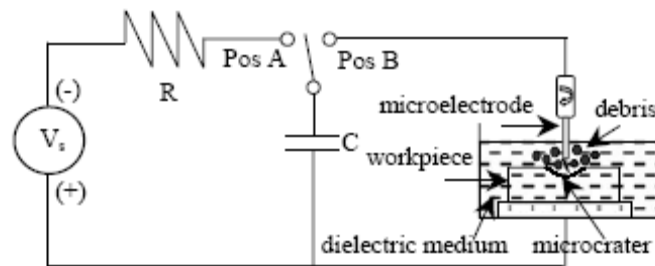


Figure 2.1 Single-discharge RC circuit of micro-EDM (Wong et al., 2003)

Allen and Chen (2007) investigated the material removal for micro-EDM on molybdenum using a MATLAB-based thermo-numerical model, which simulated single spark discharge process. Depending on the proposed model, they reported the percentage of tool wear decreases with an increase in the pulse duration and much higher for molybdenum than steel at the same machining conditions. Son et al. (2007) investigated the influences of EDM machining conditions on micro-EDM characteristics. The pulse condition is particularly focused on the pulse duration and the ratio of off-time to on-time, and the machining properties are reported on tool wear, material removal rate, and machining accuracy. Their experimental results show that the voltage and current of the pulse exert strongly to the machining properties and the shorter EDM pulses is more efficient to make a precision part with a higher material removal rate. Klocke et al. (2004) investigated the influence of the powder particles in micro-sinking-EDM on the thermal spread in the dielectric and on the influenced zone. They reported the physical properties of the powder additives play an important role in changing the recast layer composition and morphology. Their experiments result in two important conclusions; 1) ‘Al powder leads to thinnest rimzone and the highest MRR’. 2) ‘Si powder produces a

grey zone beneath the actual “white zone”’. Liu et al. (2005) reported that material removal rate (MRR) for micro-hole machining over high nickel alloys is increasing sharply with increasing discharge current, and reached a maximum at a discharge current of 500 mA when pulse duration is fixed at 4 μ s. This report reveals that a significant portion of the total energy is used to vaporize the material at lower current result in reducing in MRR, however, when the discharge current is too large (e.g. 2A) the explosive energy density is huge, and the discharge spark is drastic.

In addition, type of dielectrics fluid used during machining is also effective factor for material removal rate in micro-EDM. MRR was found to be higher when pure water was used as a dielectric liquid compared to the kerosene use was lower (Lin et al, 2007). Tool wear is found to be very small when the deionized water is used in working medium, machining time also decreases due to a fast machining federate (Chung et al, 2007)

2.3 Tool Electrode Manufacturing and Wear in Micro-EDM

Micro-tool electrode manufacturing is going to be more important for micro parts and holes machining in micro-EDM. With improving very small size tool manufacturing technology, micro-EDM mostly beginning to use, especially, for micro-hole drilling. The most powerful technique for manufacturing micro-tool is WEDG (Wire Electro-Discharge Grinding), shown in Figure 2.2, proposed firstly by Masuzawa et al. (1985). It is an important step of the improving technology in micro-EDM.

In addition to WEDG process, some other techniques also proposed by the researchers, Yamazaki et al. (2004) proposed a method to produce micro-rod electrode using machined holes as shown in Figure 2.3. With the proposed model, a straight rod can be formed with an electric capacitance of 10-220 pF and feed speed of 2 μ m at a machining time of 5 min; any rod electrode diameter can be obtained by off-centering, complicated shapes such as asymmetrical, stepped and multi-rods can be formed.

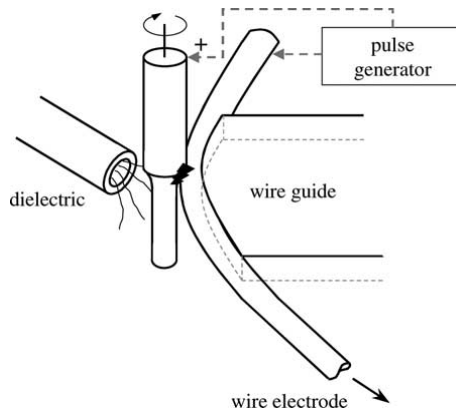


Figure 2.2 Principle of WEDG with one wire guide (Fleischer, 2004)

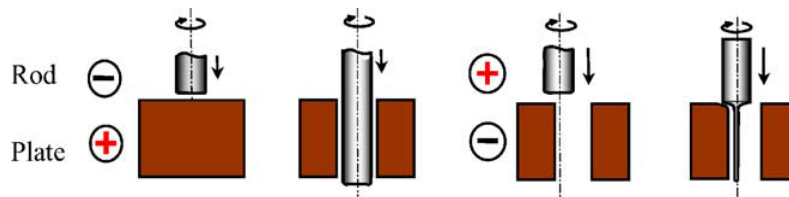


Figure 2.3 Principle of obtaining micro-rods (Yamazaki et al., 2004)

Takahata et al. (1999) developed a novel micro-EDM method using electrodes fabricated by the LIGA* process as shown in Figure 2.4. With this method, they can achieve to produce high-aspect-ratio micro structure from various kinds of materials with short machining times and to achieve high electrode wear resistance by employing electroplated copper electrodes. Multiple structures can be produced in parallel by using an electrode array. It is possible to convert micro-EDM process from serial to parallel fabrication.

* LIGA is the abbreviation from the German words, “Lithographie”, “Galvanik”, and “Abformung”
 In LIGA process, a mold insert is made by deep lithography coupled with micro electroforming; mass production is then carried out by molding technique.

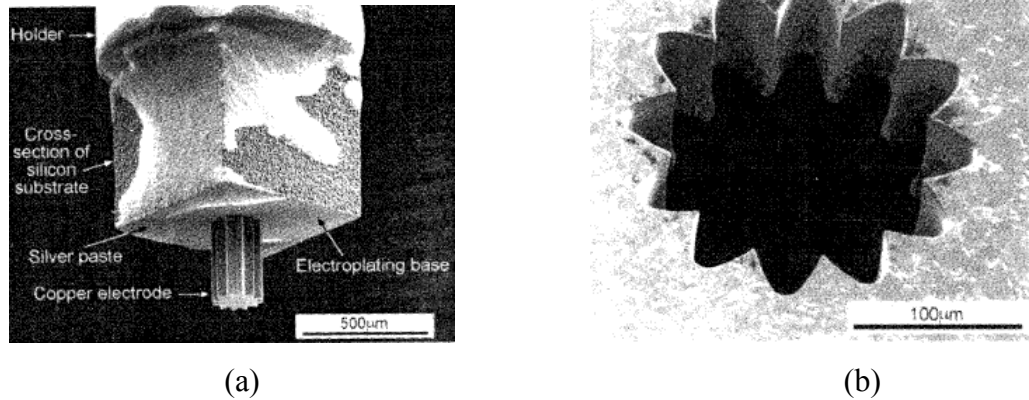


Figure 2.4 (a) SEM image of a copper structure with gear shape as a machining electrode, (b) SEM image of EDMed workpiece by the electrode shown in (a) (Takahata et al., 1999)

Fleischer et al. (2004) developed a way to produce milling tools in tungsten carbide with CNC-controlled EDM machines. Their research has shown the potential of the machining of micro-cutting tools with a diameter smaller than 100 µm.

Although EDM is an efficient machining process for the fabrication of a micro-hole with various advantages resulting from its characteristics of non-contact and thermal process, tool wear leads to significant problem resulting in deterioration in the machining accuracy. Machining accuracy of EDM is limited by tool wear, which is unavoidable consequence in EDM process because the sparks generated for the machining remove the part of the electrode simultaneously. The tool wear is characterized by corner and end wear which mean tool material removal in radial and axial directions, respectively. Therefore, the tool wear deteriorates both the depth and the shape of a machined hole in EDM drilling. In particular, this problem becomes intensified in the fabrication of a blind hole. Electrode wear is inversely related to the melting point of the material used as the electrode, the higher the melting point the lower the tool wear (Tsai and Masuzawa, 2004).

Most of the micro feed mechanisms of electrode have developed so far focus on the miniaturization of micro EDM equipment or the compensation to electrode wear along

feed direction. Introducing vibration and rotation onto electrode in feeding is certainly beneficial to keep stable and efficient machining process. In micro hole drilling, the wear of electrode is relatively significant. The fore end shape of electrode is difficult to be kept due to the radial wear of electrode directly affecting it, though the axial loss can be compensated (Li et al. 2002).

Yu et al. (1998) proposed a method based on layer-by-layer machining with maintaining the original tool shape, which is called *Uniform Wear Method*. This method is very useful for micro electrical discharge milling process; complex shape of cavity can be machined with a nearly designed aspect ratio, it provides to enable wear compensation. They stated that if a small depth of cut was used and a tool path was chosen that crossed over the previous path by the radius of the tool, the majority of the wear would occur from the end of the tool. If the tool path is long, the tool will be significantly shorter at the end of the path; therefore the next is reversed in order to achieve a flat substructure. Pham et al. (2007) investigated the electrode wear during micro-electrical discharge drilling with micro rod and micro tube electrodes, shown in Figure 2.5. They reported that wear measurement increasing dramatically after a certain depth while rod electrode is used. This is mainly expected due to deteriorated flushing conditions. Good flushing should be enabled to avoid from side sparking on the electrode. However, tubular electrode is more stabilize in deep depth when comparing to the rod electrode.

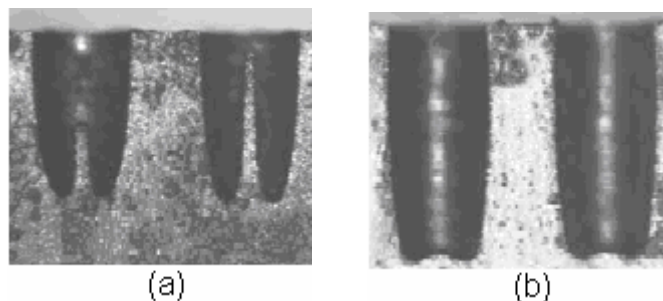


Figure 2.5 (a) Shape of micro-hole by tubular electrode (b) shape of micro-hole by rod electrode (Pham et al., 2007)

Tsai and Masuzawa (2004) investigated the relationship between the tool wear ratio and the thermal properties of tool and workpiece made of a variety of materials. And they proposed a repetitive machining method which uses reground tools until a required profile is obtained.

2.4 2D&3D Machining by micro-EDM

EDM process is a mostly favored machining technique to produce microstructures and micro mold with 3 dimensions (3D) and high aspect ratios. Feasibility of micro tool electrode by WEDG unit in micro EDM systems also gains advantages in 3D micro parts manufacturing. This type of EDM process generally called as electrical discharge milling process, because the tool electrode has a movement through the defined tool path like in milling operation. A CAD/CAM system is also needed to generate tool path for the electrode.

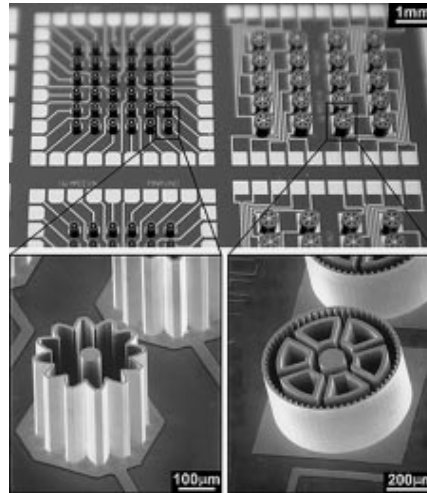
Recently published papers about micro-mold machining by using micro-EDM process are cited with their remarkable points. Electrode wear is again a drawback for 3D machining, it is necessary to compensate the worn length of the electrode. Zhao et al. (2004) have used online measurement of electrode wear to compensate the electrode wear and maintain the machining accuracy. Rajurkar and Yu proposed (2000) an approach to integrate CAD/CAM systems with micro-EDM while accounting for tool wear using recently developed uniform wear method. Using this proposed approach, some complex 3D micro shapes were machined successfully. Lim et al. (2003) have studied the machining of high aspect ratio micro-structures using micro-EDM. Parameters affecting the micro-EDM were investigated and micro-structure has been successively fabricated. They realized that the machining dept is inversely proportional to the feed rate. A micro slit die easily manufactured using a micro electrical discharge machining (micro-EDM) is proposed for micro heat sink fabrication (Wang et al. 2005). Fabrication of biocompatible microdevices has been studied by using the micro electro discharge machining (Murali and Yeo, 2004). Micro channels with feature size of 25 μm can be produced. The process is made more effective by introducing ultrasonic vibration

of the workpiece. The total time needed for fabricating these microdevices by micro-EDM is comparatively shorter than that of machining by lithographic and etching techniques. Cao et al. (2007) reported the fabrication of microscale Ta[†] mold by using micro-EDM. Surface morphology of the micro-EDMed Ta molds are characterized by scanning electron microscope, X-ray photoelectron spectroscopy, and transmission electron microscopy. Han et al. (2006) investigated the manufacturing of the smallest possible rod diameter obtained by micro-EDM. Based on their investigation results, sub-micrometer machining using SWC (Cemented tungsten carbide made of super fine particles) was attempted, and the smallest possible diameter obtained was about 2.8 μm.

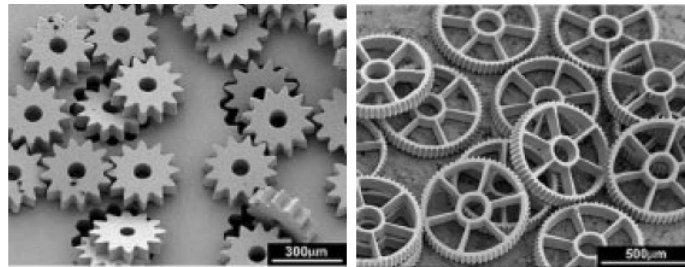
Takahata and Gianchandani (2002) proposed a micro-electro-discharge machining techniques that uses electrode arrays fabricated by LIGA process to achieve high parallelism and throughput in the machining. According to their techniques, Using electrode arrays with four circuits, batch production of 36 WC-Co gears with 300 μm outside diameter and 70 μm thickness in 15 min are produced as shown in Figure 2.6. The results obtained clearly revealed that using arrayed electrodes with separate pulse control circuits (RC pairs) for each array partition can vastly increase the machining rate.

Tseng et al. (2005) reported the integration of LIGA and micro-EDM to fabricate the micro mold for the ink jet printer nozzle plates. With this method, the positioning and alignment accuracy of the micro pins and holes have improved significantly. Li and Senturia (1992) reported the use of micro-EDM to fabricate molding tools with which plastic parts are molded having dimensions on the order of tens of microns.

[†] Ta is the abbreviation of Tantalum element.



(a)



(b)

Figure 2.6 (a) Cu electrode arrays with patterned interconnect fabricated by using LIGA technique with two-mask alignment sequence, (b) WC-Co super hard alloy gears cut from a 70- μm -thick workpiece using electrode arrays of (a) (Takahata and Gianchandani, 2002)

2.5 Micro hole Machining by Varying micro-EDM Specifications

Micro-EDM is one of the most powerful methods for drilling micro-holes in any electrically conductive materials, since circular rod electrode with a very small diameter of 5 μm can be fabricated by using WEDG unit placed on the micro-EDM machine (Masuzawa, 1997). The depth of the holes which can be drilled will be rather limited, since the side gap between electrode and workpiece is very narrow in micro-EDM. This is an obstacle to remove away debris from sparking area, and result in bad discharge called arc and short circuit. Recent study in micro-EDM is generally condensed to get high aspect ratio in micro-holes, inner and exit diameter differences, surface and geometrical shape quality, and minimum achievable size in micro-hole manufacturing.

A literature survey on micro-hole machining by using micro-EDM with different decisive specifications is presented below.

Masuzawa et al. (1989) proposed a horizontal EDM system for drilling deep, small holes. They can manage to machine deep, small hole with an aspect ratio around 10 and they can produce $\text{Ø } 55 \text{ }\mu\text{m}$ hole with a depth of $500 \text{ }\mu\text{m}$ within 30 seconds. Her et al. (2001) have studied on micro-hole machining of copper with traditional EDM machine using a tungsten carbide tool electrode. They reported that electrode wear and hole enlargement are both smaller, and a better profile of micro hole can be obtained when positive polarity machining is selected, however, electrode wear is higher when positive polarity machining is selected. In addition, the author also emphasized that material removal rate is higher when negative polarity machining and tungsten carbide electrode are selected.

In micro hole drilling, the fore end shape of electrode can not be kept stable because of the radial wear of electrode, although the axial loss can be compensated. The wear on fore-end of tool electrode alters the precision and shape of holes. In case of through hole drilling, feeding over the tool electrode gain significance so that the exit diameter of the hole is enlarged and going to be equal to the entry one (Li et al, 2002). The technique shaping the circular rod electrode with circular crosssection into the semi-circular or non circular crosssection become very efficient for machining micro-hole with high aspect ratio. The tool electrode is shaped by cutting $1/5$ to $1/4$ of the diameter off from two sides using WEDG unit (Masuzawa et al, 1989). Kim et al. (2006) proposed a method to reduce the difference between the entrance and exit diameters of the hole. By reducing secondary discharge, electrode wear, and capacitance when the tool was closed to the exit of the hole by introducing ultrasonic vibration to the EDM, a mostly straight hole was fabricated and inner shape of hole was not influenced from the proposed method. Yan et al. (2002) have studied on the precise micro hole machining with a high aspect ratios in borosilicate glass. They used a machining method which combines micro-EDM and micro ultrasonic vibration machining (MUSM). Their experimental results show that using appropriate machining parameters; the diameter variations between the entrances

and exits (DVVE) can be decreased to nearly 2 μm in micro holes with a diameter of 150 μm and depths of 500 μm . In that paper, authors claimed that DVVE can be enhanced by improving an ultrasonic amplitude or rotational speed and also they reported the degree of micro-hole roundness mostly related to the machining tool rotation speed.

Li et al. (2002) proposed that an inchworm type micro feeding mechanism in micro-EDM. With the aid of this mechanism, micro holes and micro-rods with an aspect ratio of more than 20 and 10 obtained respectively. Wansheng et al. (2002) introduced the ultrasonic vibration into micro-EDM when they made their experiments with a single side notched cylindrical tool electrode, shown in Figure 2.7. They reported that holes with a diameter of less than $\text{\O}0.2$ mm and aspect ratio of more than 15 can be machined steadily using this technology.

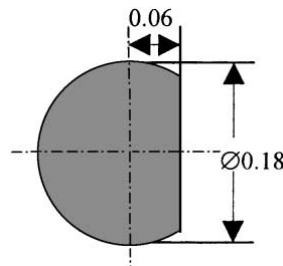


Figure 2.7 Section view of a single-notch electrode (Wansheng et al., 2002)

Yeo et al. (2004) investigated the feasibility of a magnetic field to obtain higher aspect holes on hardened tool steel using micro-EDM process. They reported that the magnetic field can assist to improve debris circulation, and they achieve to machine a hole with a depth of 1177 μm in 360 min, which is 26% higher than that of achieved in conventional micro-EDM. Hung et al. (2006) have used a helical micro-tool electrode to drill and finish micro-holes by using micro-electro-discharge machining combined with ultrasonic vibration. They reported that this method can substantially reduce the EDM gap, taper and machining time for deep micro hole drilling. Moreover, using a helical micro-tool with micro ultrasonic vibration finishing, good surface quality and less taper

of the hole wall can be obtained. Figure 2.8 shows the four methods of micro hole drilling in micro-EDM.

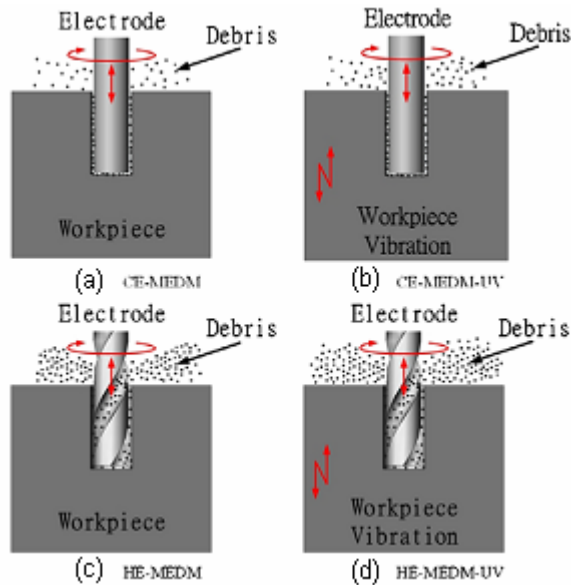


Figure 2.8 Schematic diagram of four methods during micro-hole micro-EDM drilling: (a) using a cylinder electrode for micro-EDM, (b) using a cylinder electrode for micro-EDM combined with ultrasonic vibration, (c) using a helical micro-tool electrode for micro-EDM and (d) using a helical micro-tool electrode for micro-EDM combined with ultrasonic vibration. (Hung et al., 2006)

Micro-hole machining by using micro-EDM combined with electropolishing was proposed by Hung et al. (2006). Electropolishing is applied for finishing the hole wall, high surface quality of the hole is obtained by using appropriate electrolytic voltage. Yu et al. (2002) proposed a model which provides planetary movement to the electrode. The planetary movement in micro-EDM results in sufficient gap to remove debris during drilling high aspect ratio micro holes, blind noncircular micro holes, shown in Figure 2.9, as well. Their approach is verified by manufacturing micro holes with an aspect ratio of 18 and blind noncircular micro holes with sharp corners and edges.

Diver et al. (2004) investigated that the fabrication of reverse tapered holes in EDM systems. They emphasized that the existing EDM system is not fully qualified and

produce low quality reverse tapered holes. According to their novel technique, tapered holes with a entry diameter of 100 μm and exit diameter of 160 μm can be produced. The other alternative ways of producing tapered holes are listed below (Diver et al., 2004);

- (a) “Modify the EDM parameters (e.g. voltage, frequency, current, gap ,gain, or pulse width) during machining to remove more material radially as the dept of machining increases.
- (b) Move the workpiece relative to the electrode to achieve the desired hole taper.
- (c) Change the electrode angle and position radially during drilling.
- (d) Feed and rotate the electrode at the angle required to achieve the desired hole taper.”

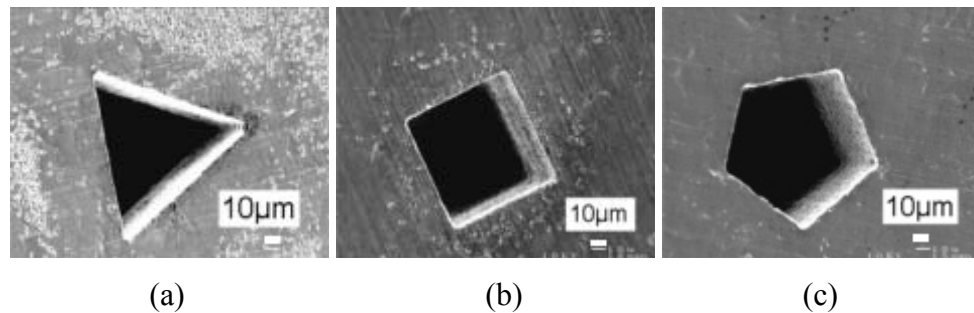


Figure 2.9 (a) triangular blind hole (b) square blind hole (c) pentagonal blind hole (Yu et al., 2002)

Weng (2006) investigated the manufacturing of microparts with an array of micro holes using the machined micrographite –copper electrode in EDM. This electrode is fabricated by using electrochemical process of anodic etching combined with electroforming process. He indicated that yielding parts can be utilized as a microwater spray nozzle in the biotechnology applications. Nakaoku et al. (2007) investigated that the basic characteristic of micro-EDM by machining micro holes in sintered diamond. They reported that micro-holes with a diameter of 50 μm can be machined in sintered diamond and machining characteristic is similar to the tungsten carbide alloy. In addition, they observed that side gap between electrode and hole wall increases with increasing open-circuit voltage. Kaminski and Capuano (2003) reported that the

parameters affecting the micro holes machining process when diameter smaller than 0.1 mm and aspect ratio bigger than 20 by electro-erosion penetration process in sheets. And circularity deviation provided by the experiment was smaller than 0.01 for 0.1 mm diameter holes.

CHAPTER 3

EXPERIMENTAL SETUPS AND PROCEDURES

In this chapter, experimental set-up and tools are described by giving their specifications and functions. Throughout the chapter, experimental procedures explained with all details for micro hole machining by using micro-EDM technique. Schematic view of the micro-EDM set-up is shown in Figure 3.1.

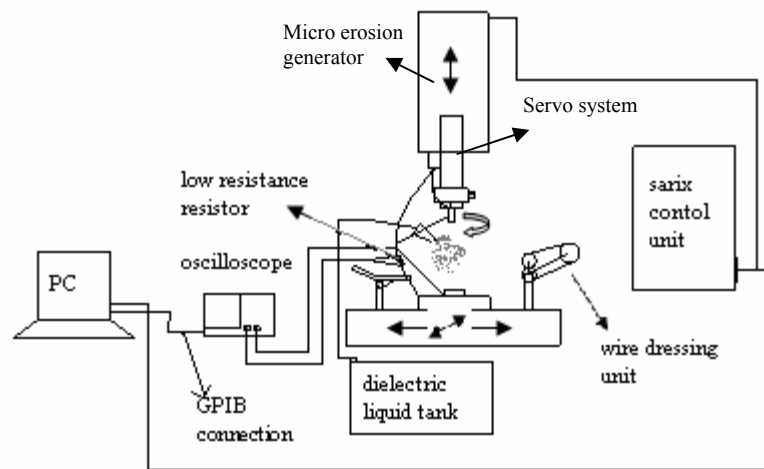


Figure 3.1 Schematic drawing of micro-EDM system

3.1 Micro-EDM Tool and Its Peripherals

A Swiss made four axis movements SARIX micro-EDM machine as it is shown in Figure 3.2 is used for micro hole machining. The machine has a SR-MPS standard micro-erosion generator. This generator is able to produce pulses from 50 ns to 2 μ s with

electrical current peak values up to 50 A. Power supply can vary voltage levels from 50 V to 250 V, but this is limited up to 100 V for the used micro-EDM machine. In addition to the micro erosion generator, the micro-EDM machine is also composed of the following parts; SX-CU control unit, SX-MMI panel and SX-DA unit. SX-CU includes the electrical circuits and control mechanisms which run the machine. SX-MMI panel is the user's command panel, the machine operator can control the machining parameters and receive machining information on TFT color screen. SX-DA unit is the dielectric liquid tank that has water-cooling system and filters the used dielectric liquid for reusing.

Wire dressing unit (Figure 3.3) is integrated to micro-EDM machine to produce small size tool electrode. It is used to reduce standard diameter of 400 μm electrode size to the desired very small size of electrode. Micro-measurement system is installed to the wire dressing unit to measure the electrode diameter whether within the expected range. To measure the exact reduced diameter of the tool electrode, an optical microscope (Figure 3.3) with 125x magnification, installed on the work-table, is used. A CAD/CAM system is used for 2D and 3D machining, Catia V5 is used for solid model of desired shapes and Esprit CAM with EDM module is used to generate G-code for milling operation. Figure 3.4 illustrates the spark observation during machining and Figure 3.5 depicts the picture of electrode dressing by wire dressing unit.

By using SX-MMI panel, electrical and technological parameters are set then drilling operation is performed. A sample of micro-hole drilled with a $\text{\O}100 \mu\text{m}$ tool electrode on the plastic mold steel plate is shown in Figure 3.6.

Micro-manufacturing process by micro-EDM and consequent processes such as measurement and sectioning process are depicted by using flowchart as shown in Figure 3.7. All the mentioned experimental process in the flowchart is explained in details in the forthcoming sections.

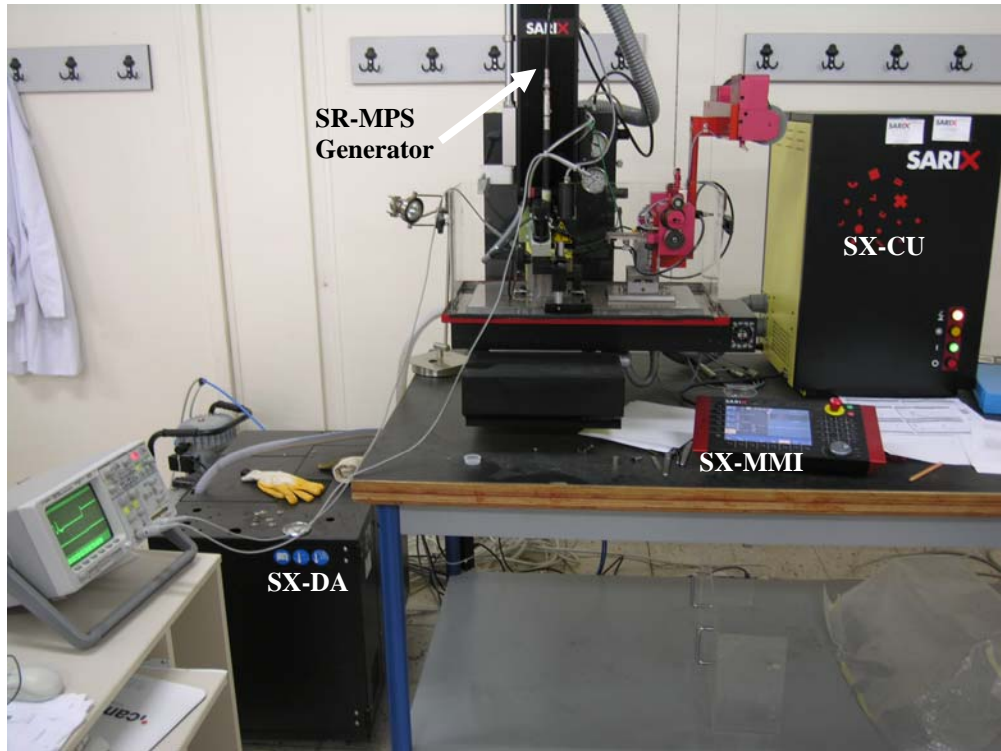


Figure 3.2 Micro-EDM machine

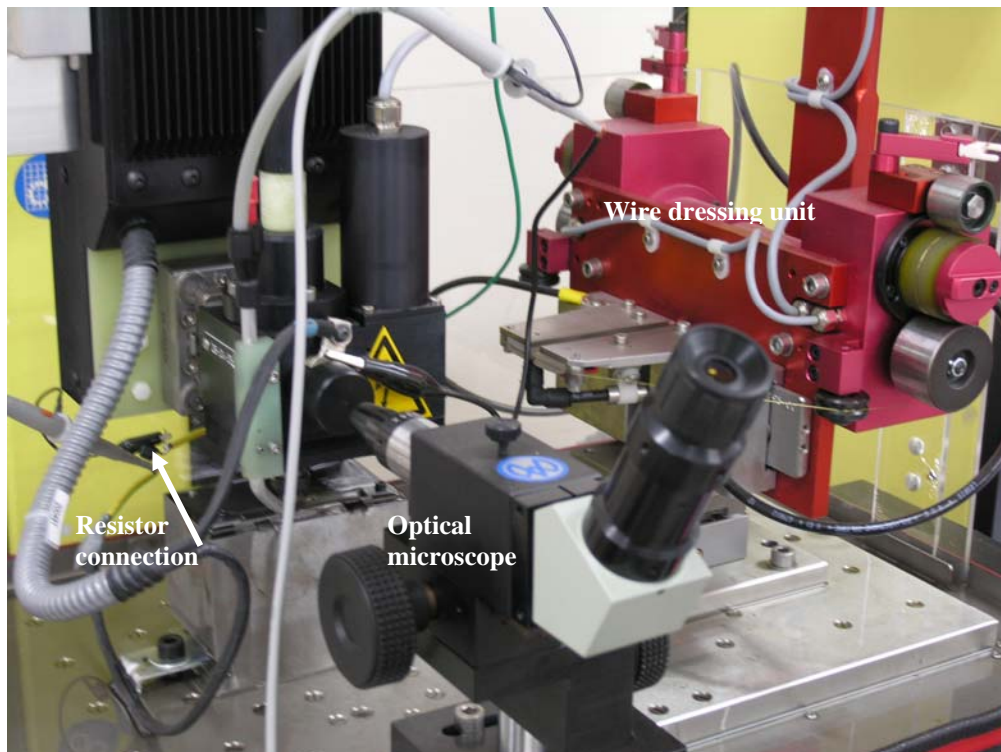


Figure 3.3 Wire dressing unit, Optical microscope with 125x magnification

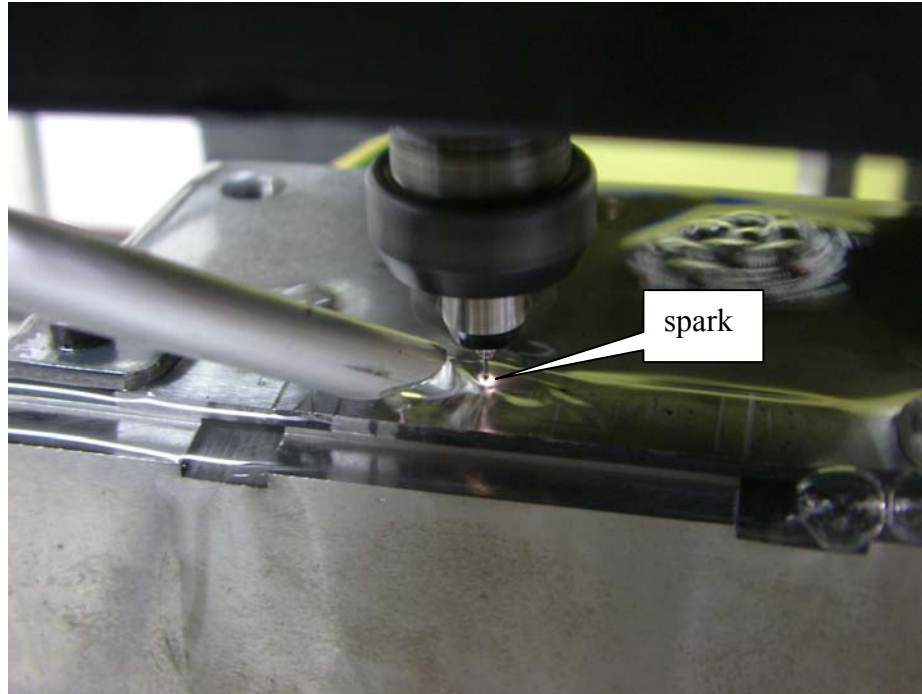


Figure 3.4 Spark observation during machining



Figure 3.5 Electrode dressing by wire dressing unit

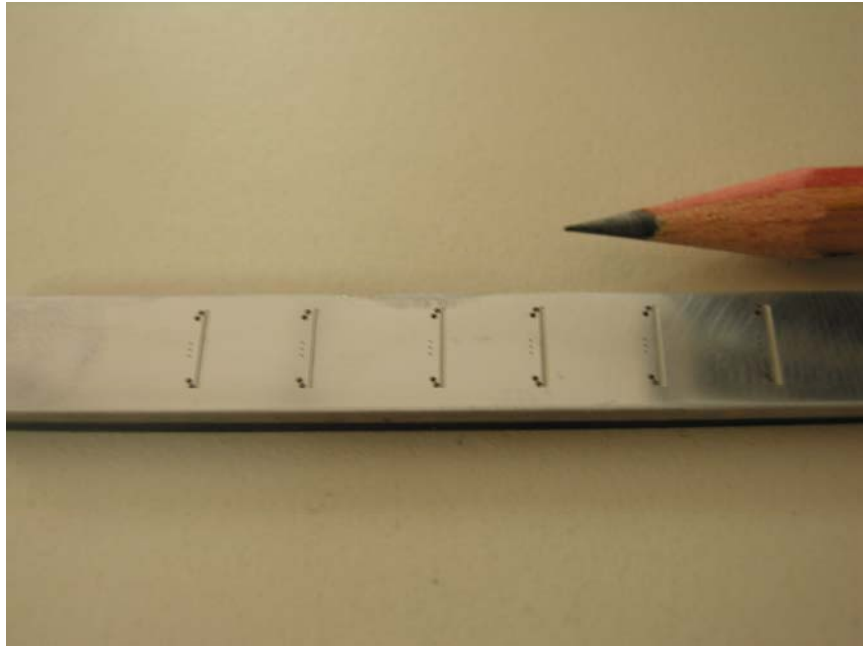


Figure 3.6 A sample of drilled micro-holes with a $\text{Ø}100\ \mu\text{m}$ tool electrode

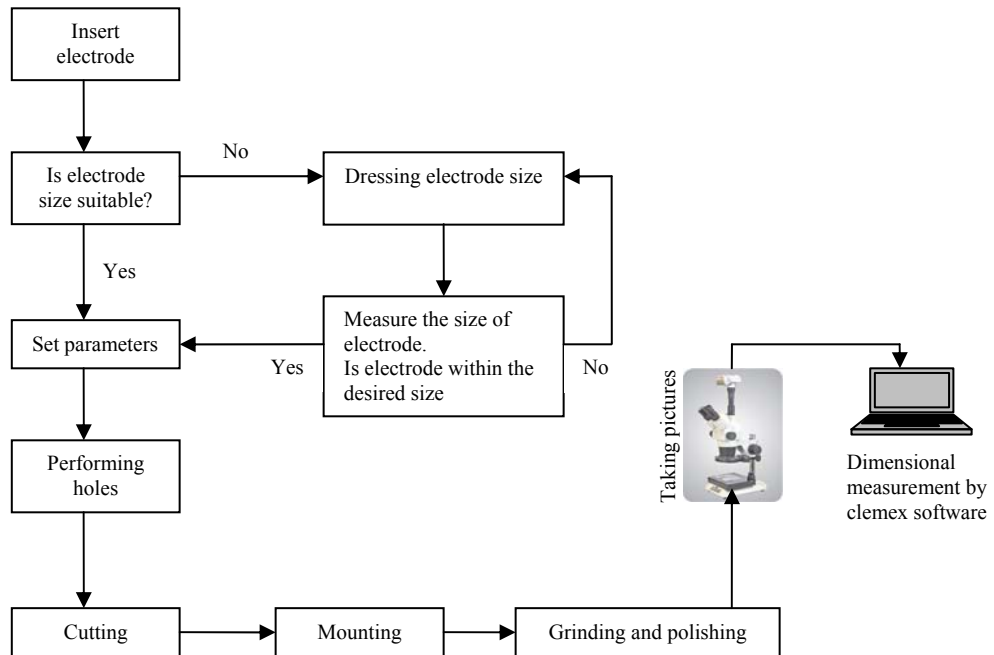


Figure 3.7 Flowchart for the experimental processes.

3.2 Material Used for Micro-Hole Machining

Plastic mold steel (70x10x2) as illustrated in Figure 3.8 is used as a workpiece material. Tungsten carbide (WC) electrodes (Figure 3.9) with a standard diameter of 400 μm and 100 μm are used as a tool electrode. Stiffness and rigidity of tungsten carbide is very high when comparing to tool steel. This is because tungsten carbide electrode size can be reduced to very small size and prevents bending or swinging during machining. Wear resistance of tungsten carbide is also better than that of tool steel. This provides advantages for micro-hole drilling since less deterioration occur in the shape of target holes. The properties of WC is given in Table 3.1. Dielectric liquid used for flushing is a hydro carbide composed of mineral and synthetic oils. Its characteristics are tabulated in Table 3.2.

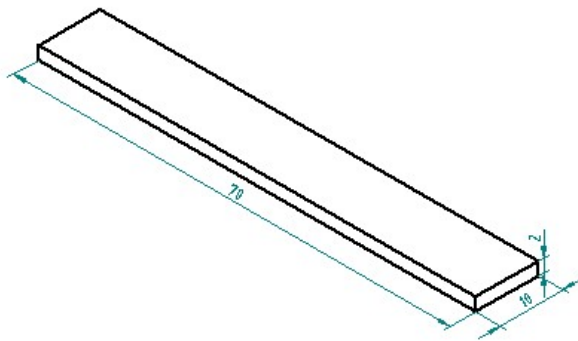


Figure 3.8 Sample of plastic mold steel (70x10x2) used for micro-EDM

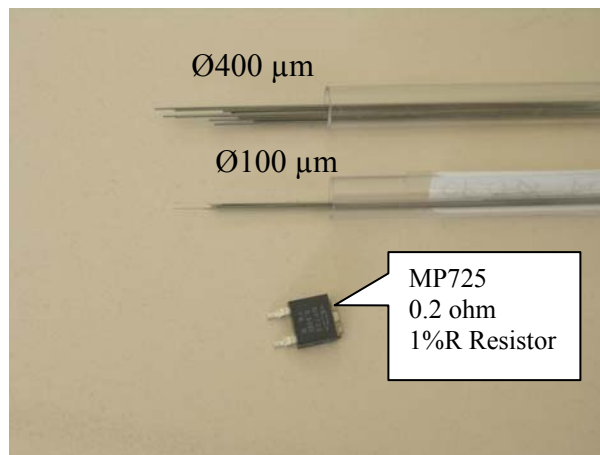


Figure 3.9 Tool electrodes and low resistance resistor

Table 3.1 Tungsten Carbide (WC) Properties:

(http://en.wikipedia.org/wiki/Tungsten_carbide)

Density and phase	: 15.8 g·cm ⁻³ , solid
Solubility in water	: Insoluble
Melting point	: 2870 °C
Boiling point	: 6000°C
Thermal conductivity	: 84.02 W·m ⁻¹ ·K ⁻¹
Tensile strength	: 0.3448 GPa
Mohs hardness	: 9

Table 3.2 Dielectric Oil Characteristics:

Dielectric Oil labeled as HEDMA111 supplied from Sarix company.

Viscosity 20 °C	: 2,4 cSt
Density 15 °C	: 0,781 Kg/l
Point of flammability	: 101 °C
Original smell	: neutral

3.3 Receiving Voltage and Current Pulse Shapes

Capturing voltage and current pulse forms in micro-EDM is very essential since by means of the pulse forms generated during machining many parameters value and type which are decisive in machining qualities are found such as current, pulse-on/off, and discharge type such as arc, and short circuits. Low inductance 0.2 ohm 1%R MP725 resistor (Figure 3.9) is connected to discharge circuit as shown in Figure 3.1 and Figure 3.3. By using this resistor current value during electrical discharge will be discovered. An Agilent 54621D mixed signal oscilloscope with a value of 60MHz and 200 MSa/sec as shown in Figure 3.10 is used to display the shape of voltage and current pulse forms and also their numerical values. A connection will be installed between oscilloscope and computer by using Agilent GPIB connection card to transfer the oscilloscope data into

the computer environment. An Agilent sample Excel data acquisition macro program is used to get a number of voltage data from the captured pulse forms.

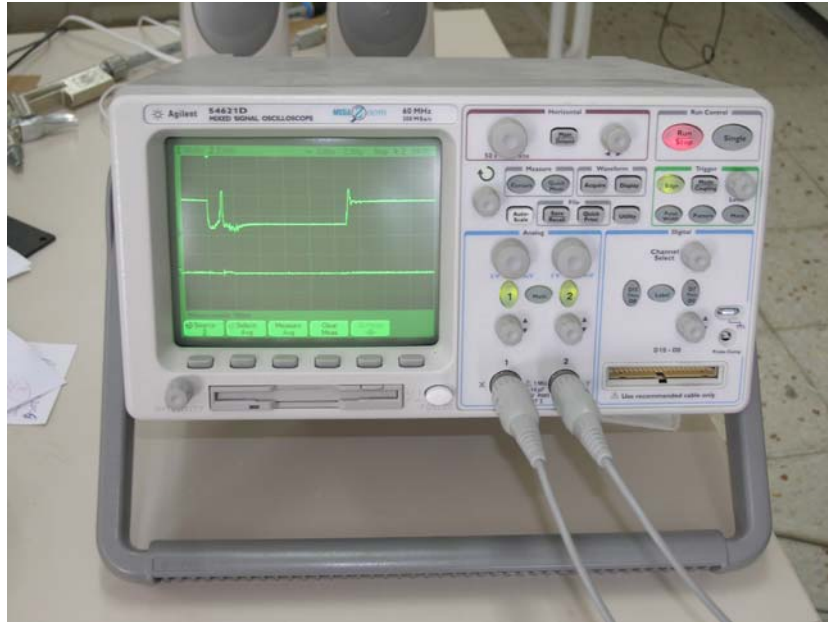


Figure 3.10 Agilent 54621D Mixed Signal Oscilloscope 60MHz/ 200Msa/sec

3.4 Taking Cross-Section of Micro-Holes

An attempt is made to observe the cross-sectional view of machined holes by using micro-EDM. This is a very beneficial work to have a knowledge about the hole shape geometry along the holes tubular section. We realized its importance especially when the cross-sectional view of the machined holes are taken accurately since considerably important defects are observed on the shape of hole geometry. The procedures for taking cross-section of machined holes are stated explicitly in following section.

The plastic mold steel plate is cut to the smaller specimen parts to observe the shape of the geometry of micro holes cross-section. Buehler precision isomet low speed saw as shown in Figure 3.11, settled in Zonguldak Karaelmas University is used to cut the specimen from the steel plate. It has a blade disc with a thickness of 0.4 mm that enables to cut the material with a little or no deformation. The blade disc is placed on the steel

plate where the blade disc almost tangential to the hole circumference then at this point plate will be cut and turns into the small specimen including generally three holes.

After cutting the specimen, the coming process is mounting. The aim of the mounting process is to handle the small and odd shaped specimens for next grinding and polishing process. For this purpose, an automatic hot mounting press (Metapress-A) as shown in Figure 3.12 is purchased from Metkon Instruments Ltd.

After mounting the specimen, the next process is the grinding and polishing. The aim of this process is to obtain highly reflective surface which is free from scratches and deformations. FORCIPOL-1 grinding and polishing machine together with FORCIMAT automatic head as shown in Figure 3.13, settled in Zonguldak Karaelmas University, is used to get a good surface for microscopic analysis. Afterwards applying the all the processes mentioned above, the specimen (Figure 3.14) will be ready for the hole cross-section shape observation by using microscopes. An overall picture of used metallographic machines is shown in Figure 3.15.



Figure 3.11 Buehler precision isomet low speed saw



Figure 3.12 Automatic hot mounting press



Figure 3.13 Grinding and polishing machine

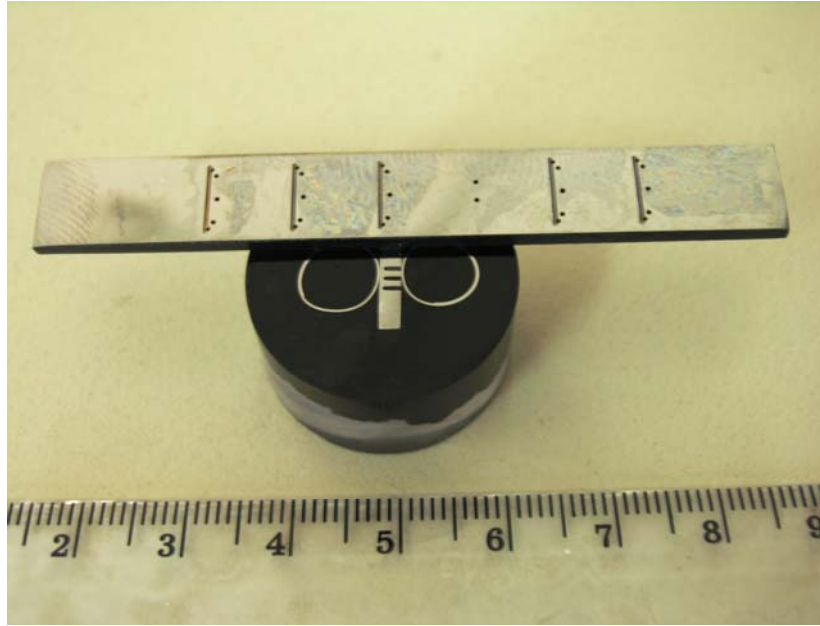


Figure 3.14 A sample of specimen



Figure 3.15 Overall picture of metallographic machines used in specimen preparation

3.5 Use of Microscope and Dimensional Measurement

Machined micro-holes and their cross-sectioned geometry are examined by using Nikon ECLIPSE LV150 optical microscope (Figure 3.16). It has five objectives with a magnification of 50x, 100x, 200x, 500x, 1000x. A 'Nikon digital camera coolpix 8400' (Figure 3.16) installed on the top of microscope is also used to take the pictures of cross-sectional view of micro-holes. The hole pictures taken by camera is sent to the computer and by means of the Clemex image analysis software dimensional measurement will be done.



Figure 3.16 Nikon microscope and digital camera

CHAPTER 4

EXPERIMENTAL RESULTS AND DISCUSSIONS

In this chapter, experimental results of machined micro-holes will be presented. Some electrical and technological parameters such as current, energy, pulse width, and frequency which are undisclosed in Sarix micro-EDM machine will be defined and their influences on machined surface will be explained depending on experimental results.

Formation of micro-holes geometry under different machining conditions is observed. Technological parameters which play an important role in determination of micro-hole geometry are investigated experimentally. Through holes and mostly blind holes are machined within the context of thesis. In through hole drilling, entrance and exit diameter variations are examined, in blind hole drilling, entrance diameter and fore end of holes are examined and the way is recommended to provide the parallelism in hole wall-side. The cross-sectional views of the holes demonstrate how the defects are formed inside the hole and they are not observed without taking cross-sectioned view. Preventive and predictive technological techniques for minimizing defects formation in hole geometry are also explained.

Achievable aspect ratios of holes under the specified machining conditions will be investigated and presented. In addition, material removal rate and tool electrode wear rate will be investigated and explained with the experimental facts. Based on the experimental results and machine technology, repeatability and accuracy of machined parts will be discussed. Throughout the experiments workpiece material, tool electrode material and dielectric liquid remain same to enable identical experimental conditions.

4.1 Hole Machining Considering Energy Parameter

A series of experiments were performed to estimate the undisclosed parameters defined in the micro-EDM machine. Those parameters only entered as a setting without a unit, which are energy and current. Although discharge energy depends on voltage and current disregarding less significant parameters, it is given in the machine settings as a type of pulse shapes and it enables to the machine discharge energy limitation. The current defined in the machine settings also carry the approximate meaning like in the energy.

To observe the influences of energy parameter in micro-EDM, a series of hole machining were performed by keeping all parameters constant except energy. Machining conditions are given in Table 4.1. Energy type will determine the shape of the discharge pulse and it is classified into six different ranges. Description of energy levels is given in Table 4.2.

In this part of the experiment, variations in hole geometry, material removal rate (workpiece and electrode), hole depth, overcut in hole diameter are investigated. This investigation reveal the effect of energy parameter on the hole machining. The voltage and current in micro-hole machining is monitored and recorded. The monitoring technique can assist in the selection and optimization of micro-hole EDM process parameters.

Shape of the pulse forms with different energy parameters are given in Figure 4.1 to Figure 4.6. Selection of lower value of energy parameter results in the lower value of discharge time and discharge current. As it shown in Figure 4.1 peak current value approximately rises to 20 A when the energy parameter set to 350, however, as it shown in Figure 4.6 peak current decreases nearly to 5 A when the energy parameter set to 14. Due to material removal relation to the discharge current, lower the current value results in higher precision in material surface, so that short pulses can be selected for finishing operation. However, long pulses should be selected for fast and rough machining

process. Discharge time (pulse on time) is also longer about 2 μs in long pulse shape when comparing to short pulses of less than 200 ns. When the short pulses are considered, shapes of the pulses are not recorded properly due to insufficient sampling rate of the oscilloscope. An advanced data acquisition device should be used to record and to keep the very short pulse shape in more reliable range.

Table 4.1 Machining conditions for varying energy parameter

Machining time	: 20 minute
Frequency	: 100 kHz
Width	: 4 μs
Open Voltage	: 80 V
Gap Voltage	: 75 V
Gain	: 10
Regulation*	: 00-00
Retraction time and length*	: 2 ms-0.2 mm
Temp. of dielectric liquid*	: $\sim 20^\circ\text{C}$
Temp. of medium (room) *	: $\sim 25^\circ\text{C}$

* Remain same throughout all experiments in the thesis

Table 4.2 Description of Energy parameters (Sarix operating manual version 1.20)

Energy Parameter	Family Description
From 13 to 15	Very short pulses
From 100 to 114	Short pulses
From 200 to 215	Long braked pulses
From 250 to 265	Long, delayed, beaked pulses
From 300 to 315	Long, delayed pulses
From 350 to 365	Long pulses

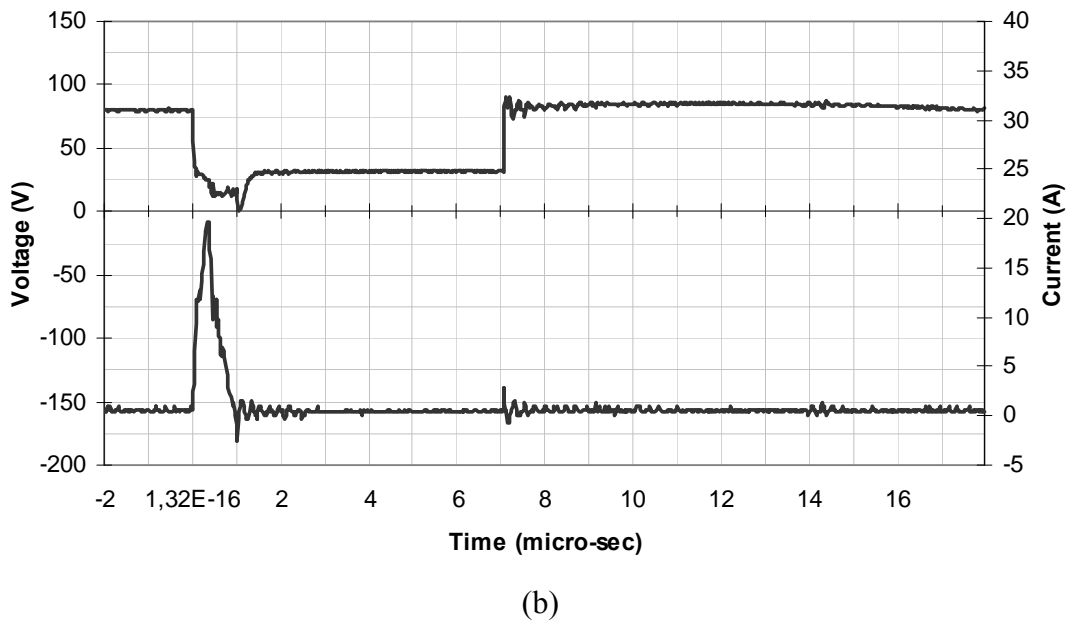
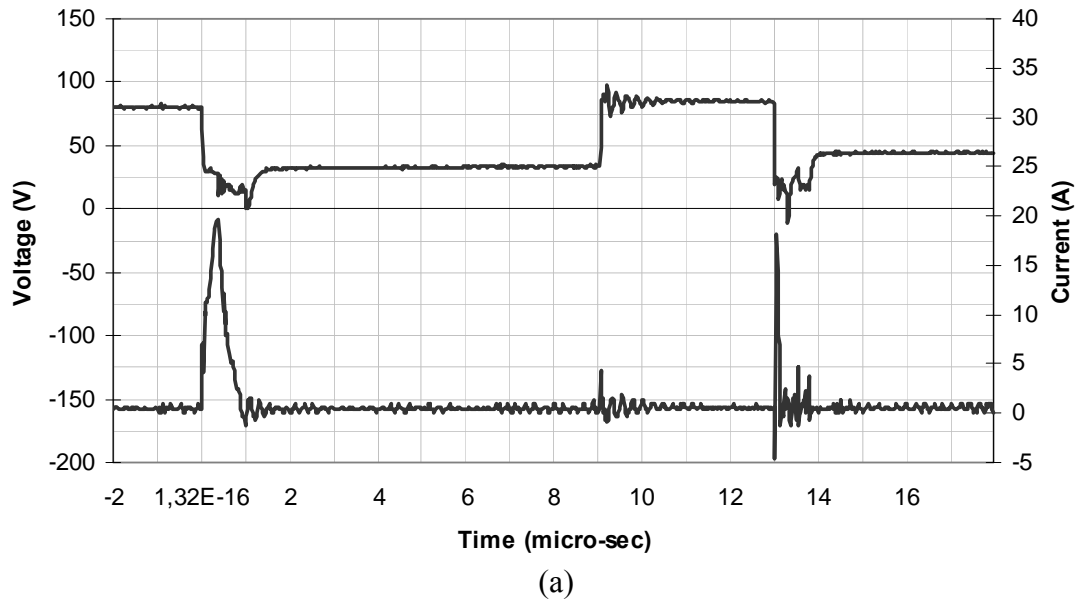
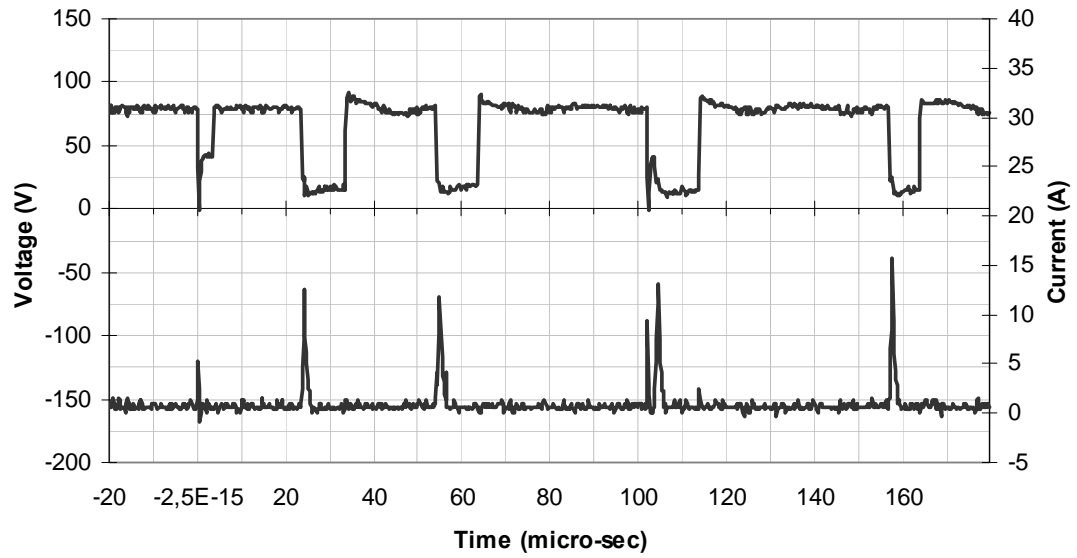
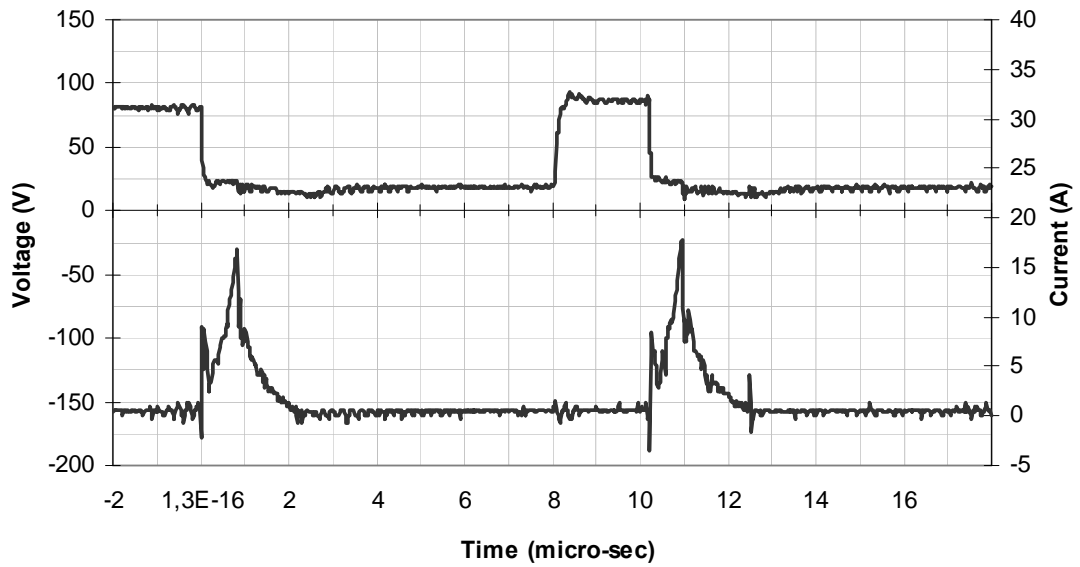


Figure 4.1 Voltage (upper case) and current (lower case) pulse form for energy level of 350 (a) Two pulses (b) One pulse

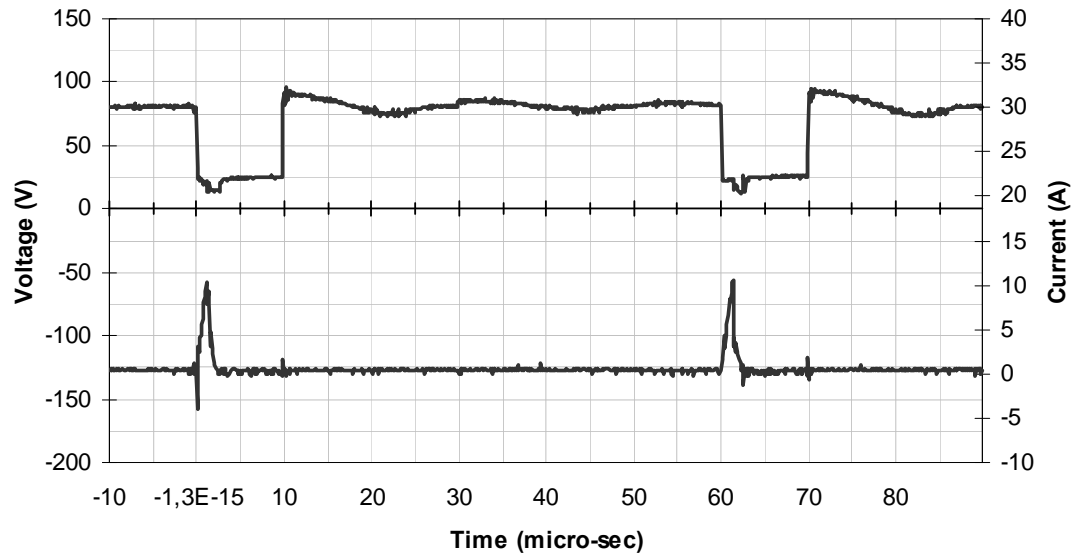


(a)

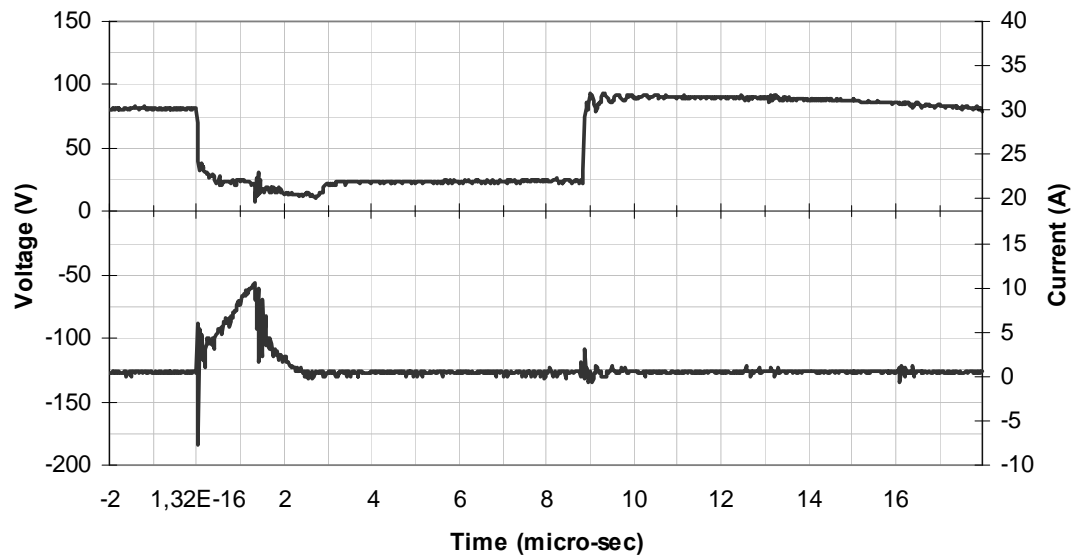


(b)

Figure 4.2 Voltage (upper case) and current (lower case) pulse form for energy level of 305 (a) squashed time scale (b) extended time scale

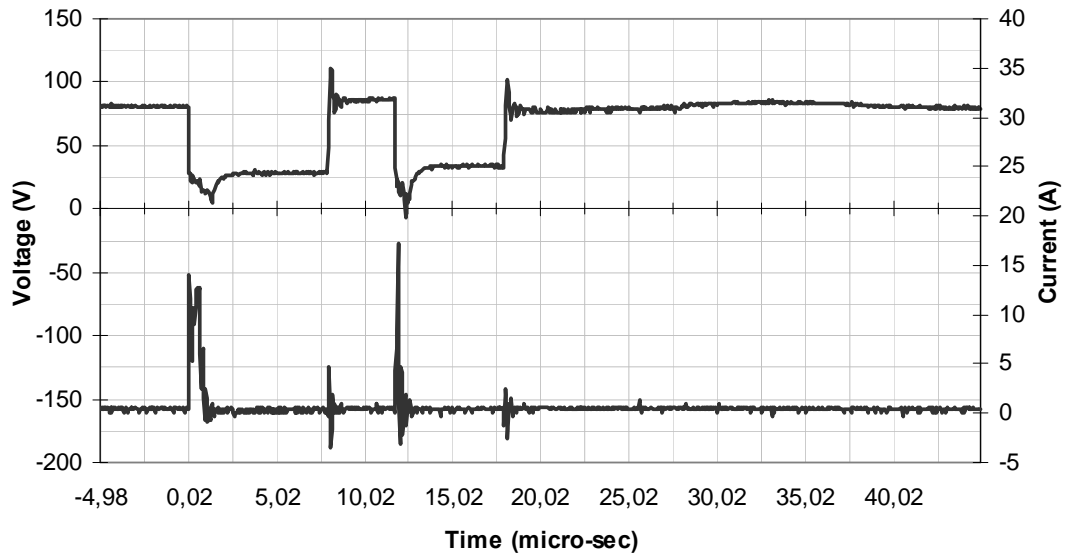


(a)

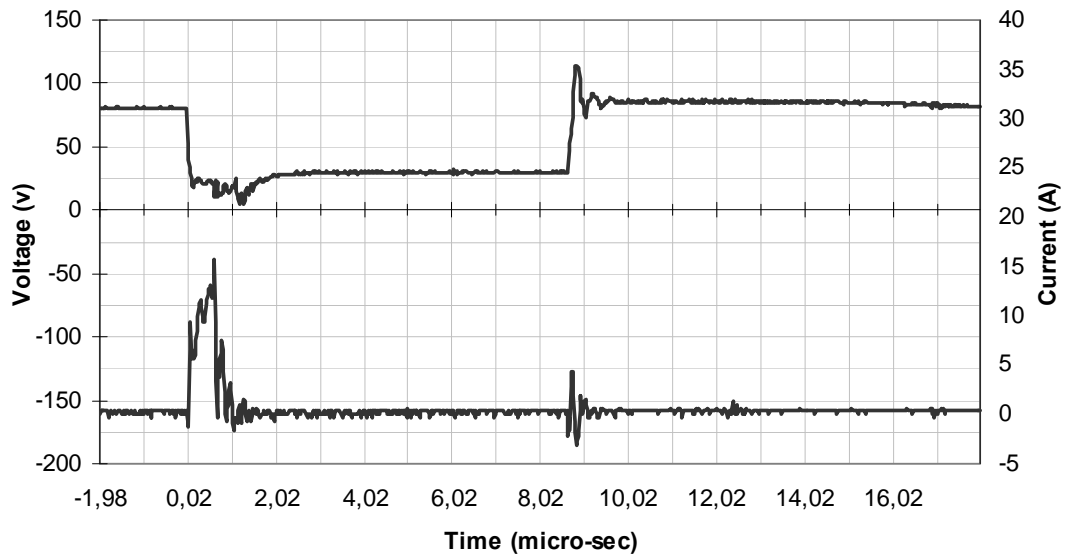


(b)

Figure 4.3 Voltage (upper case) and current (lower case) pulse form for energy level of 250 (a) squashed time scale (b) extended time scale

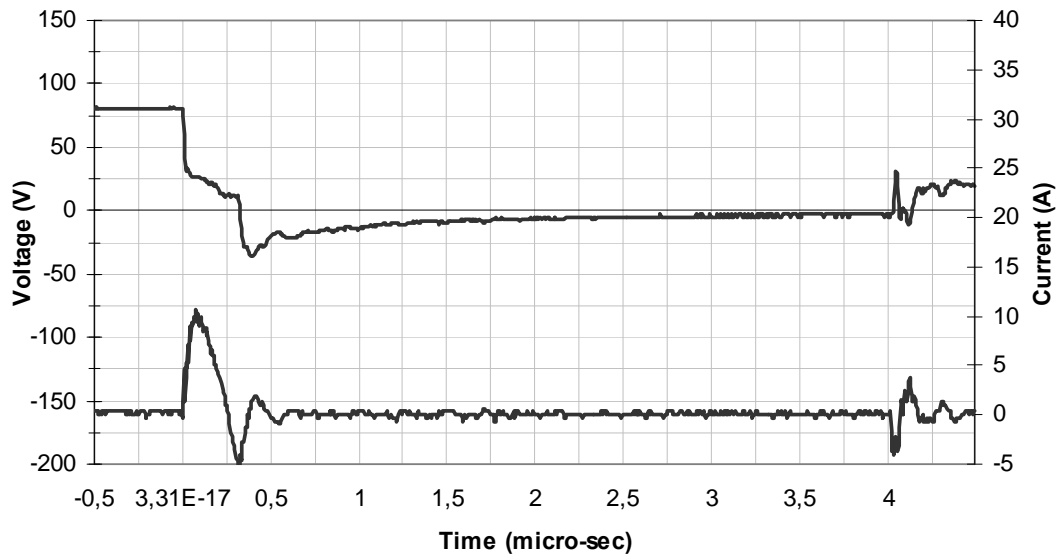


(a)

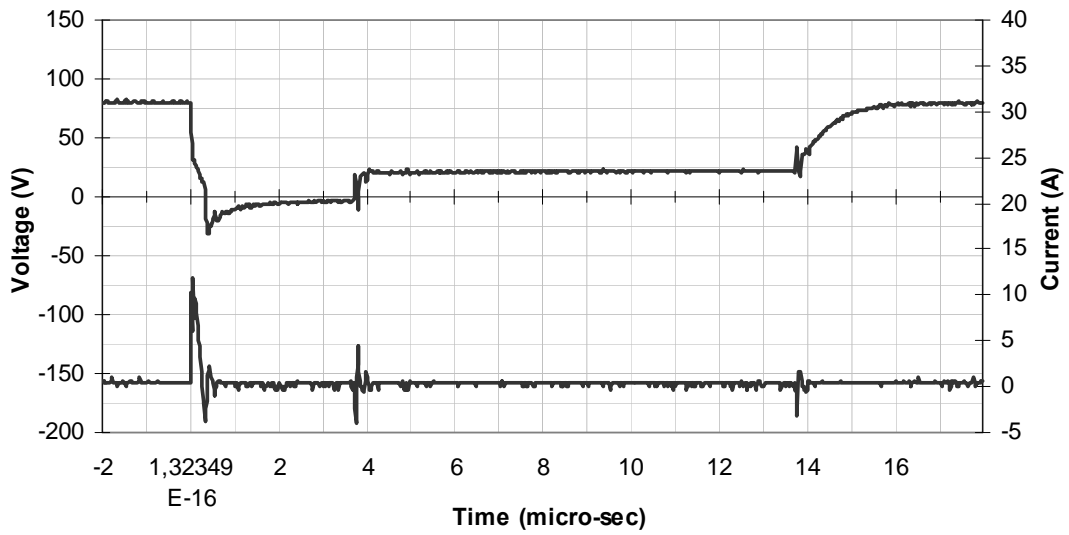


(a)

Figure 4.4 Voltage (upper case) and current (lower case) pulse form for energy level of 205 (a) squashed time scale (b) extended time scale

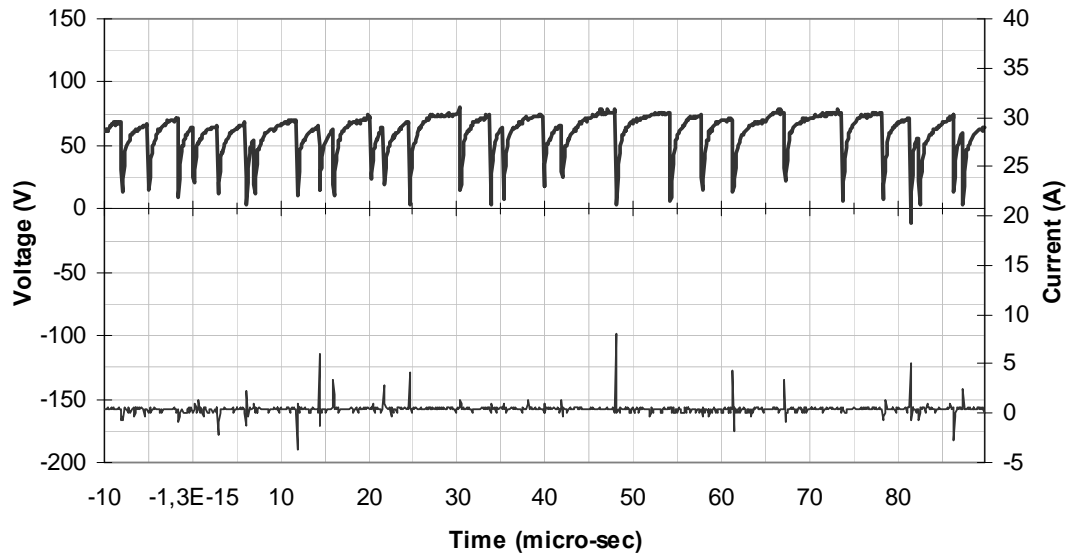


(a)

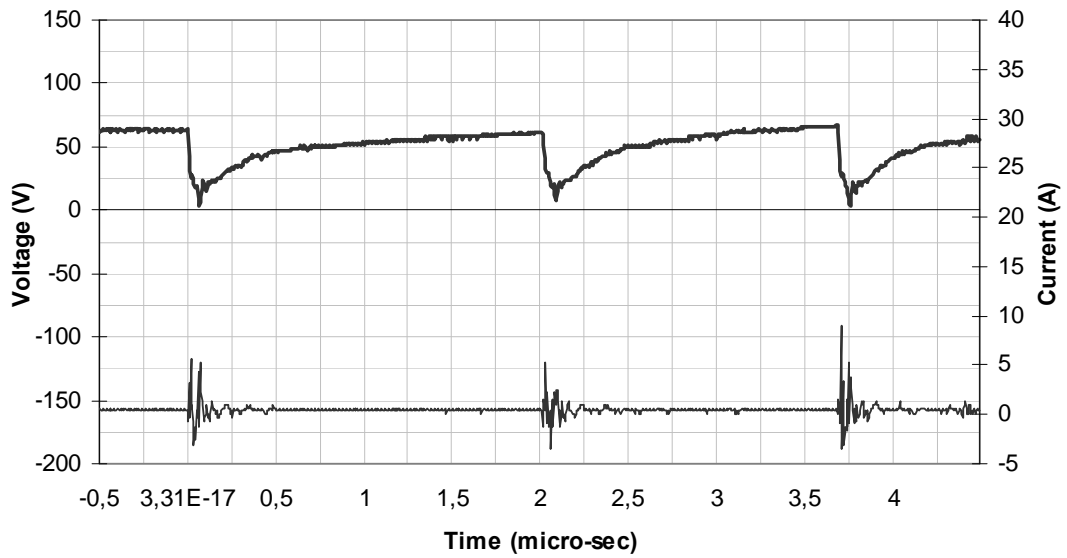


(b)

Figure 4.5 Voltage (upper case) and current (lower case) pulse form for energy level of 114 (a) squashed time scale (b) extended time scale



(a)



(b)

Figure 4.6 Voltage (upper case) and current (lower case) pulse form for energy level of 14 (a) squashed time scale (b) extended time scale

Three micro-holes were machined for each energy parameter to observe the repeatability of the process. Machined micro-hole diameter is always larger than the tool electrode diameter; the difference is varying depending on the machining conditions. Expansion in the hole diameter is called as *overcut*, caused by side spark erosion. Variation in hole diameters, electrode removal, standard deviation (STD) and overcut are tabulated in Table 4.3. According to experimental results, hole expansion (overcut) is slightly increasing when energy parameter is changing from 14 to 350. When energy parameter is set to 14 resulting in overcut of 17.58 μm and setting energy parameter 350 results in 28.5 μm overcut. This difference in overcut is due to the difference in spark intensity. Higher the energy value parameter leads to more intense spark which erodes more particles from the side surface of the micro-hole.

Figure 4.7 depicts the relation among energy parameters, target depth, machined hole depth, and worn electrode length. Target depth can be defined also a depth entered in machine setting that is the sum of the hole depth and worn electrode length. Mean hole diameter and overcut relation to the energy parameter is graphically illustrated in Figure 4.8, this graphic also verify the relations as stated earlier.

Dimensional measurement for hole diameter and machined length of hole may sometimes not consistent with the diameter of other holes machined by the similar settings. Hole diameter may be sometimes measured larger than the actual one. This inconsistency in the measurement is caused by the measurement devices and software used in the microscopic system, focusing problems arouse while magnified pictures are taken and image processing error are observed while measuring dimensions by using clemex image analysis software. Diameter of machined hole (Figure 4.9) and magnified edge for each hole (Figure 4.10) are given to analyze the geometrical shape and edge surface roughness based on the corresponding energy parameter.

Cross-sectional view of the machined holes (Figure 4.11) are analyzed in terms of the geometrical shape and parallelism of the hole wall side. According to the cross-sectional view, an almost good shape can be obtained by using the entire machining conditions.

One point in the cross-sectional view may draw attention about inconsistent cross-sectional dimension along the hole radial axis that is induced by difficulty during sectioning process. Because of the very small size grinding and polishing process, it is difficult to control whether to reach the center of the machined hole, sometimes due to over grinding or insufficient grinding process; the approximate central cross-section is taken and analyzed. Actually, disregarding the dimensional measurement, the error during sectioning process is not substantially affecting the overall geometrical shape of the machined holes.

Table 4.3 Hole diameter variation with energy type

Energy	Target depth	Removed Electrode Length	Hole depth	Hole diameter	Mean diameter	STD for H. diameter	Average overcut
14	180	31	150	447	435	10.91	17.58
	165	31	130	427			
	155	25	130	430			
105	843	161	682	438	437	10.07	18.3
	858	168	690	426			
	850	157	693	446			
114	897	237	660	435	433	2.65	16.1
	880	230	650	433			
	870	224	650	429			
205	2720	1150	1570	457	452	9.34	26
	2720	1140	1580	458			
	2820	1180	1640	441			
250	2910	1650	1260	461	448	12.33	23.5
	3060	1780	1280	443			
	3150	1790	1340	437			
305	3400	1660	1740	451	449	2.78	25
	3480	1720	1760	451			
	3460	1710	1750	446			
350	3400	1460	1940	457	457	6.71	28.5
	3380	1430	1950	464			
	3250	1400	1850	451			

* Dimensions are in μm

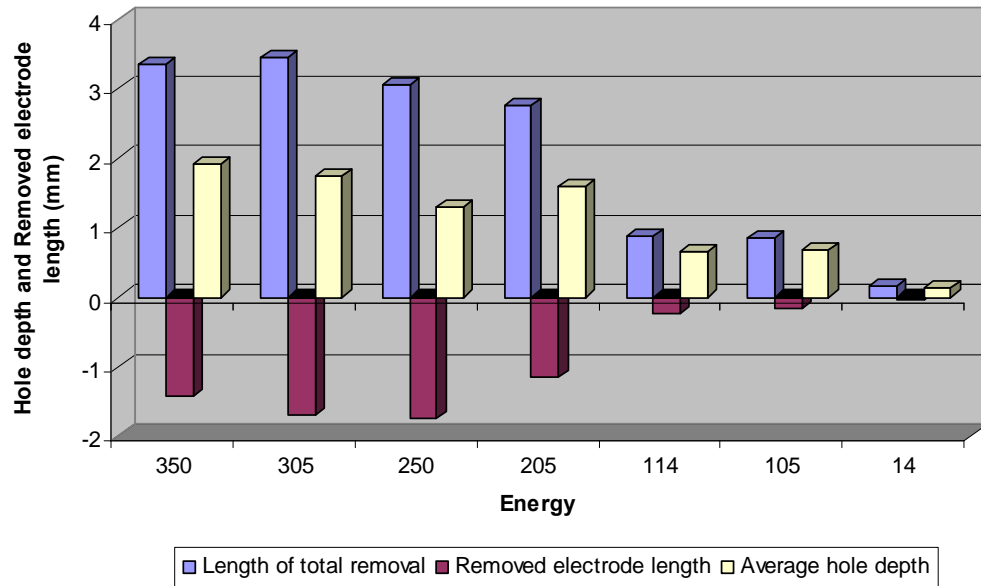


Figure 4.7 Target hole depth and removed electrode length with energy parameter

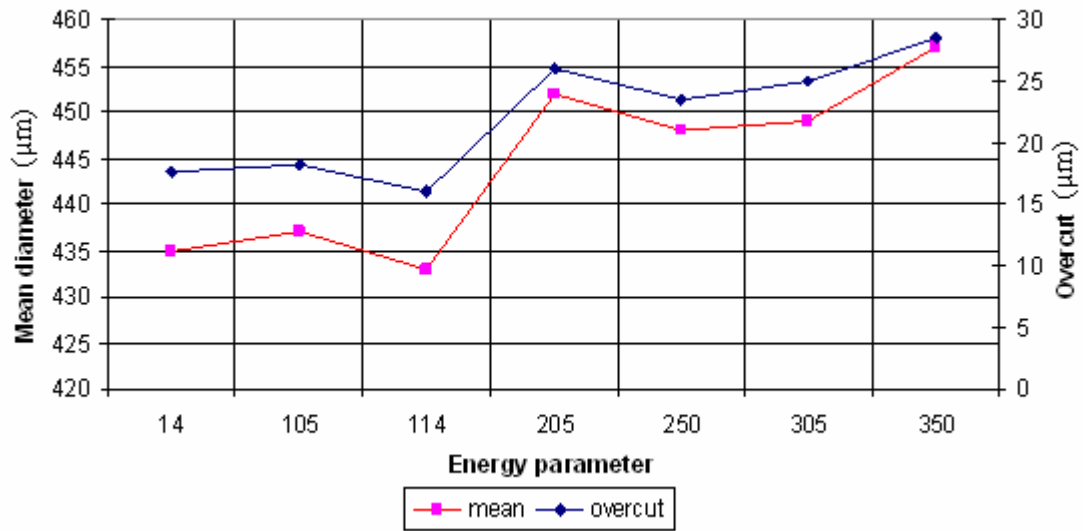


Figure 4.8 Mean hole diameter and overcut versus energy parameter

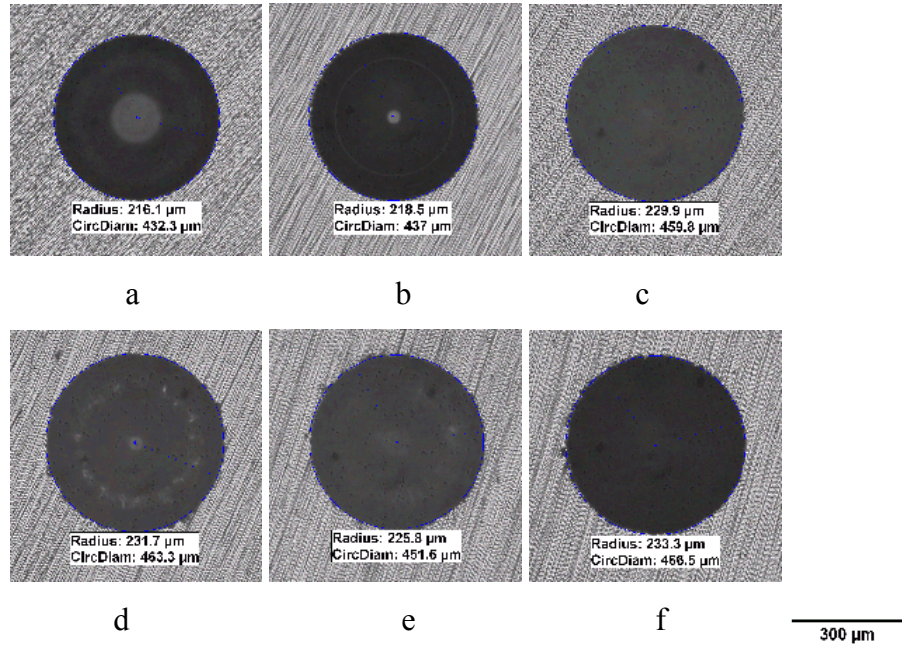


Figure 4.9 Micro hole diameter measurement from top view, diameter measurement shown on the micro-hole photographs sequenced regarding with the energy level.

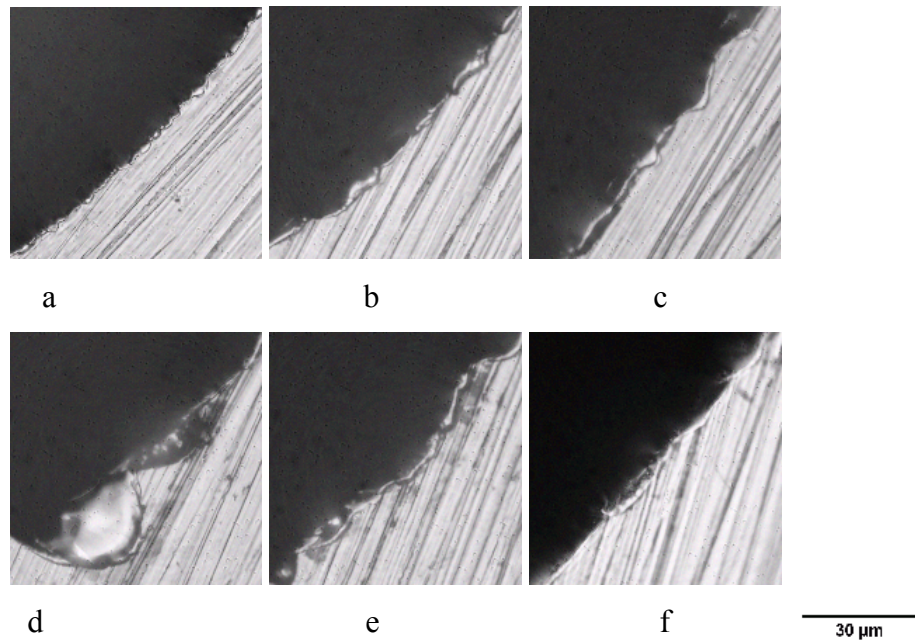


Figure 4.10 Micro-hole wall edge photographs with X1000 magnification with respect to energy level.

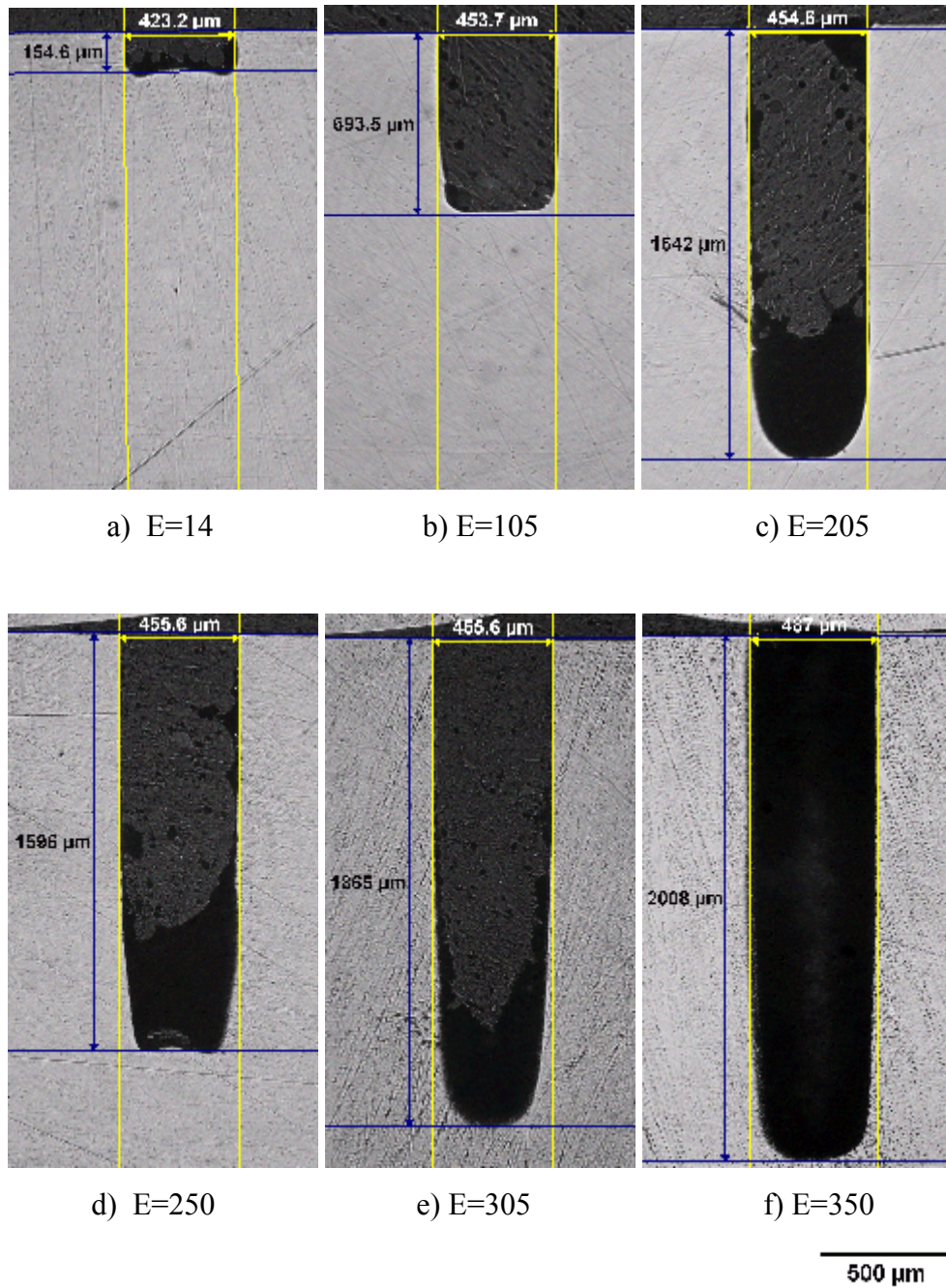


Figure 4.11 Cross-sectional photographs of micro-holes machined with different energy level.

4.2 Hole Properties Versus Machining Time

These experiments are carried out to observe and understand the formation of micro hole geometry under the constant micro-EDM parameters except machining time (Table 4.4). Increasing the machining time gradually from 1 minute to 80 minutes enable us to understand variation in hole geometry. It is understood that the variation in hole geometry occur both in hole diameter, there is an expansion due to *overcut* caused by side spark erosion, and in cross sectional geometry along the depth of hole. Towards the bottom end of the holes, narrower section is formed because it is the mirrored shape of the tool electrode. The end tip of the tool electrode is burned and gets the conic shape which is caused by electric discharge intensity. Electric discharge intensity is higher at the cornered and edge of the tool electrode. Because of this reason, the edge and corner of the tool electrode is worn more than the side and smooth surface of the tool electrode.

Table 4.4 Machining parameters for varying machining time

Width	: 4 μ s
Frequency	: 100 kHz
Current	: 60
Voltage	: 80 V
Gap voltage	: 75 V
Gain	: 10
Energy	: 105

In this experiment, 42 holes are machined, each of them is machined for different time duration which is increased gradually, to illustrate depth of holes and compare the material and electrode removal rate. Total length including hole depth and electrode removal is almost linearly increasing with the increasing machining time. The relation is depicted in Figure 4.12.

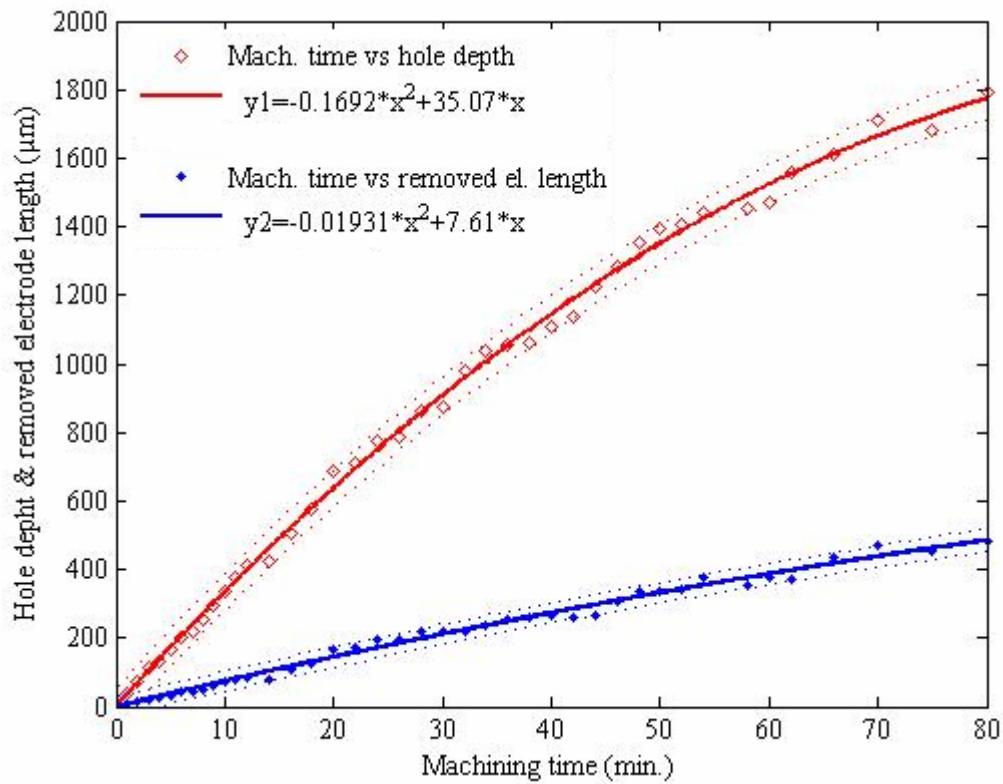


Figure 4.12 Machined hole depth and electrode removal versus machining time.

In contrast to hole depth versus machining time, hole diameter is not steadily increasing with the increasing machining time. In order to relate machining time and expanded hole diameter logically, a 20 µm-band-width is defined and observed the hole diameter increases in a 20 µm band-width with increasing machining time as shown in Figure 4.13. During the size measurement the error as explained in the previous section leads to measure the hole diameter bigger or smaller than the actual value.

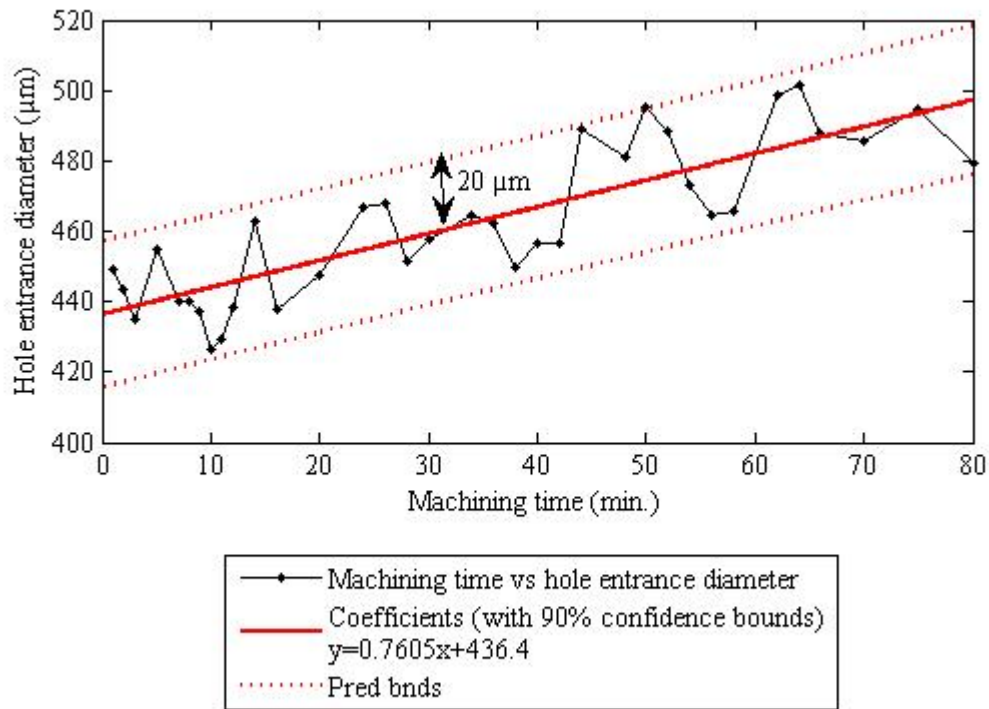
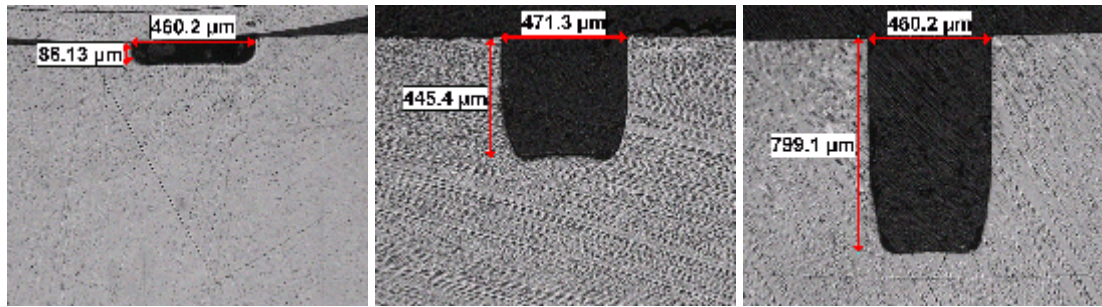


Figure 4.13 Relation between hole entrance diameter and machining time.

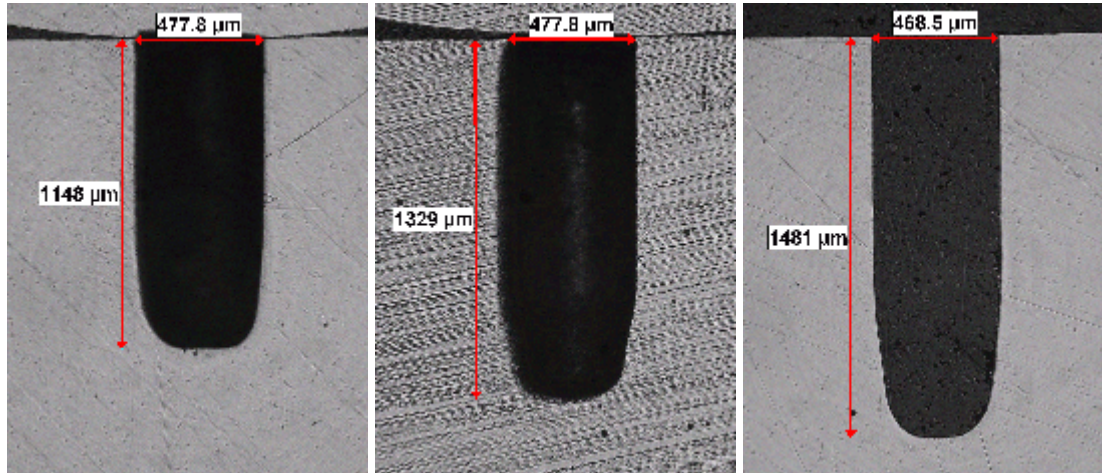
In this section of experiment with machining time from 1 min to 80 min, nine different end tip shape of hole are observed as shown in Figure 4.14. Those are selected among 42 cross-sectional views of holes; the remaining parts are illustrated in Appendix A. Having different end tip shape result from the different machining time of 2, 14, 24, 40, 46, 54, 60, 70, and 80 min. with the corresponding hole shape in Figure 4.14, respectively. The other holes having machining time around the selected values have mostly the same tip shape. The most noticeable tip shape is around the 40 min-machined hole tip, it has slightly narrower length of tip according to the former and latter machined hole tip, smoothly narrowed tip around the 24 min machining time will vanish when machining time approaches to the around 40 min., so that it can enable to the hole having very straight wall side.



a) 2 min.

b) 14 min.

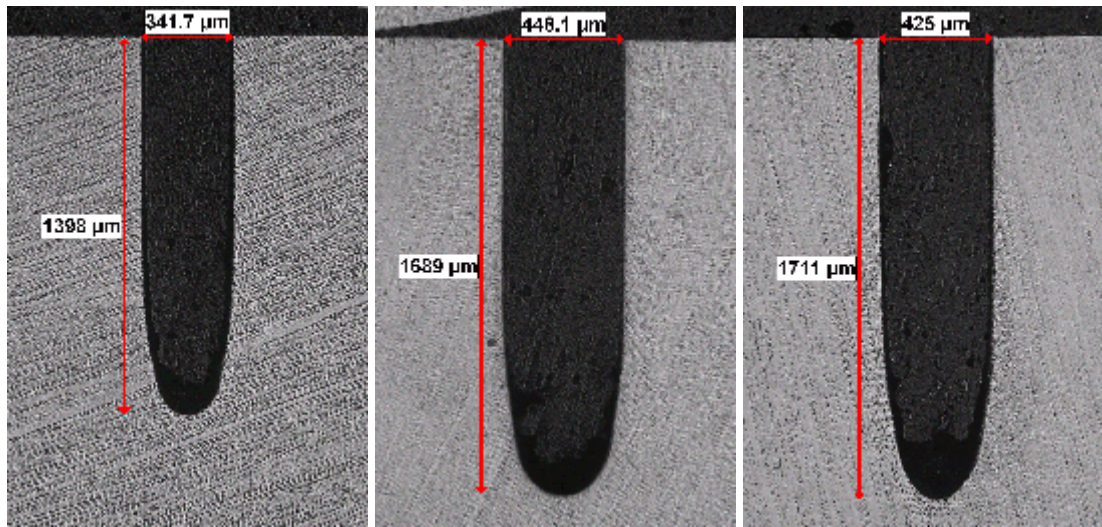
c) 24 min.



d) 40 min.

e) 46 min.

f) 54 min.



g) 60 min.

h) 70 min.

i) 80 min

400 μm

Figure 4.14 Cross-sectional geometry of micro holes with varying machining time.

Actual hole depth and diameter are measured and analyzed by using commercially available clemex image analyses software. A sample of measured picture for 24 min-machined hole is depicted in Figure 4.15. In addition to the whole picture of machined hole, the end tip shape for the specified hole is also illustrated in Figure 4.16 to contribute the understanding of machining time effect on the hole tip formation easily.

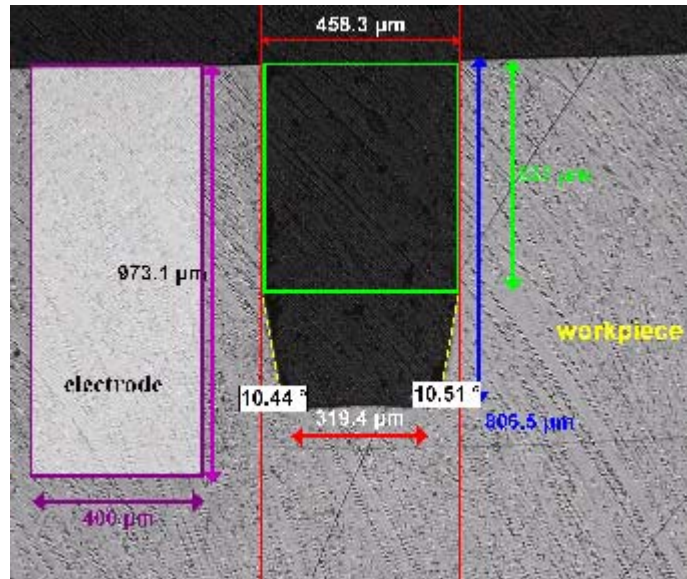


Figure 4.15 A sample of geometrical shape analysis for 24min-machined hole.

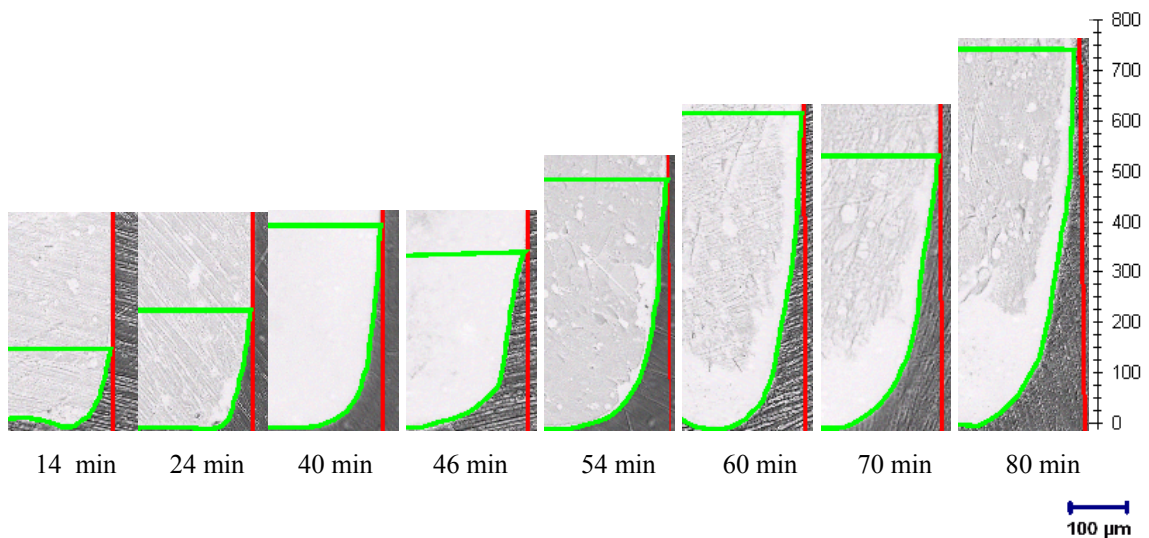


Figure 4.16 End tip shape variation of hole with increasing machining time

A hole wall side straightness can be described by eliminating the hole end as a useless part where the diameter equals to entrance diameter with %5 reduction. The straightness and parallelism of hole wall side is not distorted with the 5% diameter reduction, actually this point is observed as from where the narrower shape tip starts.

Figure 4.17 shows the total depth and useless part depth of the holes with a scale placed to the right side of the picture. A ratio between the total depth and useless part depth is calculated and necessary data are given in Table 4.5, hence, calculated ratio (total hole length / useless part length) result in a graphic as shown in Figure 4.18. As is understood from the graphic, the two end points which are machining time of 80 min and 10 min are distinguished from the others. Although in the middle points the ratio is nearly kept stable with a little change, in the end points, the ratio is increasing and decreasing for the machining time of 10 min and 80 min., respectively.

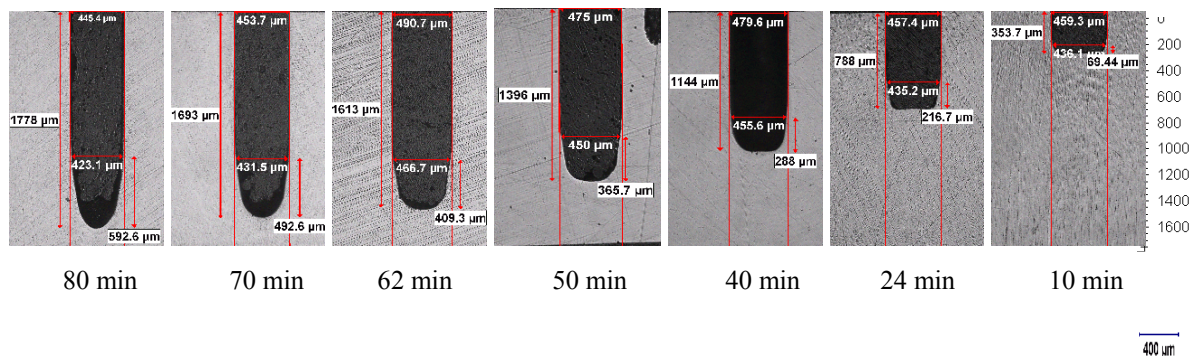


Figure 4.17 Measurement of 5% reduction of entrance diameter.

Table 4.5 Machined hole data for hole wall-side straightness calculation

Mach. time (min.)	Total length (μm)	Useless part length (μm)	Entrance diameter (μm)	5% reduced diameter (μm)	Total length / useless length (μm)
10	353,7	69,44	459,4	436,1	5,09
24	788	216,7	457,4	435,2	3,64
40	1144	288	479,6	455,6	3,97
50	1396	365,7	475	450	3,82
62	1613	409,3	490,7	466,7	3,94
70	1693	492,6	453,7	431,5	3,44
80	1778	592,6	445,4	423,1	3,00

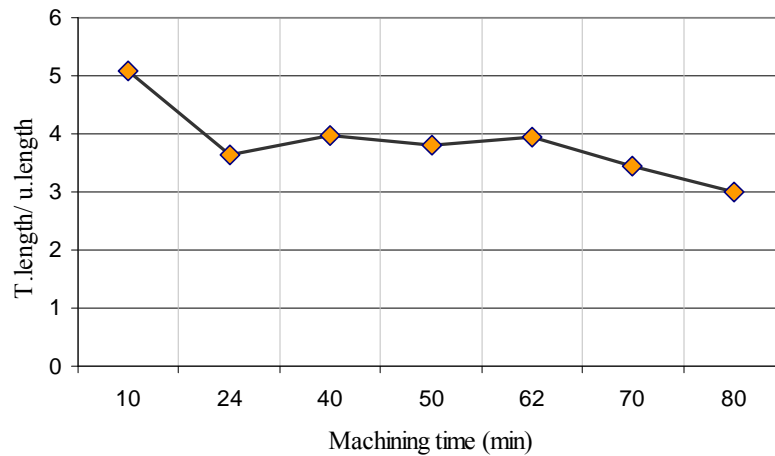


Figure 4.18 Graphical representation of machining time versus T.length/ u.length ratio

4.3 Hole Machining by Varying Width and Frequency

To understand the influence of width and frequency parameter in micro-EDM process, a series of holes are machined by keeping machining time constant at 20 min. In EDM process, pulse on/off time has a significant role in the determination of machining characteristics, but it is not defined directly in Sarix micro-EDM machine. In the

machine, time width and frequency are inserted instead of pulse on/off time. In fact the time width (t_{on}) is the period of time while the generator is activated to generate power and transferred to the electrode (Figure 4.19). Actually it is obviously explained by maintaining all the other parameters constant, the higher the ratio between t_{on} and $1/f$ (duty cycle), the higher the number of pulses probably discharged. However, it is slightly different depending on dominantly the type of energy and other parameters as stated in the Sarix SX-100 micro-EDM machine operating manual. Machining parameters for varying width are in given in Table 4.6.

Table 4.6 Machining parameters for varying width and frequency

Frequency	: 100 kHz
Open voltage	: 80V
Gap voltage	: 75 V
Current	: 60
Energy	: 105

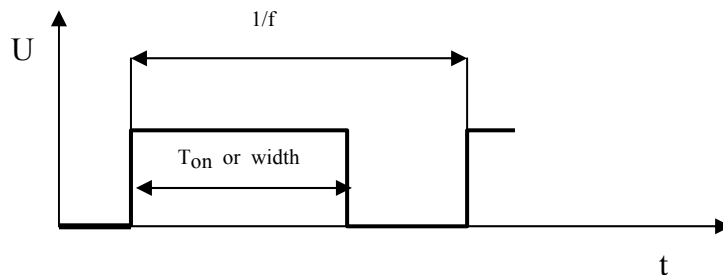


Figure 4.19 The signal that generates the pulses

Cross-sectional views of the machined holes with different width settings of 0.1, 0.5, 1, 4, 6, 8 μ s are illustrated in Figure 4.20. Holes pictures from top view are given in Appendix B. Higher the time width results in higher hole depth. Machining results are tabulated in Table 4.7 and illustrated in Figure 4.21 and Figure 4.22. Shape of the pulse forms according to the adjusted width parameter are also recorded and demonstrated in Figure 4.23. The influence of width is observed obviously when the very small width

and large width differences are compared with each other, however, pulse shape difference in very close width value is not observed easily but its effect can be seen easily on the machined hole with increasing hole depth.

Another important parameter is the frequency value; actually it has inversely the same effect on the machined part. Frequency value determine the period of time in which include summation of the pulse power generator off and on time. It should be set carefully to avoid from inconsistency during machining, frequency value must always greater than the width time. Influence of the frequency is depicted by illustrating the machined hole cross-sectional view with the different frequency values in Figure 4.24 and hole picture from top view are given in Appendix C.

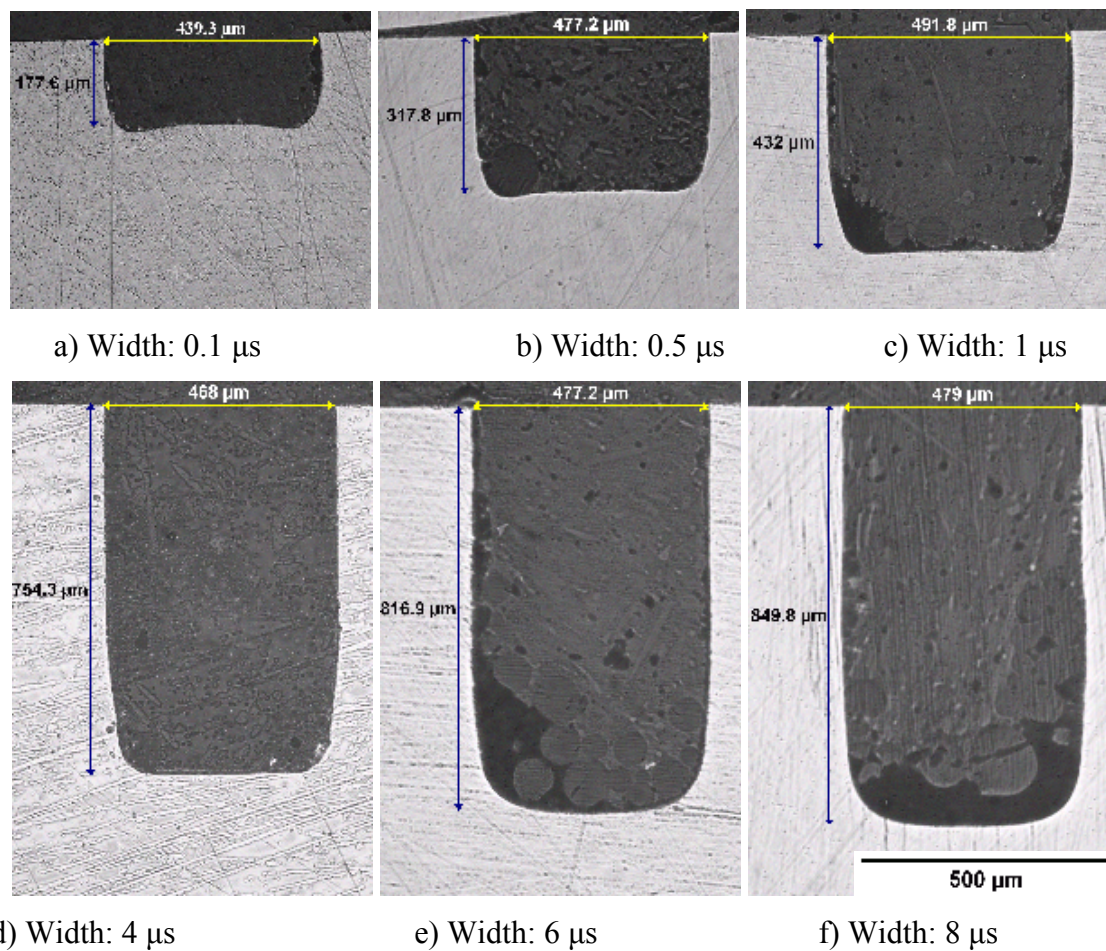


Figure 4.20 Cross-sectional views of machined holes with variant width

Table 4.7 Machining results with variant width.

Width (μs)	Target Hole Depth (mm)	El. Removal (mm)	Av. Target Hole Depth (mm)	Average El. Removal (mm)	Max. Diff. Btw. Hole depth (mm)
0.1	0.195	0.031	0.205	0.029	0.0173
	0.209	0.035			
	0.212	0.022			
0.5	0.358	0.068	0.343	0.068	0.0305
	0.327	0.067			
	0.345	0.068			
1	0.504	0.104	0.517	0.107	0.0262
	0.517	0.106			
	0.53	0.110			
2	0.656	0.120	0.682	0.131	0.0661
	0.666	0.132			
	0.723	0.140			
4	0.824	0.159	0.847	0.166	0.036
	0.858	0.168			
	0.86	0.170			
6	0.916	0.184	0.929	0.191	0.0236
	0.929	0.195			
	0.94	0.194			
8	0.954	0.191	0.989	0.204	0.0638
	0.995	0.201			
	1.018	0.219			

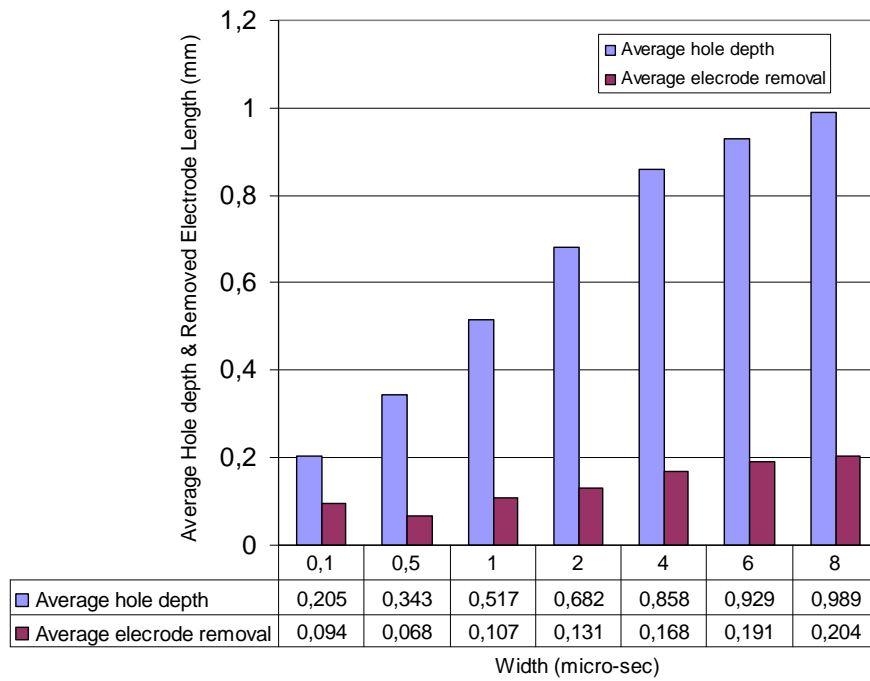


Figure 4.21 Block diagram representation of average target hole depth and electrode removal by variant width value.

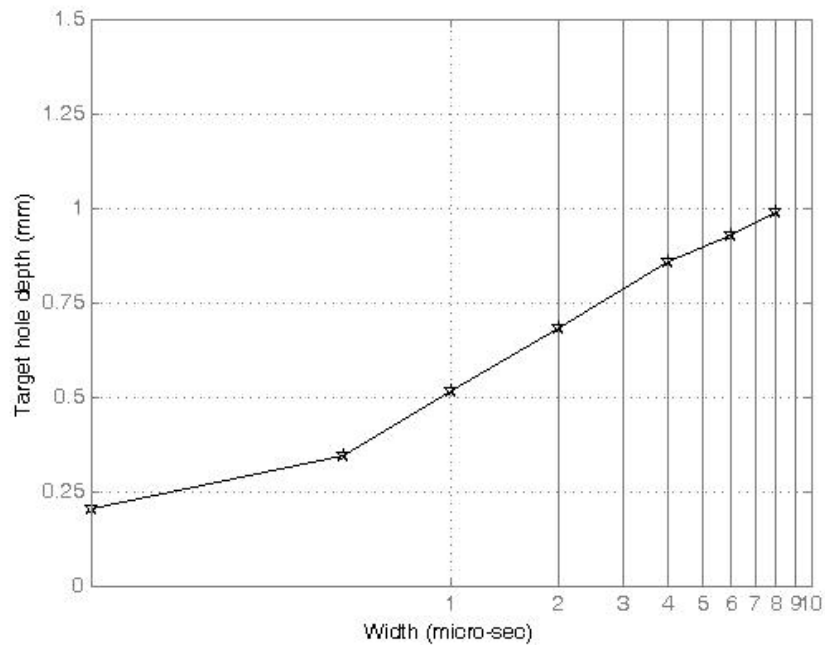


Figure 4.22 Graphical representation of target hole depth versus width

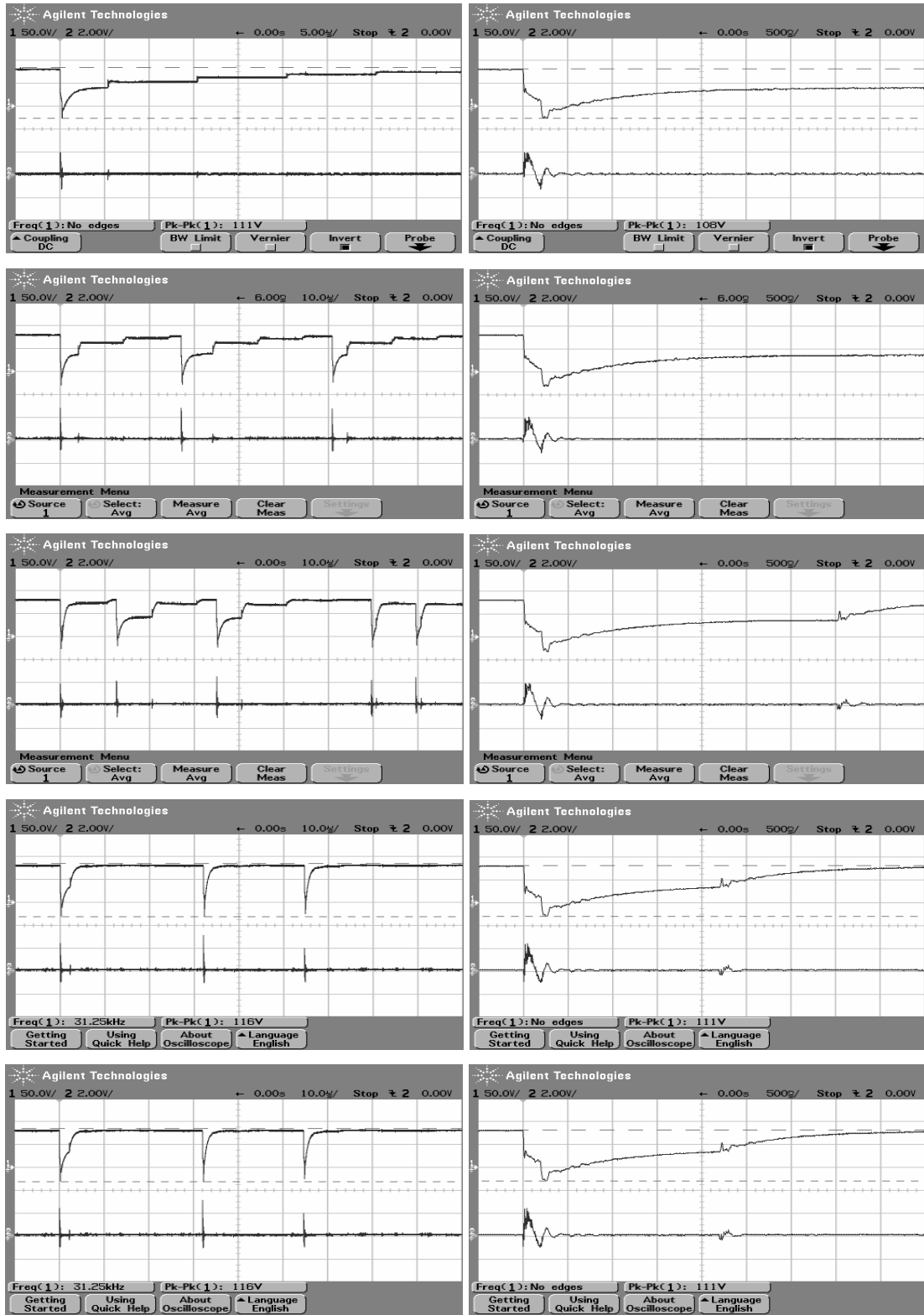
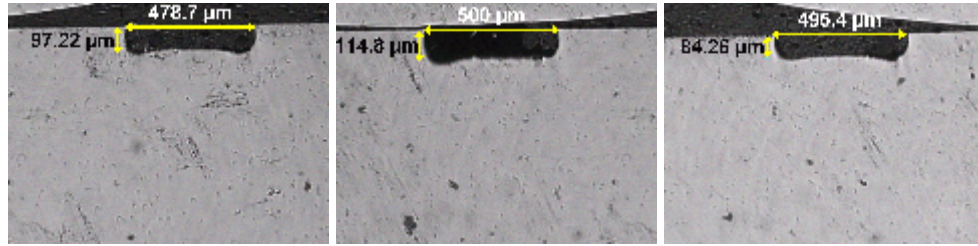
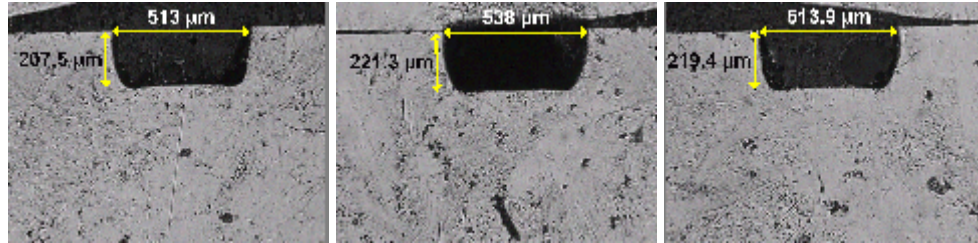


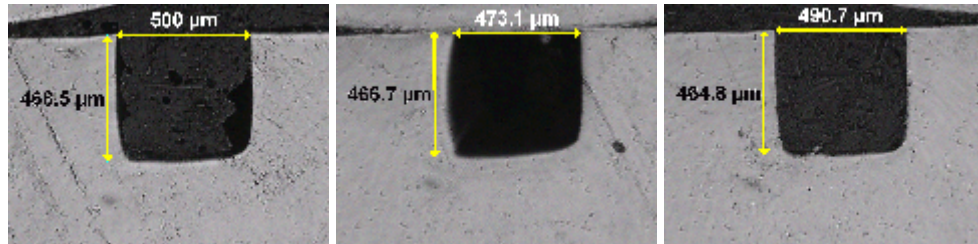
Figure 4.23 Shapes of the pulse form for different time width of 0.1, 0.5, 1, 6, 8 μ s for the each row from top to bottom, respectively.



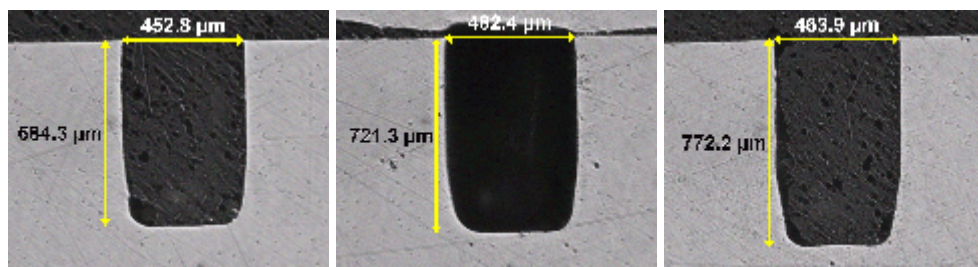
a) Machining frequency: 10 kHz



b) Machining frequency: 25 kHz



c) Machining frequency: 50 kHz



d) Machining frequency: 100 kHz



Figure 4.24 Variation in micro hole geometry with varying frequency values.

Each micro hole is machined three times to verify machining accuracy and repeatability, hence, a, b, c, and d show machined micro hole geometry with machining

frequency of 10 kHz, 25 kHz, 50 kHz, and 100 kHz respectively. Machined holes pictures from the top view are illustrated in Appendix B.

4.4 Hole Machining by Varying Open Voltage and Gap Voltage

Effects of open voltage and gap voltage on the shape of holes are investigated. In the first case, gradually increasing open voltage by keeping gap voltage constant at 50 V with machining time of 40 min. is used as an experimental condition. Holes machined by setting open voltage at 55V, 60V, 70 V, 80V, and 90V are depicted in Figure 4.25, respectively. Holes picture from top view and pulse shapes are also given in Appendix D. The most remarkable point observed in the cross-sectional view of holes is the notch formation at the end of the hole. The concluded remarks from the cross-sectional view of the holes are stated below;

- Effect of gap voltage and open voltage is obvious, bottom end of the hole are shaped as in the Figure 4.25 when the open voltage values as written in the related pictures and gap voltage remain constant at 50 V.
- Depth of micro-hole is increasing with increasing open voltage.
- The inner fraction in the tip of micro hole is increasing gradually to 70 V after this value this part is melt away.

As seen in Figure 4.25 the diameter of micro-holes are not consistent with the cross-sectional view. The reason is that the diameter of micro hole is enlarged after very small depth under micro-hole surface. But this depth is not seen in cross section view since during the formation process of bakelite; it undergoes to high pressure then probably vanishes.

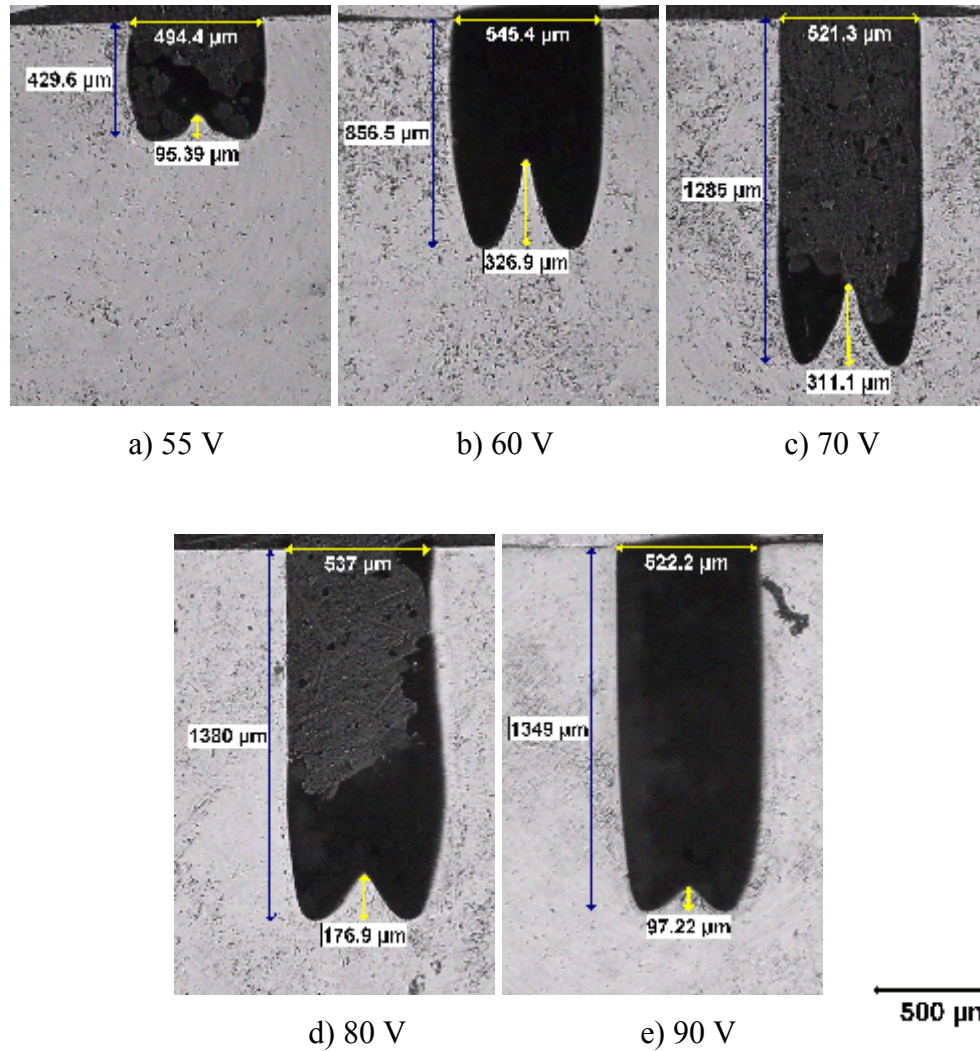


Figure 4.25 Cross-sectional views of machined holes by using varying open voltages

In the second case of experiment, the effect of gap voltage in the geometry formation of micro hole is investigated. By setting the gap voltage 95V, 90V, 80V, and 60V and keeping open voltage constant at 100 V, micro-hole manufacturing is carried out and variation in the geometry with machining different gap voltage is observed. When 95 V and 90 V are used as gap voltage, the end of the micro-holes are more straight then the other ones. When 80 V and 60 V are used as gap voltage the end tip of the micro-holes turn into the different shape as shown in Figure 4.26. These results also verify the statement declared as in the first case. The experiment for each voltage value is repeated three times to show the reliability of experiments. In some of the machining, although

the fore end of the machined holes shape are consistent with each other, the hole depths are sometimes are not preserved within the same level as shown in Figure 4.26. This problem is considered to be arisen from the application of different machining time or use of not sufficiently clear tool electrode that should be free from any carbon particles for good discharge result.

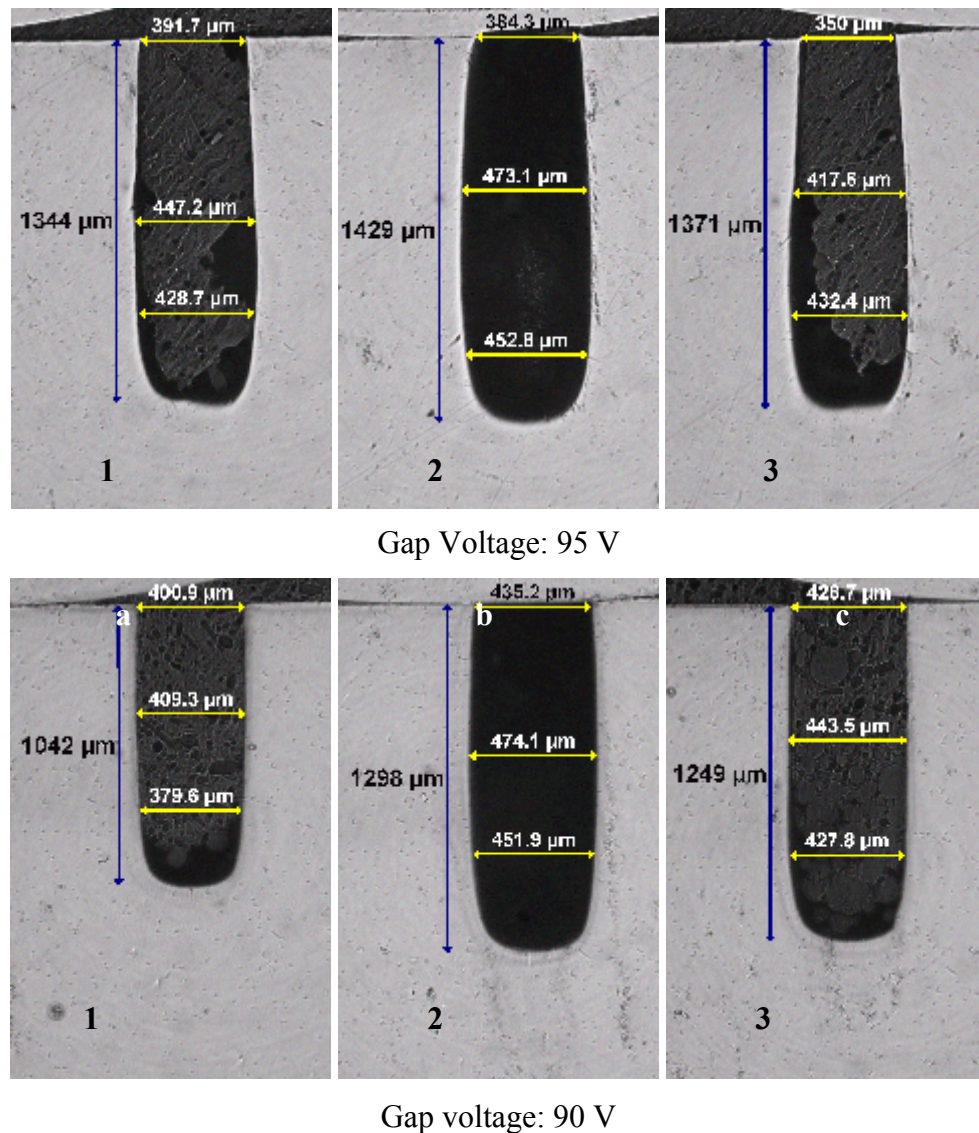
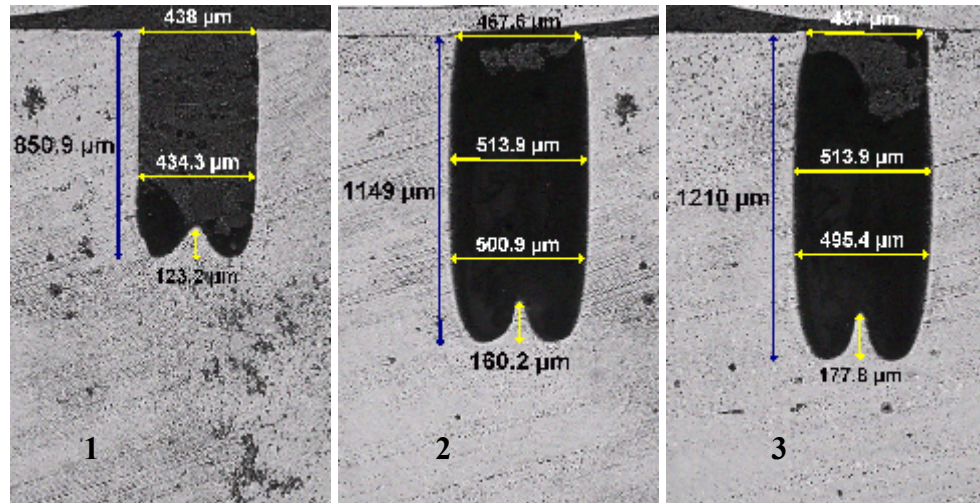
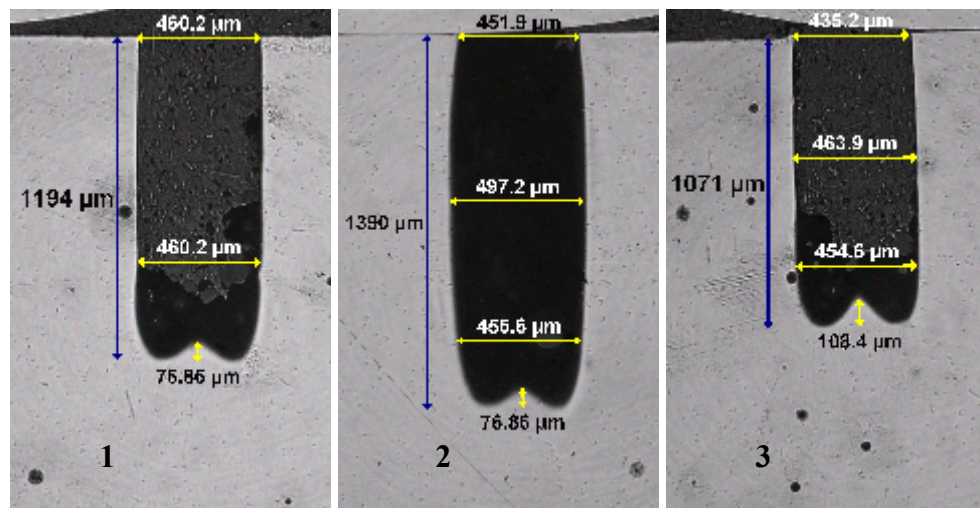


Figure 4.26 Cross-sectional views of machined holes by using variant gap voltage. Each machining were repeated three times and represented by 1, 2, and 3.(cont)



Gap voltage: 80 V



Gap voltage: 60 V

Machining time for 1) 44 min. 2) 41 min. 3) 40 min. for 60 V

500 μm

Figure 4.26 (cont) Cross-sectional views of machined holes by using variant gap voltage. Each machining were repeated three times and represented by 1, 2, and 3.

4.5 Manufacturing of Micro-Holes by Using Ø100 μm Tool Electrode

In this experiment, by using Ø100 μm electrode, variation in geometry of micro-hole, straightness of micro-hole wall side, i.e. parallelism of wall side through cross-sectional view of micro-holes, effectiveness of type of pulses in micro-hole manufacturing, aspect ratio of micro-holes, expansion in holes diameter are investigated. Machining

parameters are given in Table 4.8. Cross-sectional views of machined micro-holes with different machining time depicted in Figure 4.27. Concluded remarks are stated in the coming sections.

Table 4.8 Machining parameters for hole machining by Ø100 µm electrode

Width	: 5 µs
Frequency	: 100 kHz
Open Voltage	: 90 V
Gap Voltage	: 85 V
Gain	: 10

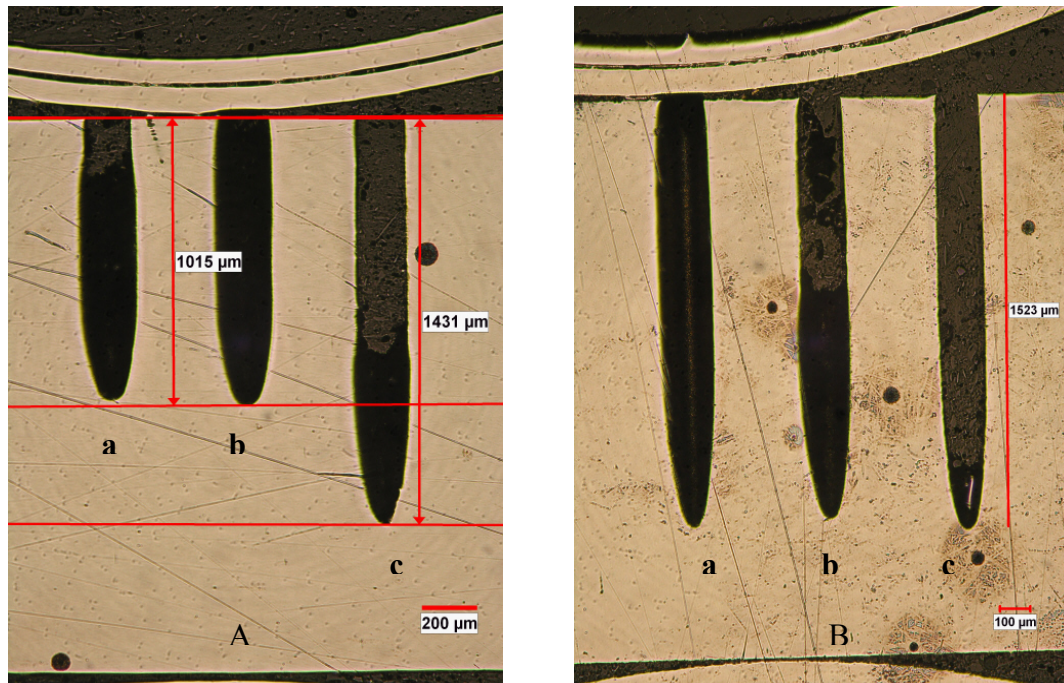


Figure 4.27 Cross-sectional view of holes machined by Ø100 µm electrode with a machining time of A) (a) and (b) 20 min. (c) 30 min., B) (a), (b) and (c) 40 min while energy parameter is set to 14.

Following remarks can be concluded by considering above pictures and machining settings.

- Entrance diameter of micro-holes are smaller than the diameter of the consequent section of micro-holes and this expansion in hole diameters occur where the flushing conditions and debris concentrations are nearly same with thereafter point.
- Maximum possible aspect ratio, within the acceptable machining time, using $\text{Ø}100\ \mu\text{m}$ electrode is about 16. This value can be increased a little but much more time will be consumed.
- Machining ratio, depth of micro-hole over machining time, gradually decreases with increasing machining time.

The other most significant remark realized by means of this experimental work is the influence of the energy parameter while using smaller size electrode such as $\text{Ø}100\ \mu\text{m}$. When the $\text{Ø}100\ \mu\text{m}$ electrode is used to machine micro-hole, energy parameter of 14 or 13 which generate very short pulses should be selected, otherwise, it is impossible to machine a correctly drilled hole such as using energy parameter of 105 or 114. Figure 4.28 illustrates the above statement explicitly, as shown in the related picture nearly aspect ratio of 17 is obtained by using 14 as a energy parameter, whereas by using 105 or 114 as a energy parameter only a little cavity which is far from becoming micro-hole is obtained.

The reason of this undesired machining with smaller size electrode by using energy parameter apart from 13 and 14 is found to be overcharge on the very small size electrode. While the longer pulse form is selected by setting energy parameter energy intensity is increased dramatically on the tip of electrode and the energy on the electrode body immediately wants to discharge to the workpiece and this phenomena occur consecutively many times without waiting for suitable conditions and which result in short circuit away from eroding workpiece.

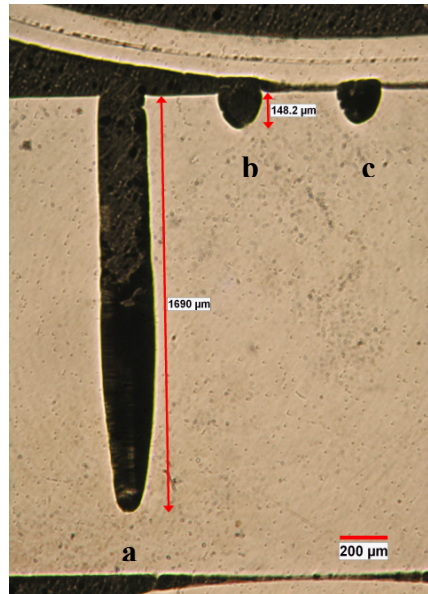


Figure 4.28 Cross-sectional view of holes machined by $\text{\O}100\ \mu\text{m}$ electrode with a machining time of 60 min. and energy parameter for a) 14, b)105 and c) 114.

Micro-hole drilling with the lower energy values is repeatable for desired depth with the same machining time but this can not be valid for higher energy values, Fig. 4.29 shows the cross-section of machined holes with same energy level, it is 350, and same machining time. As a result, depth of micro-hole can not be predictable with increasing energy level. After certain dept of micro-hole, tip of the micro-hole is turn into the worn tip. Worn tip of micro-hole increases with increasing micro-hole depth

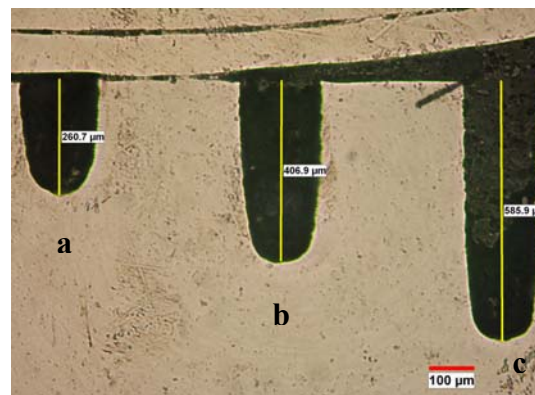


Figure 4.29 Cross-sectional view of holes machined by $\text{\O}100\ \mu\text{m}$ electrode with a machining time of 15 min. and energy parameter of 350 for a, b, and c.

4.6 Defect Formation Inside Machined Hole

During the manufacturing of micro-holes with the related machining conditions, defective shape formation was observed as stated earlier. Some distorted holes cross-sectional views are given with different machining time in Figure 4.30. Machining parameters are given in Table 4.9 and time depended machining table and machining results are given in Table 4.10. We have realized that what cause this deterioration inside the hole, used energy parameter and gain increase the aggressiveness of the machining and together with insufficient flushing condition after certain depth leads to increase in the debris material condensation in the sparking gap. This highly condensed gap with eroded particle make easy to short circuit and undesirable arc, and flushing gap is blocked with the molten material. The eroded particles are adhered to the electrode, so electrode shape is away from cylindrical shape. Thus, newly formed rotating electrode start to erode workpiece and result in a cavity with its mirrored shape.

In order to avoid from this deterioration inside the hole, energy parameter should be changed with the short pulse form and gain value should also be decreased. Defects formation can also be observed via the voltage and current pulse forms recorded by Agilent oscilloscope. When the defective region starts to be formed, the oscilloscope shows frequently pulse types turns into short circuit and arc. Figure 4.33 illustrates recorded type of pulses with instantaneous machining time during the hole machining in 4.31. Figure 4.32 shows the Scanning Electron Microscope (SEM) photograph of corresponding hole. As seen in the Figure 4.33, short circuits and arc occur frequently between machining time of 12-13 min. Pulse forms for the other holes are also given in Appendix F.

Table 4.9 Machining parameters for defected holes

Energy	: 206
Gain	: 20
Frequency	: 120 kHz
Width	: 5 μ s

Table 4.10 Time depended machining table

Hole number	Machining time (min)	Electrode wear (mm)	Total depth (mm)
1-1	1	0.273	0.609
1-2	2	0.479	1.116
1-3	3	0.596	1.450
2-1	5	0.788	1.880
2-2	7	0.989	2.270
2-3	9	1.384	2.840
3-1	11	1,045	2.588
3-2	14	1.200	2.566
3-3	17	1.333	3.220
4-1	20	1.329	3.248
4-2	14	1.526	4.500
4-3	25	1.533	3.998
5	16,3	1.515	4.000
6	23	1.289	4.500

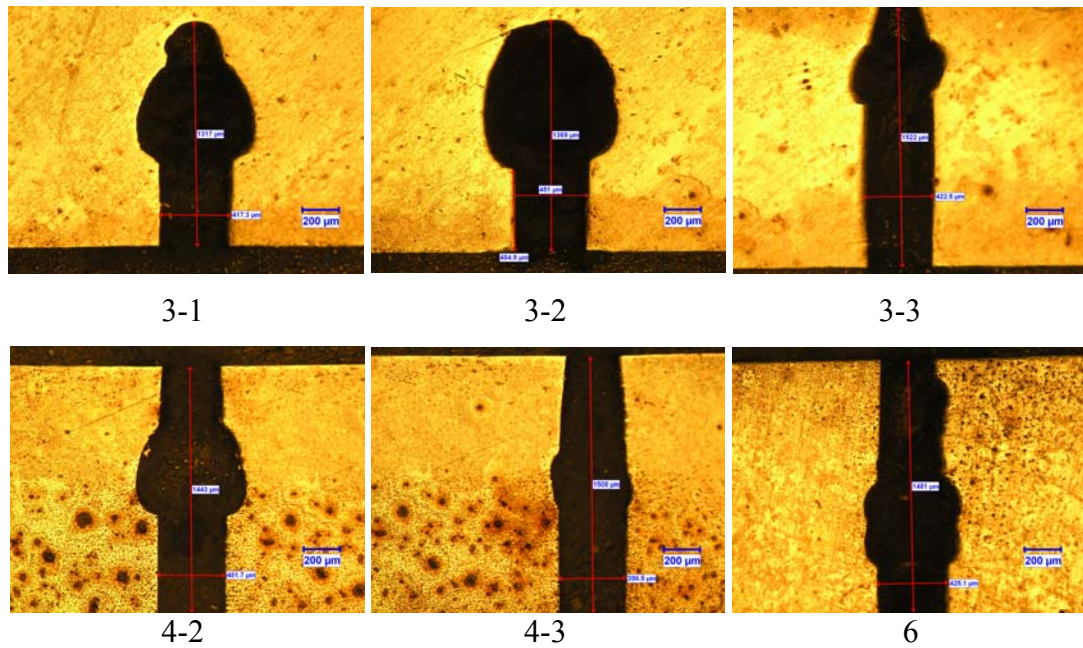


Figure 4.30 A series of hole machining defectively (numbers assigned to each pictures are given considering total machined holes as given in Appendix F)

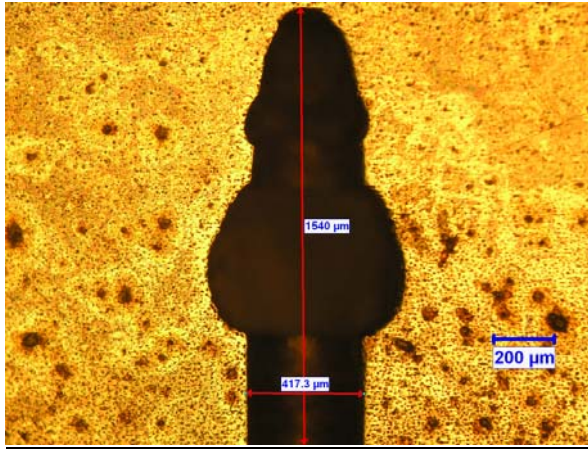


Figure 4.31 Defective hole shape labeled with (4-1)

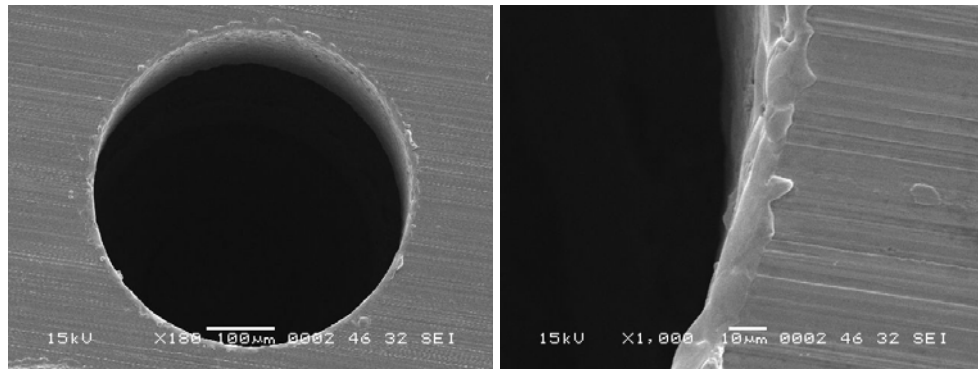
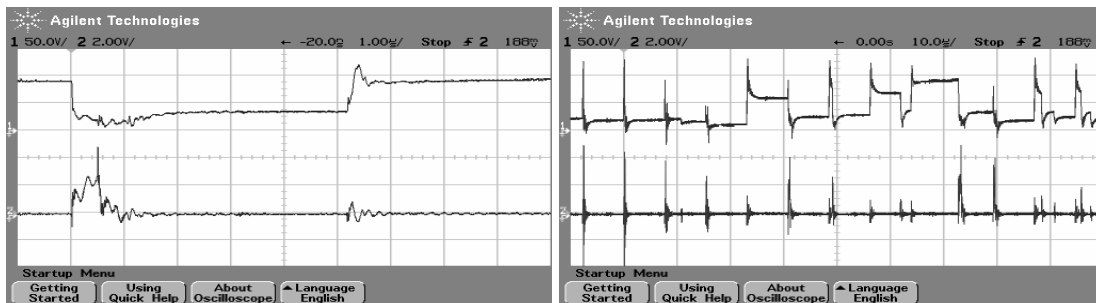


Figure 4.32 SEM photographs of defective hole from top view



2min

4 min

Figure 4.33 Recorded pulse forms of defective hole in Figure 4.31 with instant machining time shown under the captured pulse shapes (cont).

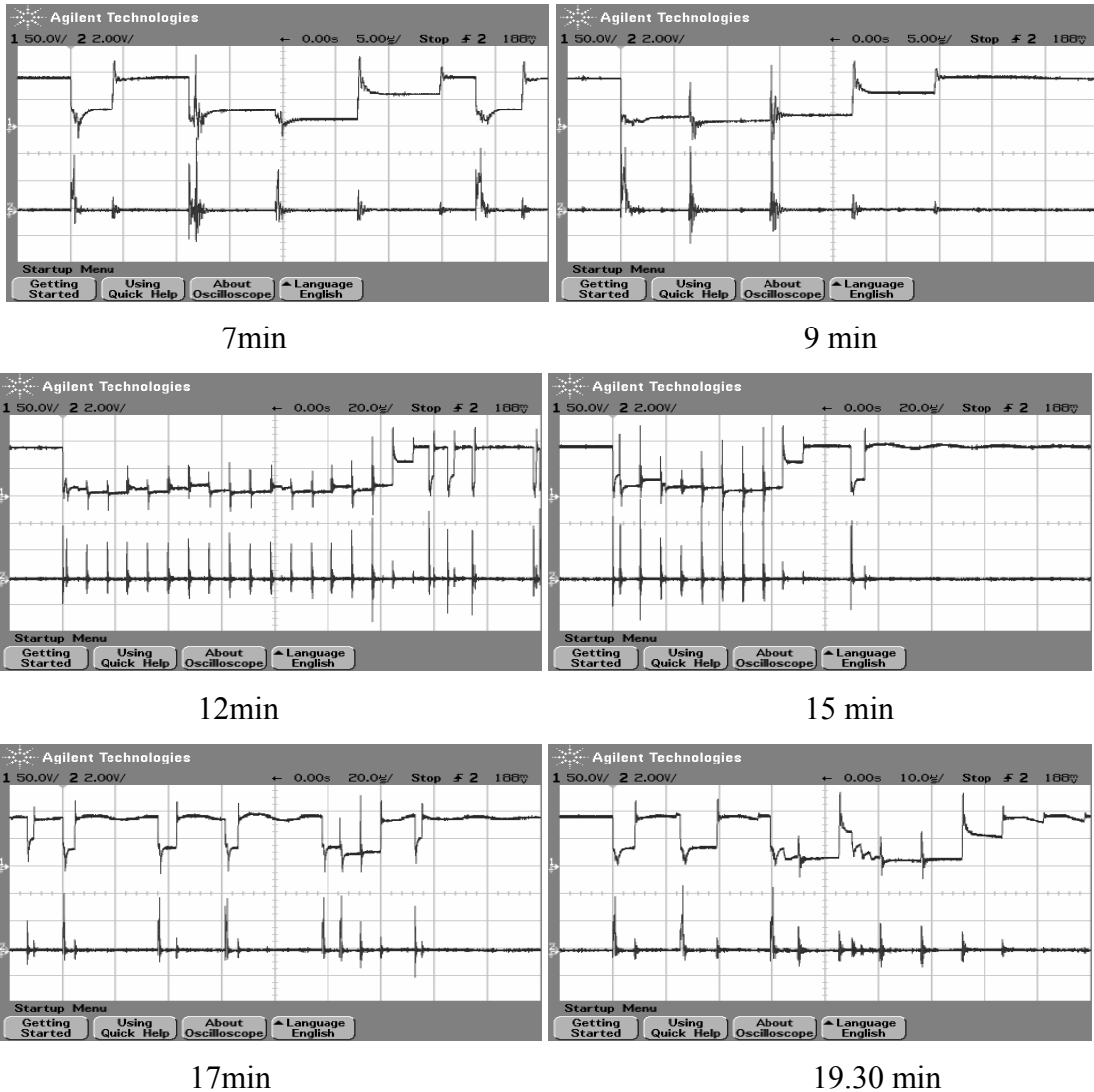


Figure 4.33 (cont) Recorded pulse forms of defective hole in Figure 4.31 with instant machining time shown under the captured pulse shapes.

The possible solution to eliminate the distortion inside the hole shape.

- Use of lower energy parameter and gain depending on current and voltage value
- Increase flushing pressure and clamp rotational speed
- Use of vibrating worktable such as ultrasonic vibration method
- Use of tubular electrode; it has constant flushing through the gap so the debris can be easily removed away from the sparking area.

4.7 Preventive Machining Parameters for Defect Formation and Achievable Aspect Ratio by Smaller Tool Electrode

After obtaining the cross-sectional view of machined holes, some undesirable geometrical shapes (Figure 4.34, (4), (5), (6)) are observed along the hole tubular section, but this defective geometry can not be realized without sectional view. This undesired machining effect are tried to be removed by changing the machining characteristics, hence, we obtained sufficiently smooth shape of hole cross-section as shown in Figure 4.34 -(2), -(7), -(9). The machining parameters of each machined holes and other results are given in Appendix E.

According to the machining conditions, the most predominant parameters that lead to the unexpected defected shape are found to be energy level and gain. The selection of energy level around 205 and gain value higher than 10 or 15 result in the defective geometrical shape. Use of these parameters together within the specified range leads to the higher material deformation inside the hole than that of use individually. In the machining of hole with a number of 4, 5 and 6 in Figure 4.29, energy parameter is set to 250,250, and 206, and gain is set to 20, 20, and 10, respectively. However, In the machining of hole with a number of 2, 7, and 8, energy parameter is set to 350, 105, 105 and gain is set to 10, 10,10, respectively and more smooth and parallel wall side is obtained. Characteristics of the type of energy parameter were stated in the earlier sections.

An attempt also was made to manufacture smaller size of holes under 100 μm diameter. Machining conditions are given in the table Appendix-E. Smaller size of the electrode used in the hole machining is about $\text{Ø}15 \mu\text{m}$ but its cross-sectional view was not taken successfully due to having a very small size, during grinding operation almost totally sectioned parts vanished. As shown in Figure 4.35 the cross-sectional view of the micro-holes are partly over grinding, nevertheless remaining parts of the cross-sectional view is useful to have knowledge about aspect ratios and straightness of the hole wall side. For the machining of hole labeled by 12, the micro-hole with a nearly 740 μm

depth was drilled by using $\text{Ø}32 \mu\text{m}$ tool electrode and aspect ratio of over 20 was obtained in 100 min.

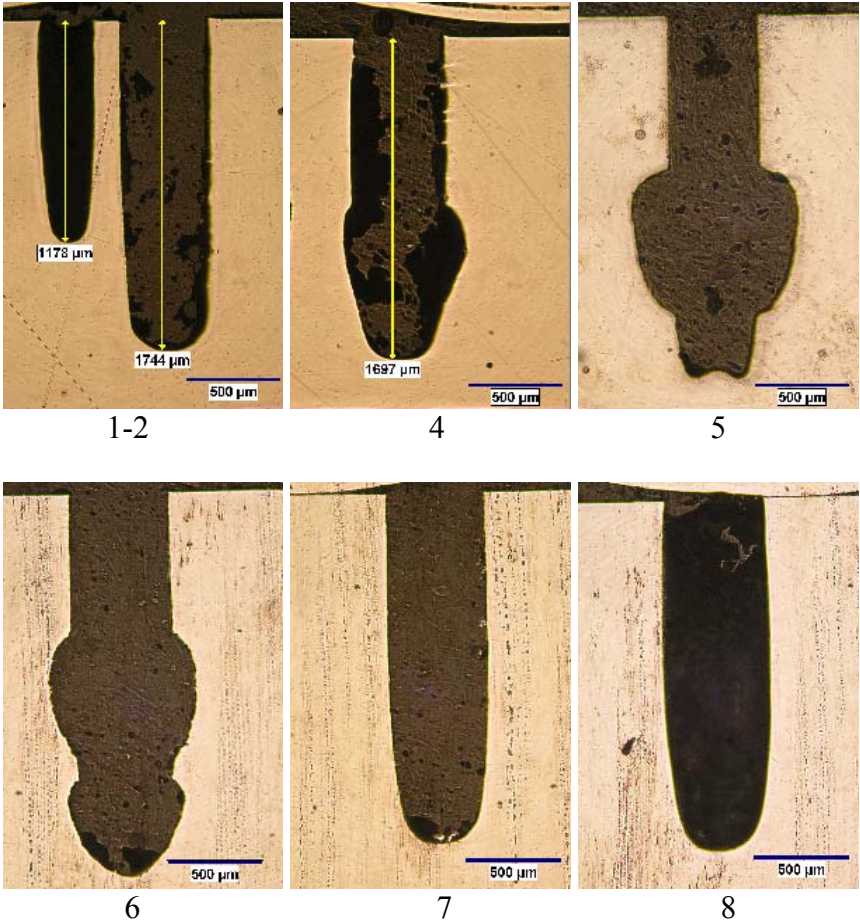


Figure 4.34 Cross-sectional views of defective and smooth machined holes

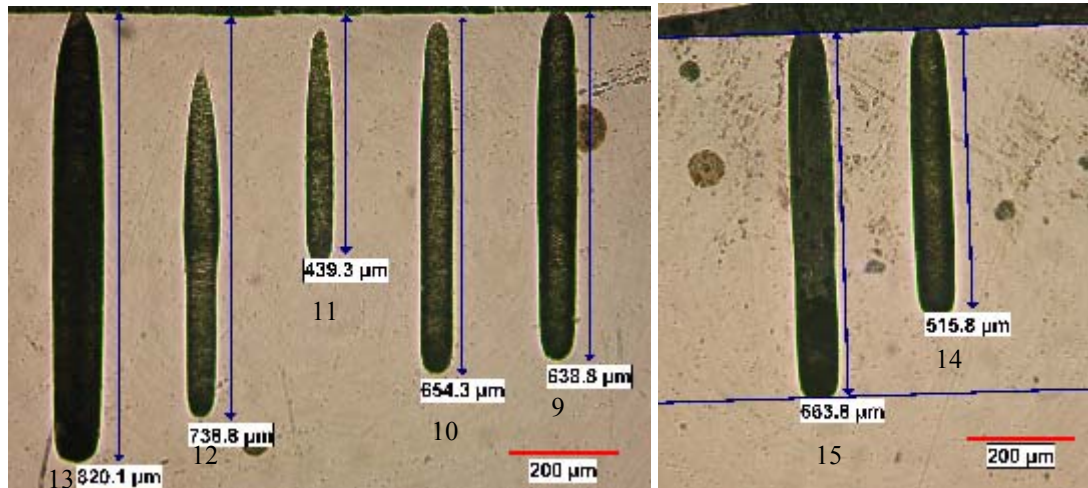


Figure 4.35 Cross-sectional views of machined micro-holes

Although manufacturing of very small size hole under $\text{Ø } 100 \text{ }\mu\text{m}$ seems to be machined successfully, a circularity problem arises while electrode size is around $\text{Ø } 30 \text{ }\mu\text{m}$. Increasing machining time and smaller the electrode size with rotating clamp leads to the divergence from circularity of the micro-hole, and the shape tends to become elliptical shape (Figure 4.36). However, these type of holes can be used for many industrial and research applications where the circularity is not primarily essential. Divergence problem has not observed up to now in the machining of slightly bigger size holes than that of $\text{Ø } 100 \text{ }\mu\text{m}$.

As depicted in the Figure 4.36 with a hole number of 7 and 8, a circle is fit to the hole shape and no inconsistency is observed, almost good circularity is obtained when bigger size electrode is used. As for hole 13 and 14, no good circle is fit to the hole, so we need to define a circularity in the micro-hole manufacturing, two circle is drawn by referencing the most inner three point and the most outer three point on the hole circumference, the size difference between circles gives us the divergence from the perfect circle. For instance, for hole 13, the outer circle diameter is $74.01 \text{ }\mu\text{m}$ and the inner circle diameter is $70.25 \text{ }\mu\text{m}$, half of the difference is $1.88 \text{ }\mu\text{m}$ which represent divergence from the perfect circularity.

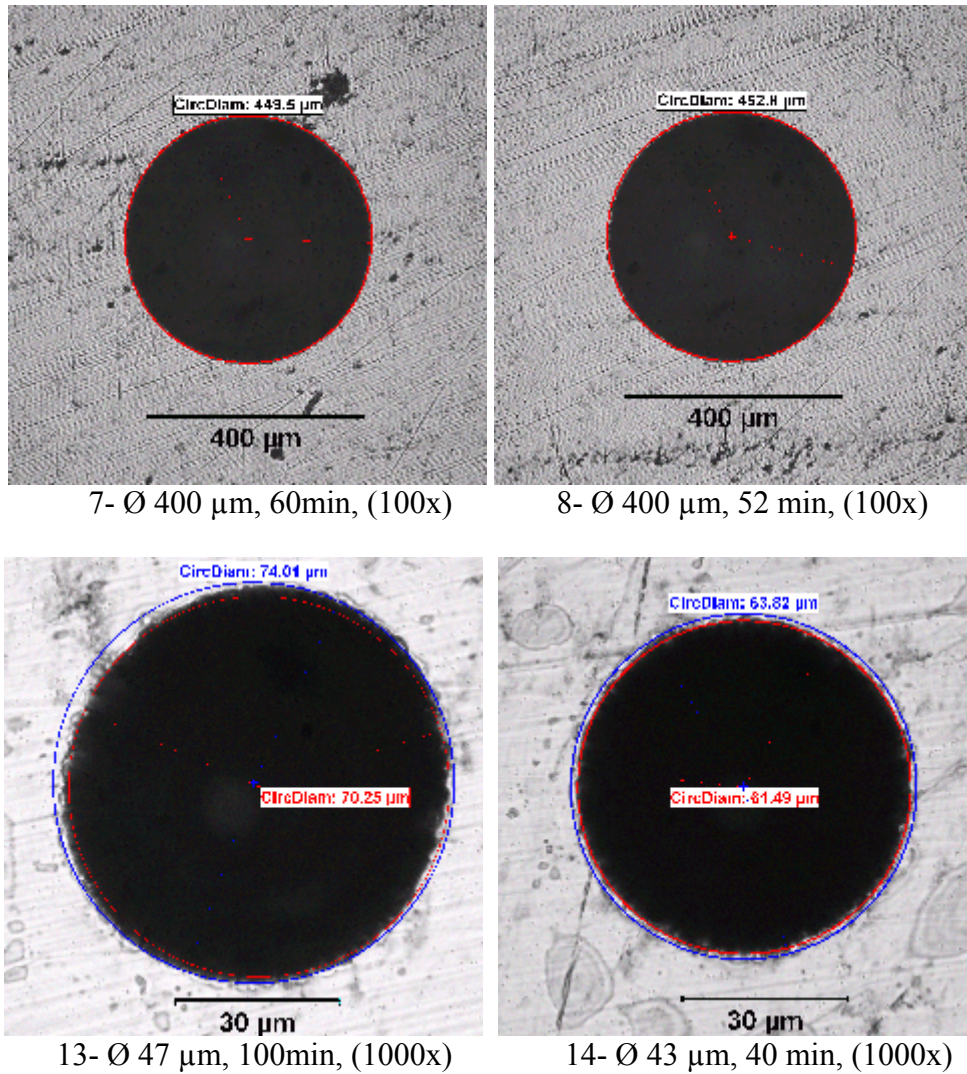


Figure 4.36 Micro-holes to show circularity, label in the bottom of each picture represent hole number, electrode size, machining time and microscopic magnification, respectively.

Another significant point realized in above pictures, the hole radial expansion is drastically increasing while machining time is increased. This is obvious in hole 13 and 14.

4.8 Through Hole machining

An attempt is made to machine through holes on the 2mm-thick plate. Machining conditions are given in Table 4.11. During machining of through holes, there are some possible difficulties to be encountered. These difficulties are revealed during a series of through holes machining and possible remedy are recommended and applied to the entire job.

Formation of tapered shape in the hole making is the mostly encountered geometry problem because the exact through holes must be viewed as a cylindrical shape. These situations are illustrated schematically in Figure 4.37. This tapered shape formation in hole machining by using EDM is caused by the worn tip of the tool electrode, when deeper hole is machined, tapered degree increases since the fore end of the electrode worn much more with the increasing hole depth or machining time. The widely used possible solution recommended by the researchers is the over-travel of tool electrode through the workpiece as shown in Figure 4.38, so that worn tip of the electrode can exit to the out of machining area and exit diameter of the hole come to the same size with entrance diameter. Thus, tapered shape is eliminated and approximately exact cylindrical shape can be obtained.

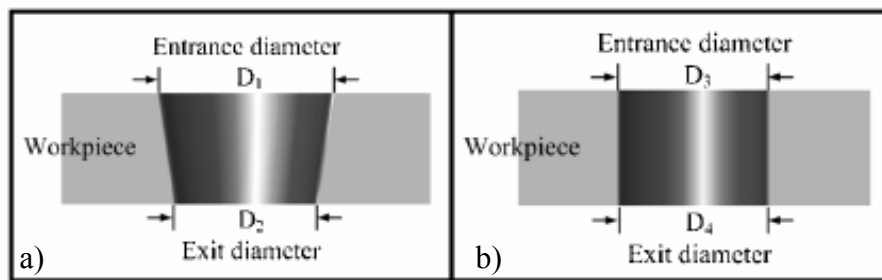


Figure 4.37 Schematic views of (a) tapered shape hole and (b) exactly cylindrical shape hole (Hung et al., 2006)

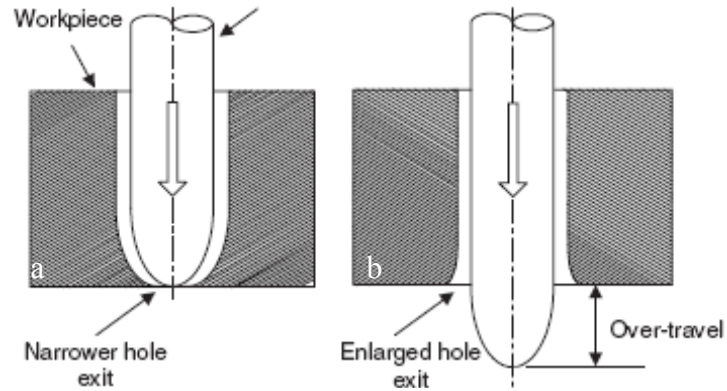


Figure 4.38 Schematic illustration of electrode over-travel to avoid from tapered shape (a) Worn tip of rod electrode causes a narrower hole exit and (b) enlarged hole exit is generated due to the over-travel of rod electrode (Kao and Shih, 2006)

A series of hole machining were performed by considering over-travel of electrode, length of over-travel is changed to observe the variation in the exit diameter. Six holes are machined with setting machining parameters as in the Table 4.11 and machining time and over-travel value are tabulated according to the corresponding hole number in Table 4.12. Entrance diameter enlargement are observed as in the Figure 4.39 with the corresponding hole number.

Table 4.11 Machining parameters (rough condition) for through hole drilling

Width	: 4 μ s,	Voltage	: 90	Gain: 30
Frequency	: 130 kHz,	Gap Voltage	: 80	
Current	: 55,	Energy	: 206	

Table 4.12 Over-travel settings for each hole

Hole number	Mach. time (min)	Target hole depth (mm)	Electrode wear (mm)	Over-travel* (mm)	Mach. Type
1	13	3.5	1.317	0.183	Rough
2	29	3.75	1.412	0.338	Rough
3	68	4	1.765	0.235	Rough
4	45	4.5	1.571	0.929	Rough
5	25	5	1.429	1.571	Rough
6	21	5.5	1.338	2.162	Rough

*Over travel: Target hole depth-(worn electrode length+ specimen thickness (2mm))

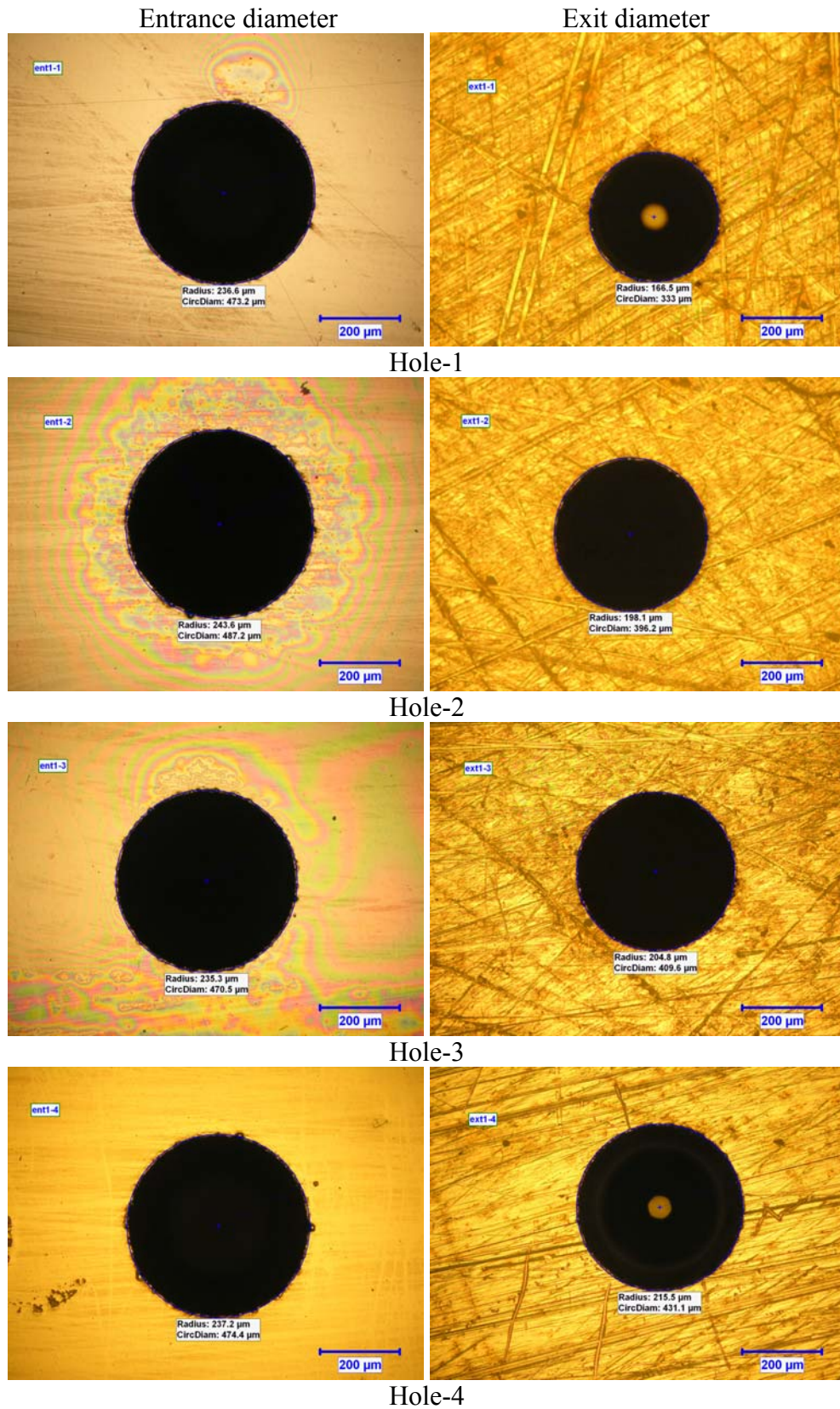


Figure 4.39 Machined holes entrance and exit diameter pictures by applying electrode over-travel (cont)

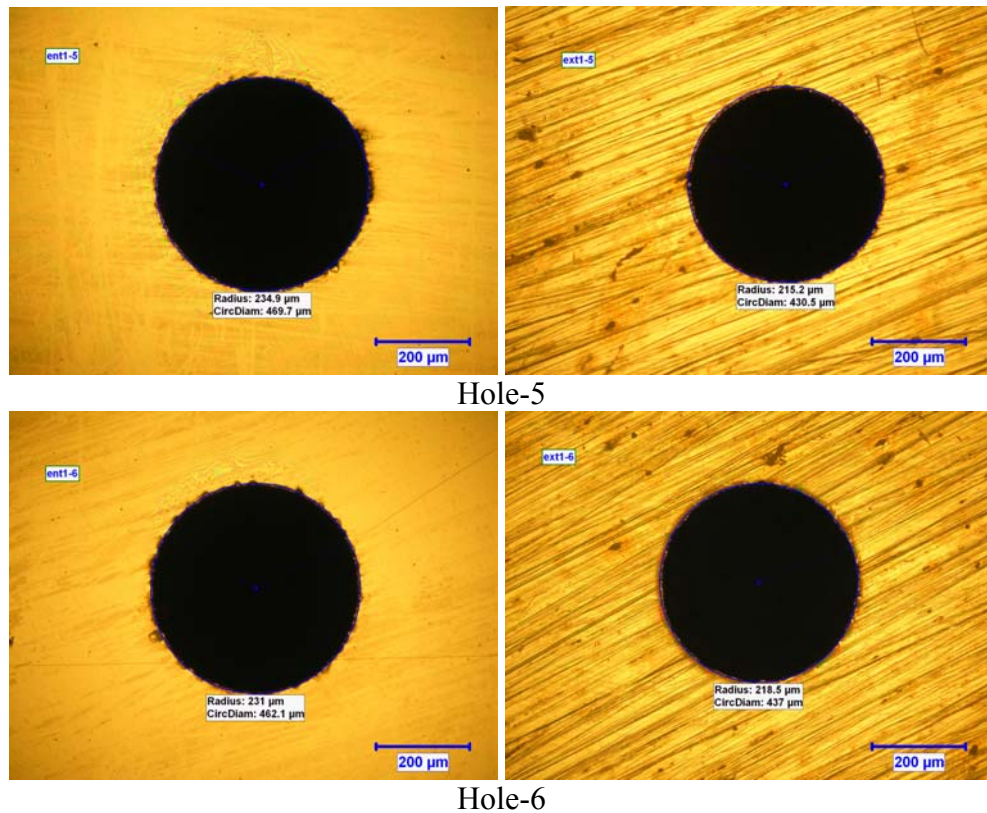


Figure 4.39 (cont) Machined holes entrance and exit diameter pictures by applying electrode over-travel.

We have proposed a classical EDM approach to produce micro-holes with lower difference between entrance and exit diameter, and obtain better surface roughness, this technique can be applied by introducing second electrode after the first machining operations. Machining with new electrode and setting finish machining parameters provide better circularity, good surface roughness, and lower tapered shape when compared to the machining only applying electrode over-travel. There is no repetition problem when exact machining coordinate is found to be ready after cutting used electrode tip since Sarix machine has a high resolution of 1μm working table moving along $-x$ and $-y$ axis. The first machining is done using rough machining parameters but the second machining is done by using finish machining parameters and second machining time is very small according to the first one, because previously machined holes provide good flushing condition. The finish parameter is different from rough machining parameter in the energy parameter and frequency, 100 and 150 kHz are used

respectively and the others remain same. Machining type and target hole depth are given in Table 4.12 and entrance and exit diameter of the machined holes are illustrated in Figure 4.40. As it shown in Figure 4.40, exit of the holes are smoother and higher circularity degree than that of only applying electrode over-travel due to secondary finish machining. Another significant point realized from the Table 4.12 and Table 4.13 is on the machining time. Although machining time for each hole should be very closing to the each other, we observed that the comparatively different values of machining time. Actually this problem is well-known due to earlier experiments. The reason is that undesired machining take place inside the hole as it stated in Figure 4.31 and its related expression.

Table 4.13 Settings for hole machining with secondary electrode

Hole number	Mach. Time (min)	Target hole depth (mm)	Electrode wear (mm)	Mach. Type
1-1	14.30	3.5	1.254	Rough (Energy=206)
1-2	10	3.5	Negligible amount	Finish (Energy=100)
2-1	20	3.75	1.536	Rough (Energy=206)
2-2	14	3.75	Negligible amount	Finish (Energy=100)
3-1	50	4	1.548	Rough (Energy=206)
3-2	9	4	Negligible amount	Finish (Energy=100)
4-1	12.30	4.5	1.163	Rough (Energy=206)
4-2	10	4	Negligible amount	Finish (Energy=100)
5-1	50	5	15.114	Rough (Energy=206)
5-2	8	4	Negligible amount	Finish (Energy=100)
6-1	40	5	14.235	Rough (Energy=206)
6-2	8	4	Negligible amount	Finish (Energy=100)

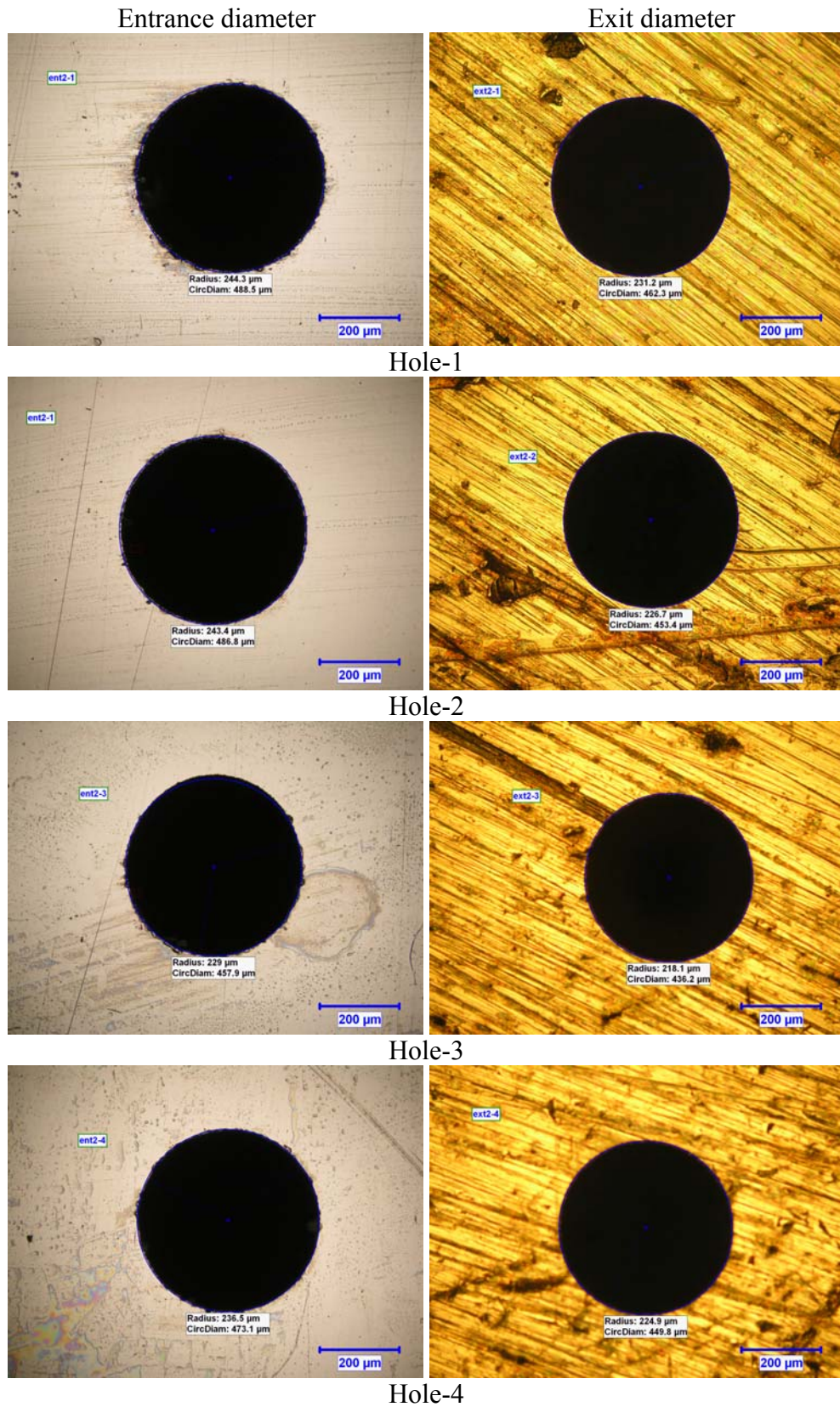
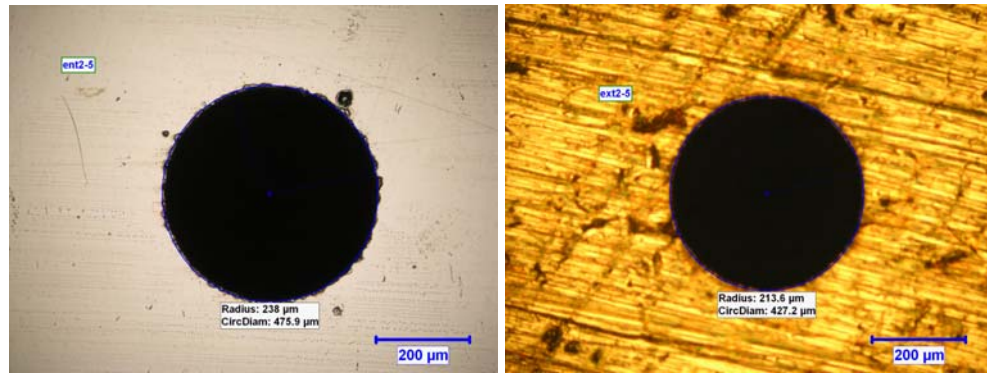
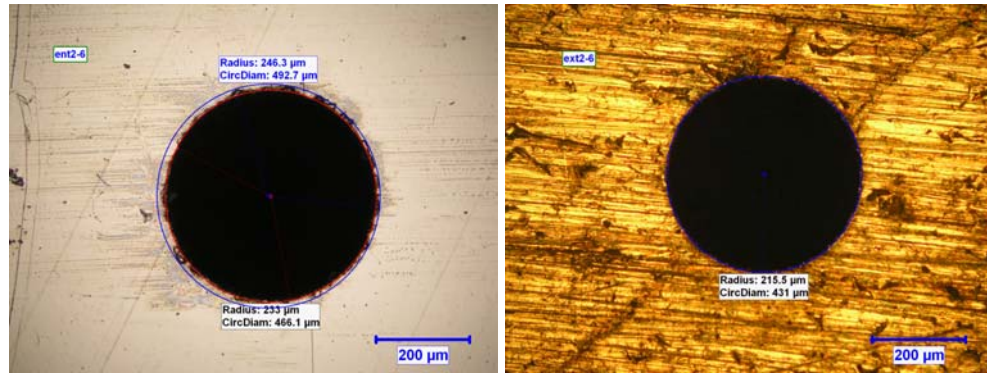


Figure 4.40 Entrance and exit diameter photos of holes machined by using two electrodes (cont).



Hole-5



Hole-6

Figure 4.40 (cont) Entrance and exit diameter photos of holes machined by using two electrodes.

As it observed in the holes pictures, entrance diameters are larger and more rough than exit diameters, and their close regions on the hole wall show nearly same characteristics. In order to overcome this inconsistency over the hole sections, use of slightly small electrode than desired hole size for firstly rough machining are proposed, then small big electrode can be used for secondly finish machining. Most smooth and less taper hole can be obtained by means of this application.

CHAPTER 5

CONCLUSIONS AND FUTURE WORK

Micro-electrical discharge machining process is a widely used micro fabrication technique to produce micro-parts and components needed in the micro-mechatronic systems and industrial applications. Micro-EDM technique was discussed extensively by using previous literatures. Micro-hole fabrication is a primary task for this thesis because micro-hole is the most simple and widely used micro products that can be manufactured by using micro-EDM.

Manufacturing of micro-holes by using micro-EDM is the first completed study on micro-EDM in Turkey. For this purpose, Sarix high precision micro-EDM machine was purchased from Switzerland and it has many undisclosed parameters which are effective in the determination of machining characteristics. In order to reveal the machining characteristics and predict the machined shape of holes, this thesis is completed with the outstanding concluding remarks.

The statements below can be concluded from the experimental results and observations;

- 1- Energy parameter is the most predominant parameter which assigns the type of pulses produced by the micro-erosion generator. According to captured pulse form results, approximately 125 ns and 1 μ s discharge time are recorded when energy parameter are set to 14 and 205, respectively. The peak current read from the oscilloscope are approximately 5 A and 15 A while considering the former energy parameter, respectively.

- 2- By using higher the energy parameter, higher discharge time and peak current, results in higher hole depth while surface roughness and shape of holes go to be distorted. In addition, electrode removal also increases with the mentioned energy parameter.
- 3- Expansion in the hole diameter increases with the increasing machining time and longer the voltage pulse. However, less consistency in the holes diameter is obtained.
- 4- Narrower section length of a hole, end tip of the hole, start to be formed after where the 5% reduction of hole entrance diameter is measured.
- 5- By using higher the width and lower the frequency, higher hole depth can be obtained but the frequency value must always greater than time width.
- 6- Open voltage and gap voltage should be close to each other, approximately 5 V or 10 V difference is suitable for effective machining.
- 7- Lower gain value should be used, approximately 10, in order to prevent the undesired shape formation inside the hole.
- 8- Approximately 20 aspect ratios are obtained by using $\text{Ø}100\ \mu\text{m}$ tool electrode.
- 9- Circularity of the micro-holes around $\text{Ø}30\ \mu\text{m}$ size is away from the correct circle which turns into the elliptical shape when the higher machining time approximately 100 min. is applied.

As future work;

With the completion of this thesis, machining characteristics and machining behavior of micro-EDM can be estimated and predicted easily. By using the approved machining parameters, through micro-holes with a diameter less than $50\ \mu\text{m}$ can be performed to analyze aspect ratios, surface roughness, circularity, and straightness of the hole wall-side in detail. A software based model can be developed to predict the machined hole geometry in advance by considering end tip shape and cross-sectional view. This model provides us to save waste of time consumed during the sacrificial experiments.

In this study, dielectric oil is used as a flushing liquid, dielectric liquid can be changed to different dielectric liquid, such as dielectric water or kerosene, and efficiency on the machined parts can be compared. Apart from the micro-hole manufacturing, a study can be focused on the manufacturing of micro-channels widely used for micro-cooling systems or 3D machining can performed to produce mini/micro complex shape parts or cavities.

By using the recommended machining parameters in the thesis, all the planned micro machining process by micro-EDM can be achieved successfully.

REFERENCES

1. Allen, P., Chen, X., 2007 “Process simulation of micro electro-discharge machining on molybdenum” *J. Mater. Process. Technol.* **186** 346-355.
2. Chung, D.K., Kim, B.H., Chu, C.N., 2007 “Micro electrical discharge milling using deionized water as a dielectric fluid”, *J. Micromech. Microeng.* **17** 867-874.
3. Cao, D.M., Jiang, J., Meng, W.J., Jiang, J.C., Wang, W., 2007 “Fabrication of high-aspect-ratio microscale Ta mold inserts with micro electrical discharge machining”, *Microsystem Technologies* **13** 503-510
4. Diver, C., Atkinson, J., Helml, H.J., Li, L., 2004 “Micro-EDM drilling of tapered holes for industrial applications”, *J. Mater. Process. Technol.* **149** 296-303.
5. Dhanik, S., Joshi, S.S., 2005 “Modeling of a Single Resistance Capacitance Pulse Discharge in Micro-Electro Discharge Machining”, *Journal of Manufacturing Science and Engineering*, **127** 759-767.
6. Ekmekçi, B., 2004 “Theoretical and Experimental Investigation of Residual Stresses in Electric Discharge Machining”, PhD Thesis, METU.
7. Erden, A., 1977 “Theoretical and Experimental Investigation on Electric Discharge Machining”, PhD Thesis, METU.
8. Fleischer, J., Masuzawa, T., Schmidt, J., Knoll, M., 2004 “New applications for micro-EDM”, *J. Mater. Process. Technol.* **149** 246-249.
9. Gangadhar, A., Sunmugam, M.S., Philip, P.K., 1992 “Pulse train studies in EDM with controlled pulse relaxation” *Int. J. Machine Tools Manuf.* **32** 651-657.

10. Ho, K.H., Newman, S. T., 2003 “State of the art electrical discharge machining (EDM)”, *Int. J. Machine Tools Manuf.* **43** 1287-1300.
11. Han, F., Chen, L., Yu, D., Zhou, X., 2007 “Basic study on pulse generator for micro-EDM” *Int. J. Adv. Manuf. Tech.* **33** 474-479.
12. Han, F., Yamada, Y., Kawakami, T., Kunieda, M., 2006 “Experimental attempts of sub-micrometer order size machining using micro-EDM”, *Precis. Eng.* **30** 123-131.
13. Her, M.G., Weng, F.T., 2001 “Micro-hole Machining of Copper Using the Electro-discharge Machining Process with a Tungsten Carbide Electrode Compared with a Copper Electrode”, *Int. J. Adv. Manuf. Tech.* **17** 715-719.
14. Hung, J.C., Lin, J.K., Yan, B.H., Liu, H.S., Ho, P.H., 2006 “Using a helical micro-tool in micro-EDM combined with ultrasonic vibration for micro-hole machining”, *J. Micromech. Microeng.* **16** 2705-2713.
15. Hung, J.C., Yan, B.H., Liu, H.S., Chow, H.M., 2006 “Micro-hole machining using micro-EDM combined with electropolishing”, *J. Micromech. Microeng.* **16** 1480-1486.
16. Kao, C.C., Shih, A.J., 2006 “Sub-nanosecond monitoring of micro-hole electrical discharge machining pulses and modeling of discharge ringing”, *Int. J. Machine Tools Manuf.* **46** 1996-2008.
17. Kim, Y.T., Park, S.J., Lee, S.J., 2005 “Micro/Meso-scale Shapes Machining by Micro EDM Process” *Int. Journal of Precision Eng. And Manufacturing* **6** 5-11.
18. Klocke, F., Lung, D., Antonoglou, G., Thomaidis, D., 2004 “The effects of powder suspended dielectrics on the thermal influenced zone by electrodischarge machining with small discharge energies” *J. Mater. Process. Technol.* **149** 191-197.

19. Kim, D.J., Yi, S.M., Lee, Y.S., Chu, C.N., 2006 “Straight hole micro EDM with a cylindrical tool using a variable capacitance method accompanied by ultrasonic vibration”, *J. Micromech. Microeng.* **16** 1092-1097.
20. Kaminski, P.C., Capuano, M.N., 2003 “Micro hole machining by conventional penetration electrical discharge machine”, *Int. J. Machine Tools Manuf.* **43** 1143-1149.
21. Liu, H.S., Yan, B.H., Huang, F.Y., Qiu, K.H., 2005 “A study on the characterization of high nickel alloy micro-holes using micro-EDM and their applications” *J. Mater. Process. Technol.* **169** 418-426.
22. Lin, C.T., Chow, H.M., Yang, L.D., Chen, Y.F., 2007 “Feasibility study of micro-slit EDM machining using pure water” *Int. J. Adv. Manuf. Tech.* **34** 104-110.
23. Li, Y., Guo, M., Zhou, Z., Hu, M., 2002 “Micro electro discharge machine with an inchworm type of micro feed mechanism” *Precision Eng., J. of the Int. Societies. for Precision Eng. and Nanotechnology* **26** 7-14.
24. Li, H., Senturia, S.D., 1992 “Molding of Plastic Components Using Micro-EDM Tools” *Thirteenth IEEE/CHMT International Electronics Manufacturing Technology Symposium*, 145-149.
25. Lim, H.S., Wong, Y.S., Rahman, M., Edwin Lee, M.K., 2003 “A study on the machining of high-aspect ratio micro-structures using micro-EDM” *J. Mater. Process. Technol.* **140** 318-325.
26. Masuzawa, T., 2000 “State of the art of micromachining” *Ann. CIRP* **49** 473-488.
27. Masuzawa, T., Tsukamoto, J., Fujino, M., 1989 “Drilling of Deep Microholes by EDM”, *Ann. CIRP* **38** 195-198.
28. Masuzawa, T., Fujimoto M, Kobayashi, K., 1985 “Wire electro-discharge grinding for micromachining” *Ann. CIRP* **34** 431-434.

29. Masuzawa, T., 1997 “Three-dimensional micro-machining by machine tools” *Ann. CIRP* **46** 621-628.
30. Moylan, S.P., Chandrasekar, S., Benavides, G.L., 2005 “High-Speed Micro-Electro-Discharge Machining” *Sandia Report, Sandia National Laboratories*, SAND2005-5023, Printed September.
31. Murali, M., Yeo, S.H., 2004 “Rapid Biocompatible Micro Device Fabrication by Micro Electro-Discharge Machining”, *Biomedical Microdevices* 6:1, 41-45, 2004 Kluwer Academic Publishers, Manufactured in The Netherlands.
32. Nakaoku, H., Masuzawa, T., Fujino, M., 2007 “Micro-EDM of sintered diamond”, *J. Mater. Process. Technol.* **187-188** 274-278
33. Pham, D.T., Ivanov, A., Bigot, S., Popov, K., Dimov, S., 2007 “An investigation of tube and rod electrode wear in micro EDM drilling”, *Int. J. Adv. Manuf. Tech.* **33** 103-109.
34. Qu, J., 2002 “Development of cylindrical wire electrical discharge machining process and investigation of surface integrity and mechanical property of edm surface layers”, PhD Thesis, North Carolina State University.
35. Rajurkar, K.P., Yu, Z.Y., 2000 “3D Micro-EDM Using CAD/CAM”, *Ann. CIRP* **49** 127-130.
36. Rajurkar, K.P., Navelkar, V.V., Springer J.E., 1987 “High speed pulse train analysis for real-time EDM control”, *SME Technical Paper*.
37. Sarix Operating Manual version 1.20 for SX-100 Micro-Erosion Machine.
38. Son, S., Lim, H., Kumar, A.S., Rahman, M., 2007 “Influences of pulsed power condition on the machining properties in micro-EDM” *J. Mater. Process. Technol.* **190** 73-76.

39. Takahata, K., Shibaike, N., Guckel, H., 1999 “A Novel Micro Electro-Discharge Machining Method Using Electrodes Fabricated by The LIGA Process” *Twelfth IEEE Int. Conference on MEMS* 238-243.
40. Tsai, Y.Y., Masuzawa, T., 2004 “An index to evaluate the wear resistance of the electrode in micro-EDM” *J. Mater. Process. Technol.* **149** 304-309.
41. Takahata, K., Gianchandani, Y.B., 2002 “Batch Mode Micro-Electro-Discharge Machining” *Journal of Microelectromechanical systems* **11** 102-110.
42. Tseng, S.C., Chen, Y.C., Kuo, C.L., 2005 “A study of integration of LIGA and M-EDM technology on the microinjection molding of ink-jet printers’ nozzle plates”, *Microsystem Technologies* **12** 116-119.
43. Uhlmann, E., Piltz, S., Doll, U., 2005 “Machining of micro/miniature dies and moulds by electrical discharge machining-Recent development”, *J. Mater. Process. Technol.* **167** 488-493.
44. Wang, A.C., Yan, B.H., Tang, Y.X., Huang, F.Y., 2005 “The feasibility study on a fabricated micro slit die using micro EDM”, *Int. J. Adv. Manuf. Tech.* **25** 10-16.
45. Wansheng, Z., Zhenlong, W., Shichun, D., Guanxin, C., Hongyu, W., 2002 “Ultrasonic and electric discharge machining to deep and small hole on titanium alloy”, *J. Mater. Process. Technol.* **120** 101-106.
46. Weng, F.T., 2006 “Electrodischarge machining of a coaxial array of microholes using a graphite-copper electrode”, *Int. J. Adv. Manuf. Tech* **27** 1097-1100.
47. Wong, Y.S., Rahman, M., Lim, H.S., Han, H., Ravi, N., 2003 “Investigation of micro-EDM material removal characteristics using single RC-pulse discharges”, *J. Mater. Process. Technol.* **140** 303-307
48. Yamazaki, M., Suziki, T., Mori, N., Kunieda M., 2004 “EDM of micro-rods by self-drilled holes”, *J. Mater. Process. Technol.* **149**134-138.

49. Yan, B.H., Wang, A.C., Huang, C.Y., Huang, F.Y., 2002 “Study of precision micro-holes in borosilicate glass using micro EDM combined with micro ultrasonic vibration machining”, *Int. J. Machine Tools Manuf.* **42** 1105-1112.
50. Yeo, S.H., Murali, M., Cheah, H.T., 2004 “Magnetic field assisted micro electro-discharge machining”, *J. Micromech. Microeng.* **14** 1526-1529.
51. Yu, Z., Masuzawa, T., Fujino, M., 1998 “Micro-EDM for Three Dimensional Cavities-Development of Uniform Wear Method”, *Ann. CIRP.* **47** 169-172.
52. Yu, Z.Y., Rajurkar, K.P., Shen, H., 2002 “High Aspect Ratio and Complex Shaped Blind Micro Holes by Micro EDM”, *Ann. CIRP* **51** 359-362.
53. Zhao, W., Yang, Y., Wang, Z., Zhang, Y., 2004 “A CAD/CAM system for micro-ED-milling of small 3D freeform cavity”, *J. Mater. Process. Technol* **149** 573-578.

APPENDIX A

HOLE SHAPES WITH VARYING MACHINING TIME

Geometrical shape variations of micro-holes are observed from the cross-sectional view as in Figure A.1. Constant machining conditions and energy parameter are used for this experiment.

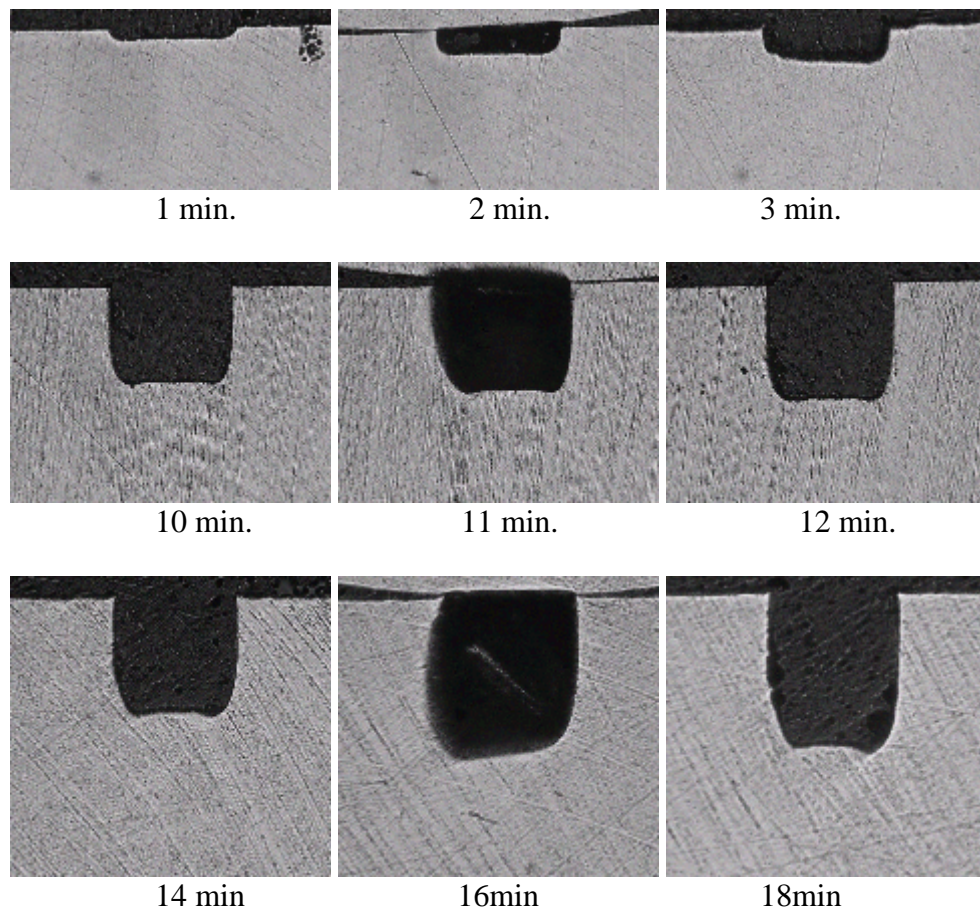


Figure A.1 Micro-holes cross-sectional shape with different machining time from 1min. to 80 min. and constant machining parameters as given in Table 4.4.

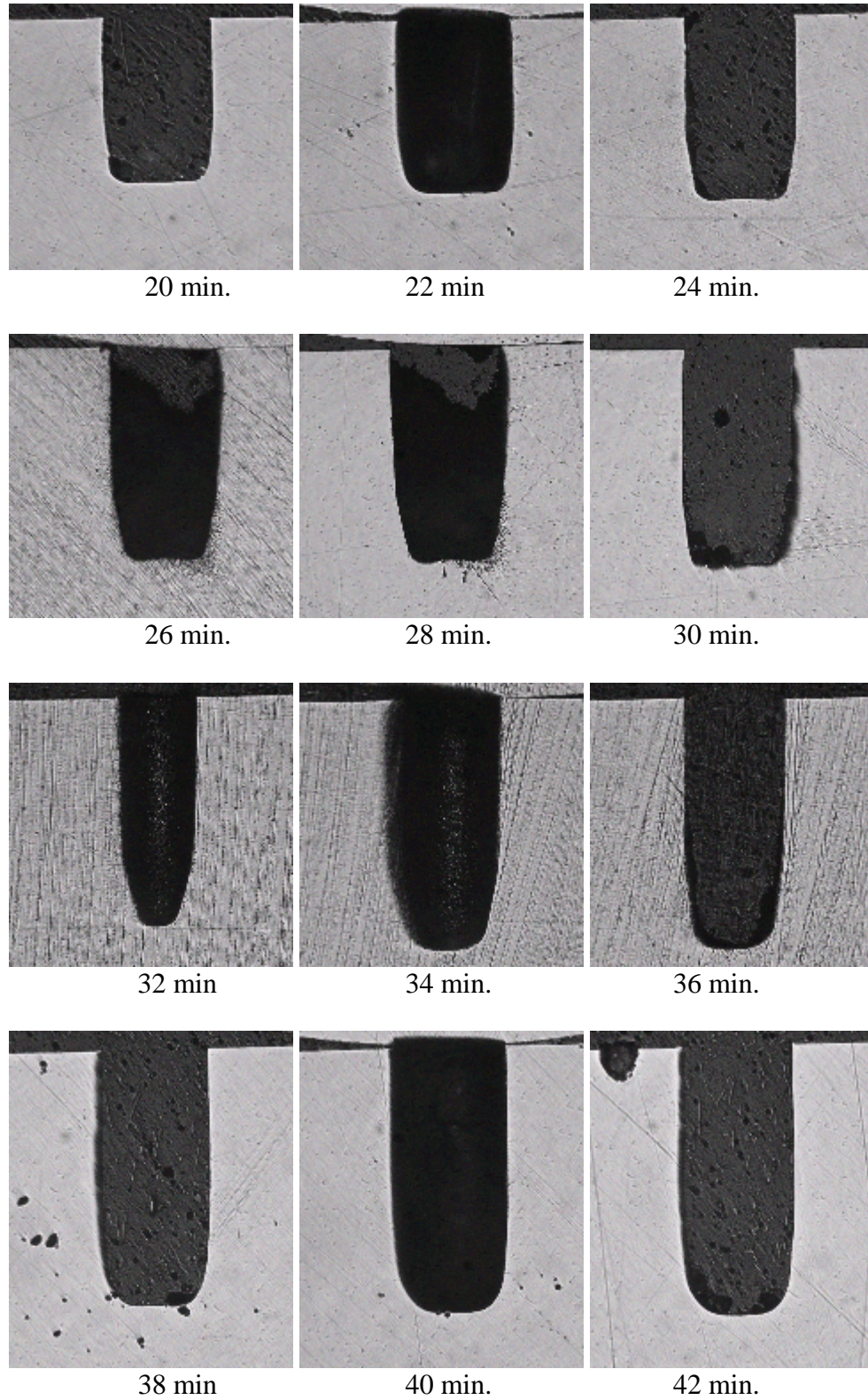


Figure A.1 (cont) Micro-holes cross-sectional shape with different machining time from 1min. to 80 min. and constant machining parameters as given in Table 4.4.

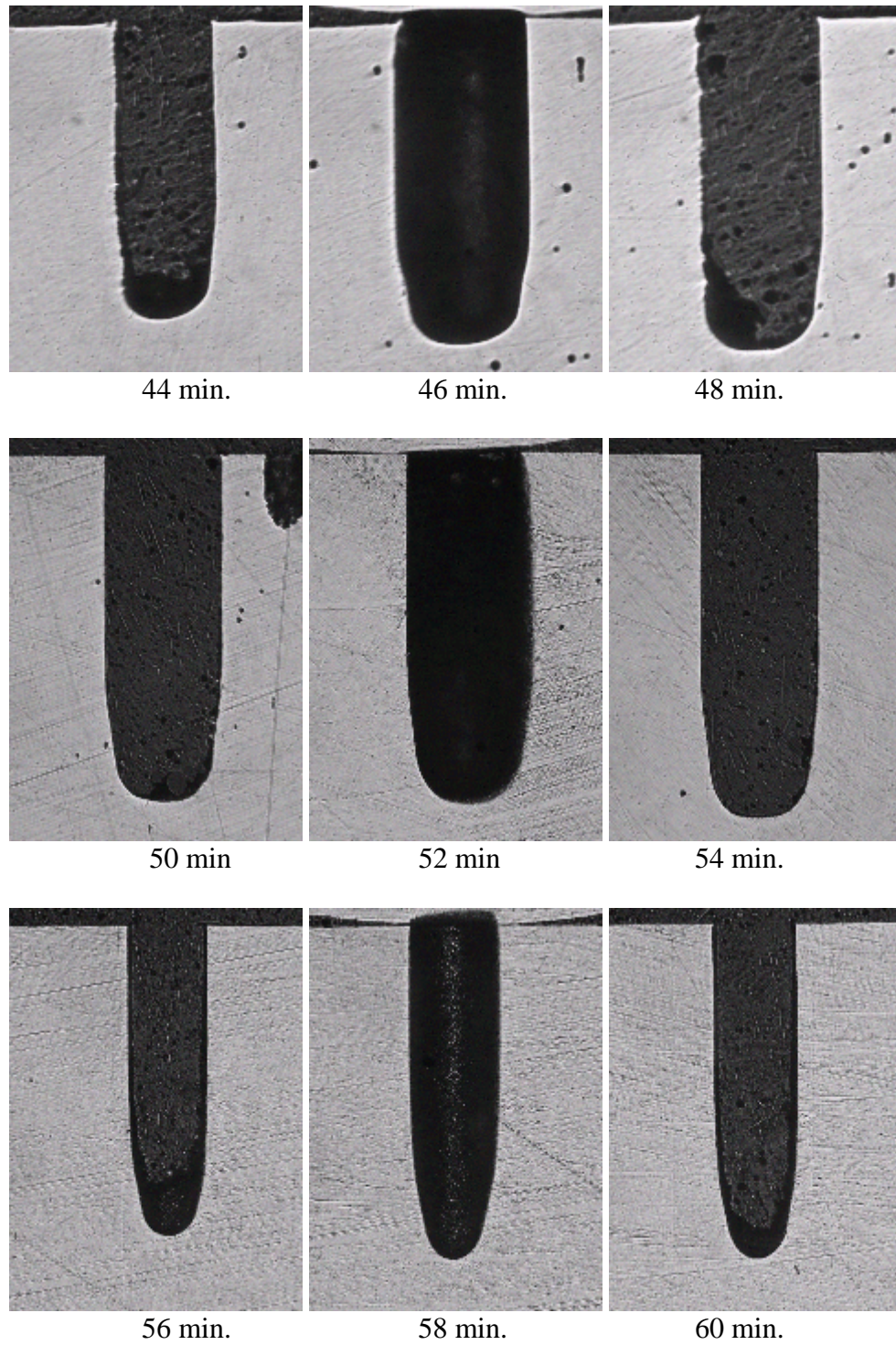


Figure A.1 (cont) Micro-holes cross-sectional shape with different machining time from 1min. to 80 min. and constant machining parameters as given in Table 4.4.

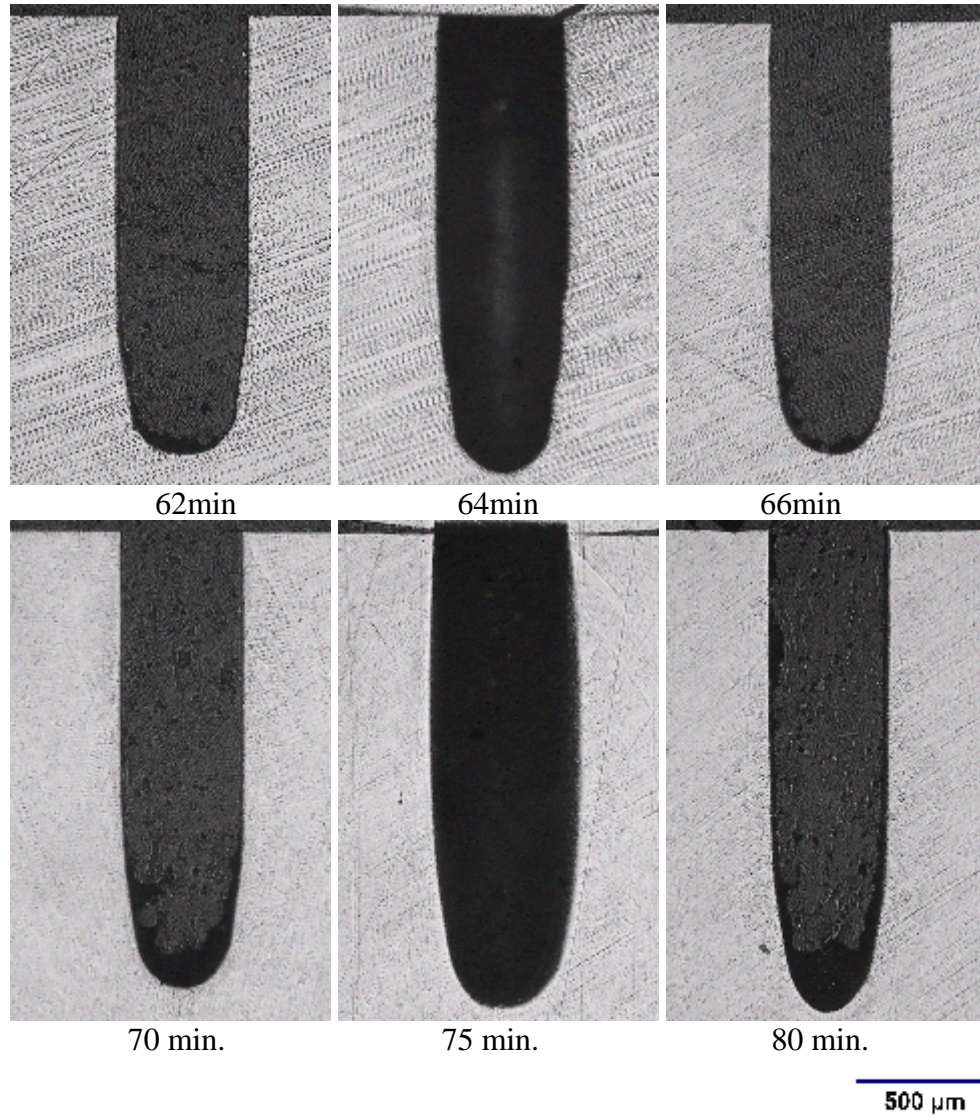


Figure A.1 (cont) Micro-holes cross-sectional shape with different machining time from 1min. to 80 min. and constant machining parameters as given in Table 4.4.

APPENDIX B

HOLE SHAPES WITH VARYING TIME WIDTH

Diameter variations of micro-holes are illustrated in Figure B.1 and cross-sectional shape of machined holes are given in Figure B.2. Machining was repeated three times for the same width to verify the repeatability of experiments.

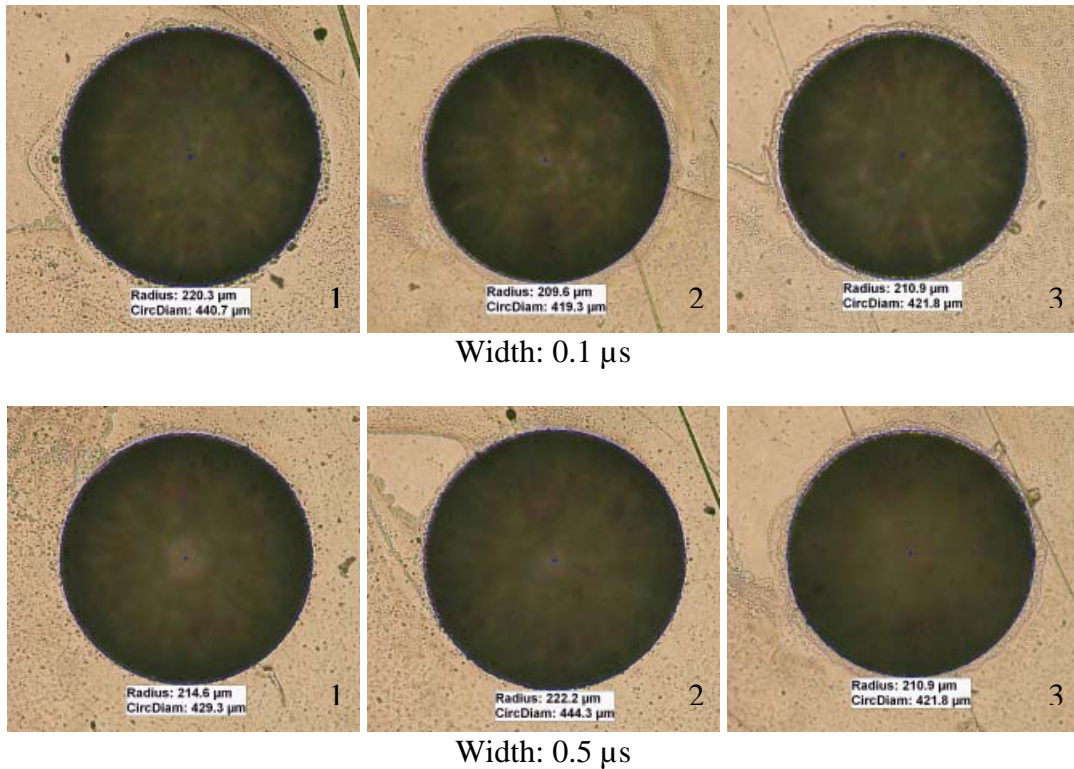
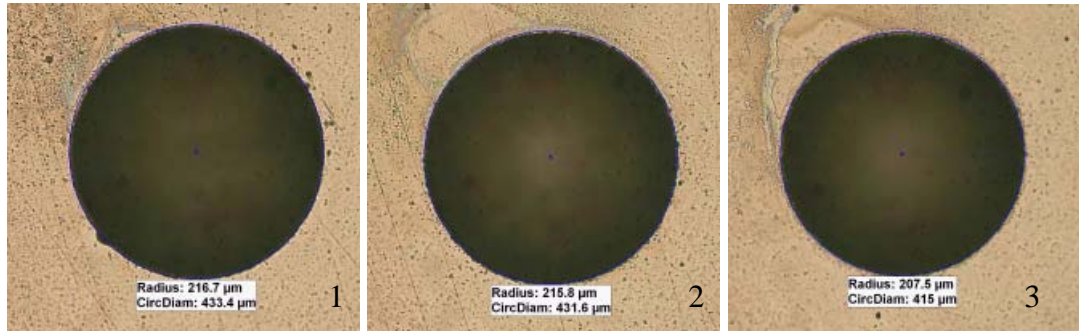
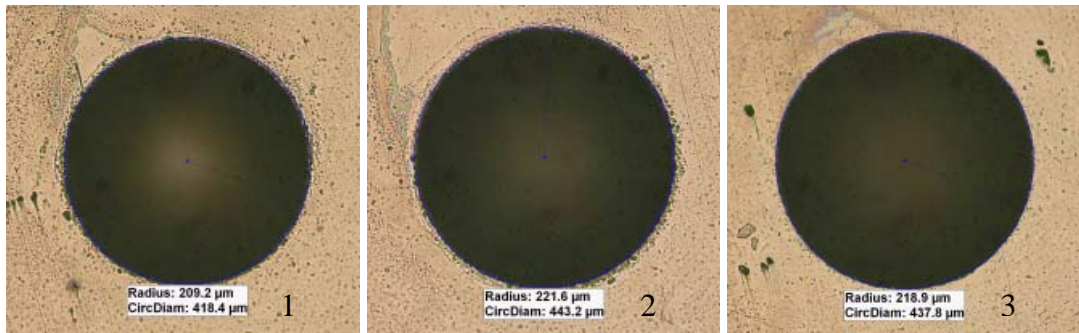


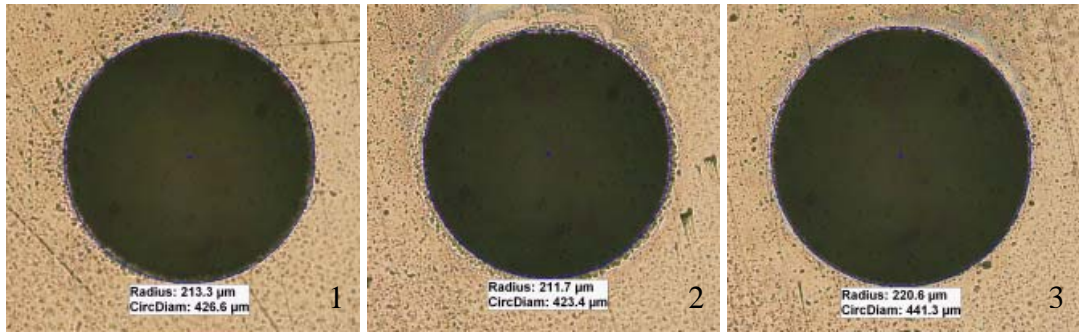
Figure B.1 Micro-hole photographs from top view by using variant width time



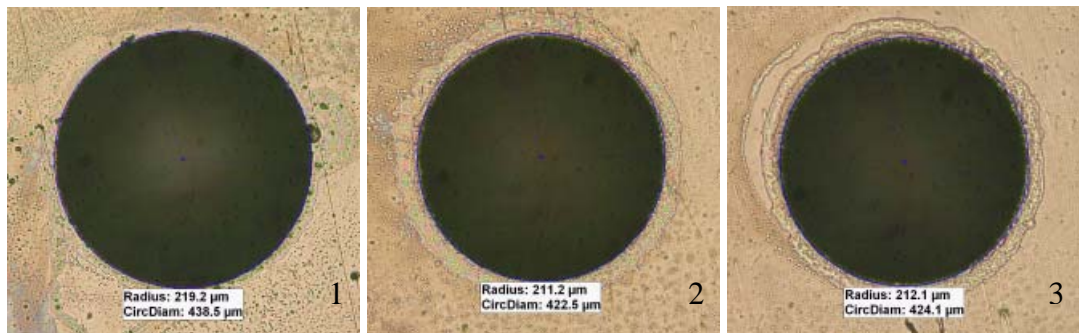
Width: 1 μ s



Width: 2 μ s



Width: 6 μ s



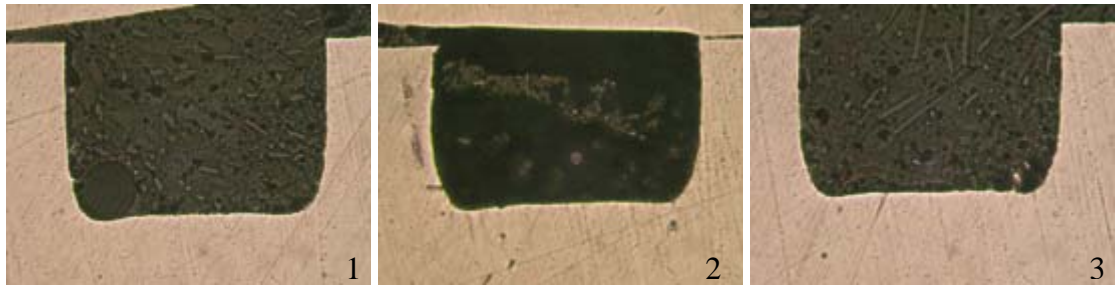
Width: 8 μ s



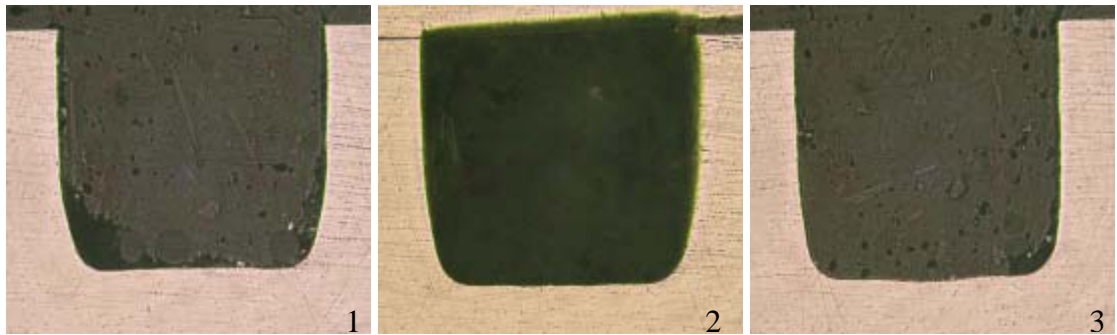
Figure B.1 (cont) Micro-hole photographs from top view by using variant width time



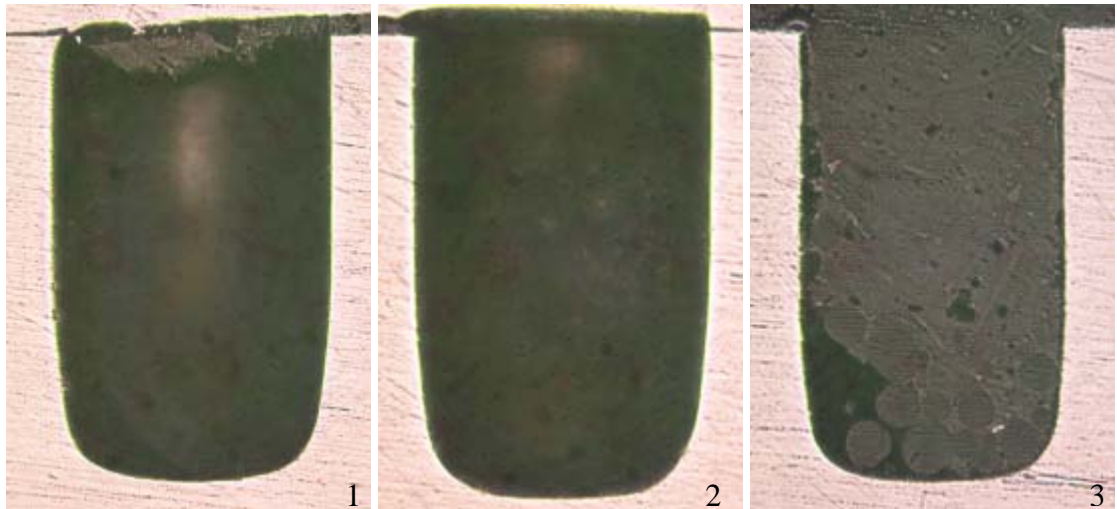
Width: 0.1 μ s



Width: 0.5 μ s



Width: 1 μ s



Width: 6 μ s

Figure B.2 Cross-sectional photographs of micro-holes by using variant width time.

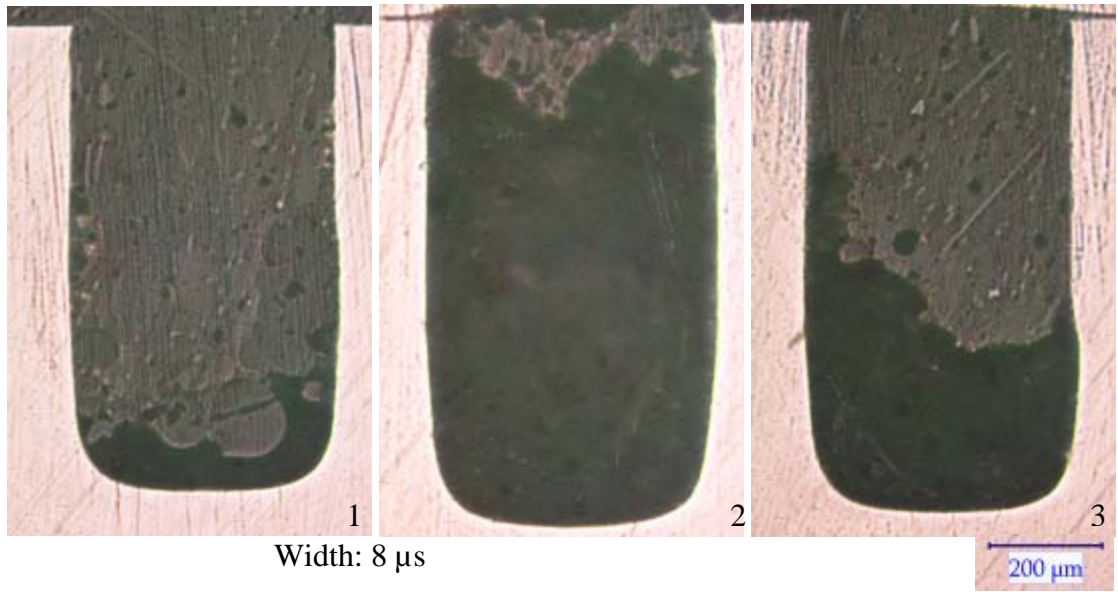


Figure B.2 (cont) Cross-sectional photographs of micro-holes by using variant width time.

APPENDIX C

HOLES SHAPES WITH VARYING FREQUENCY

Micro-holes were machined to see the effect of frequency is illustrated in Figure C.1. Each machining repeated three times to verify the reliability of results.

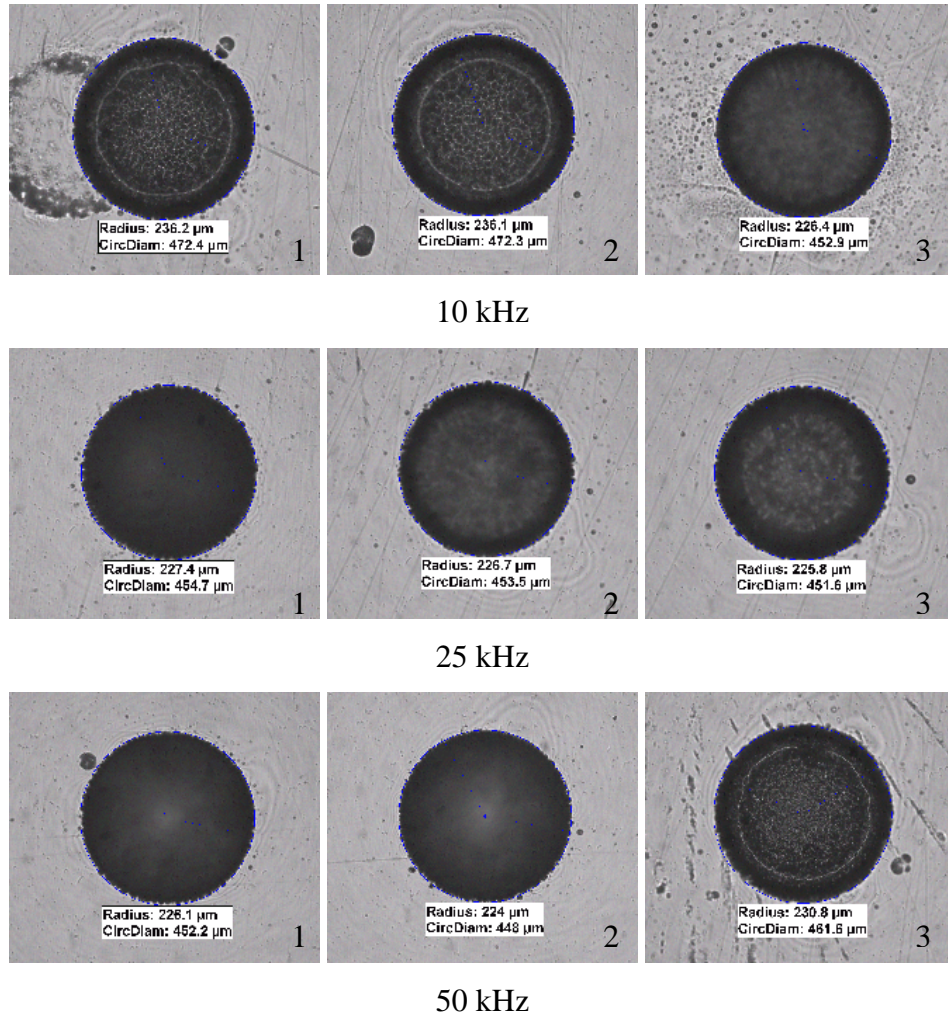


Figure C.1 Micro hole photographs machined with different frequency values of 10 kHz, 25 kHz, 50 kHz, 100 kHz, and 150 kHz r for each row, respectively.

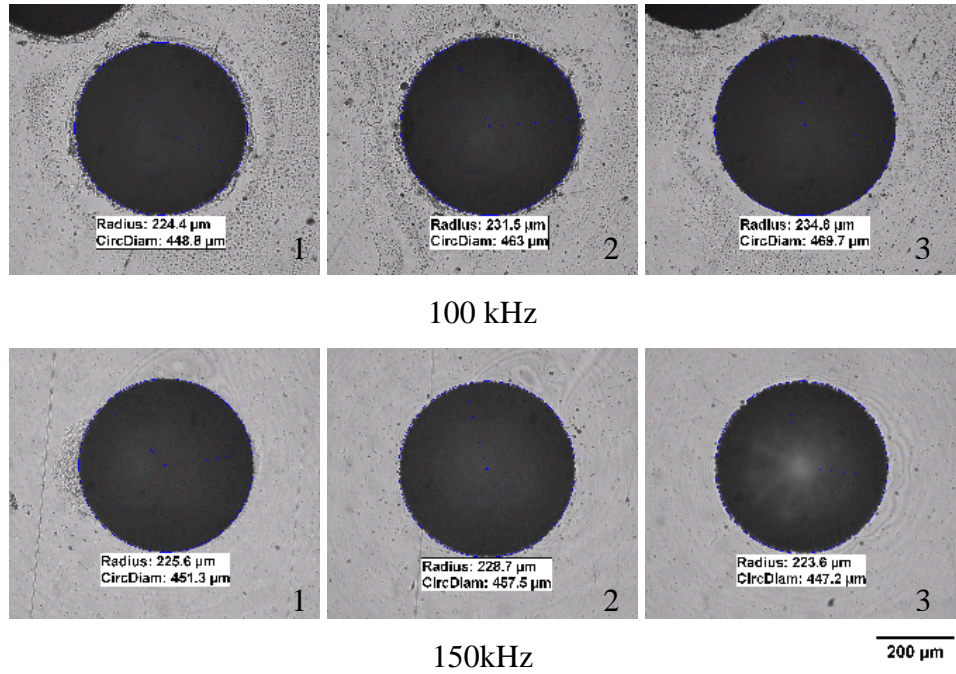


Figure C.1 (cont) Micro hole photographs machined with different frequency values of 10 kHz, 25 kHz, 50 kHz, 100 kHz, and 150 kHz r for each row, respectively.

APPENDIX D

HOLE AND PULSE SHAPES WITH VARYING OPEN VOLTAGE

Micro-holes machined by using variant open voltage are illustrated from top view and magnified edge view in Figure D.1.

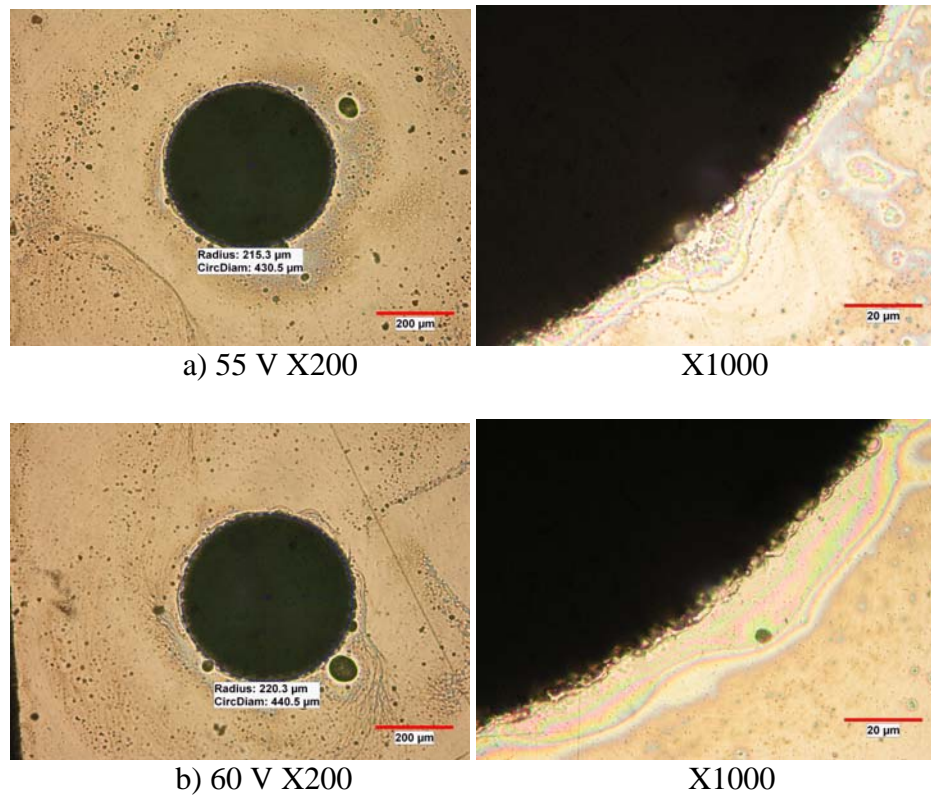
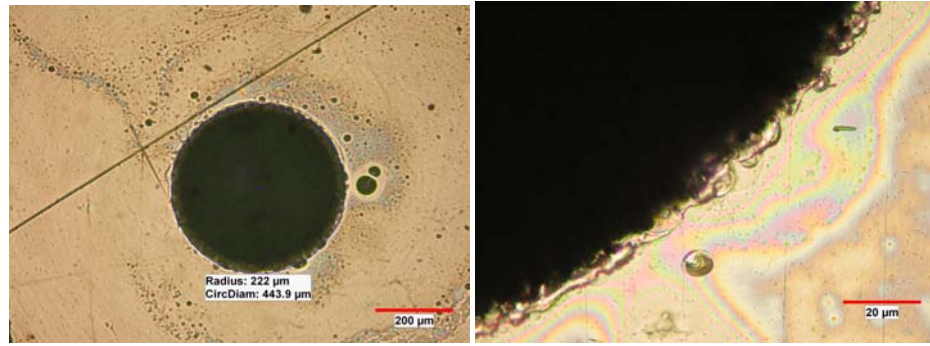
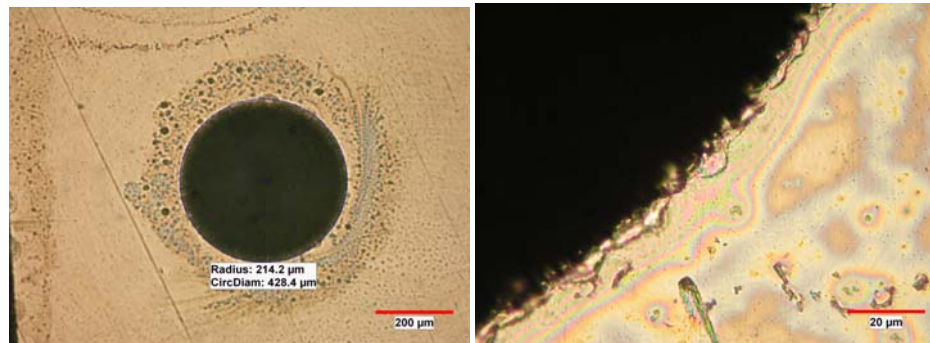


Figure D.1 Machined hole photos by setting gap voltage 50 V and gradually increasing open voltage value as given beneath the related pictures. 1000x magnified pictures of each holes are also illustrated to discuss the quality of the hole wall surface with varying open voltage value.



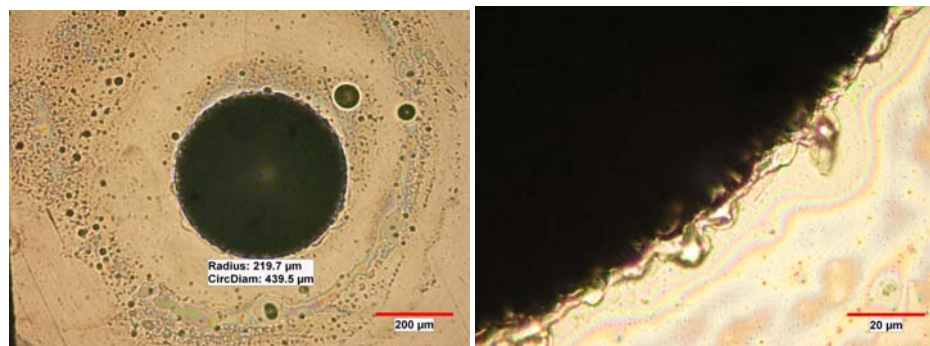
c) 70 V X200

X1000



d) 80 V X200

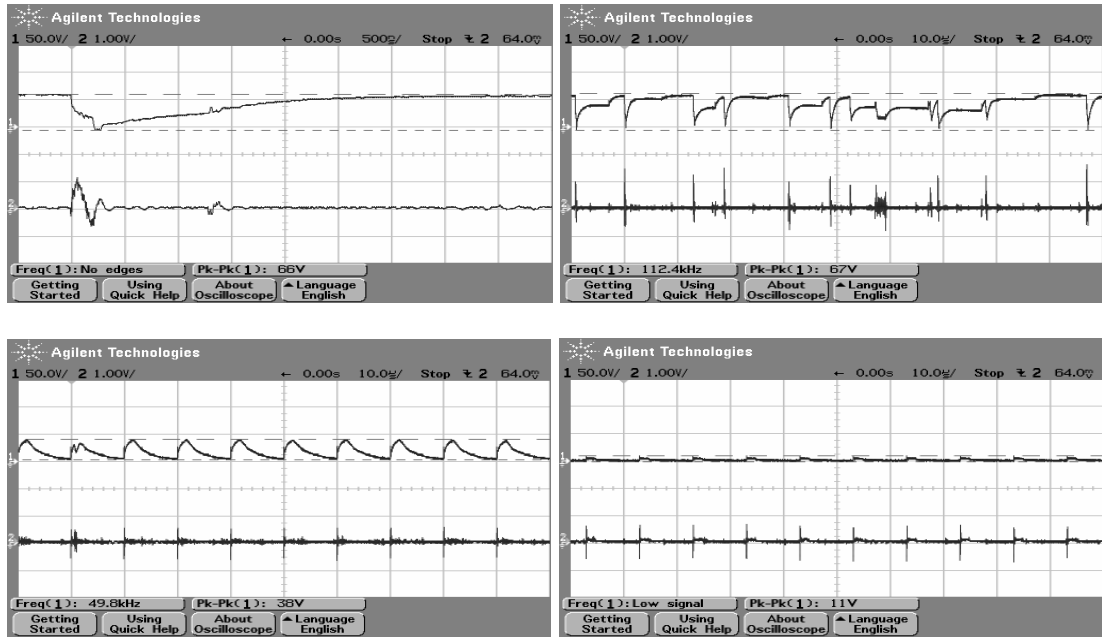
X1000



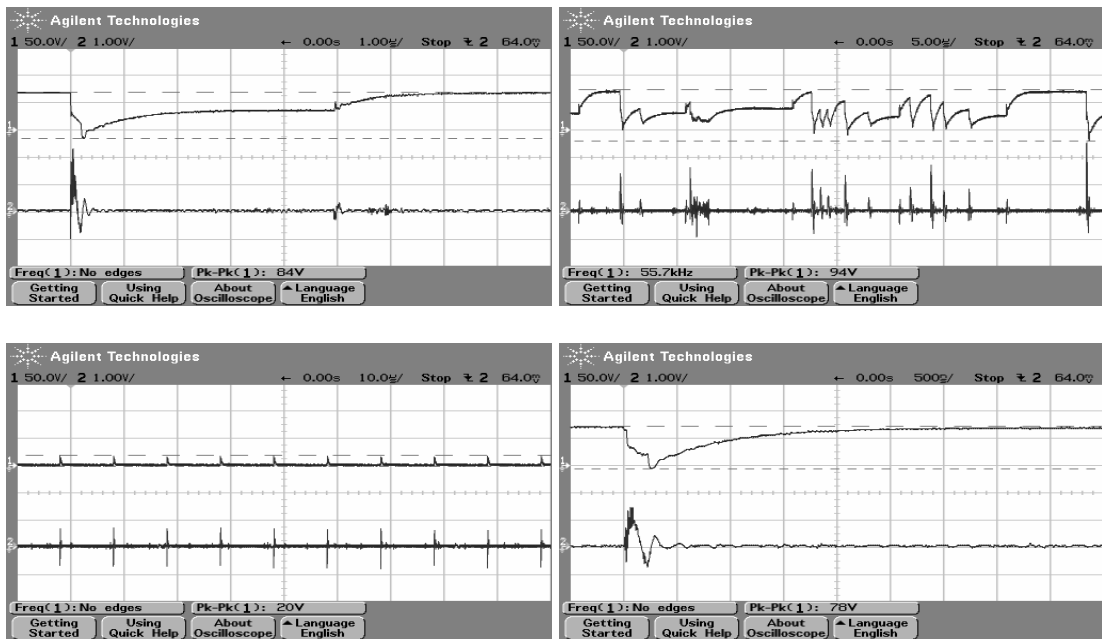
e) 90 V X200

X1000

Figure D.1 (cont) Machined hole photos by setting gap voltage 50 V and gradually increasing open voltage value as given beneath the related pictures. 1000x magnified pictures of each holes are also illustrated to discuss the quality of the hole wall surface with varying open voltage value.

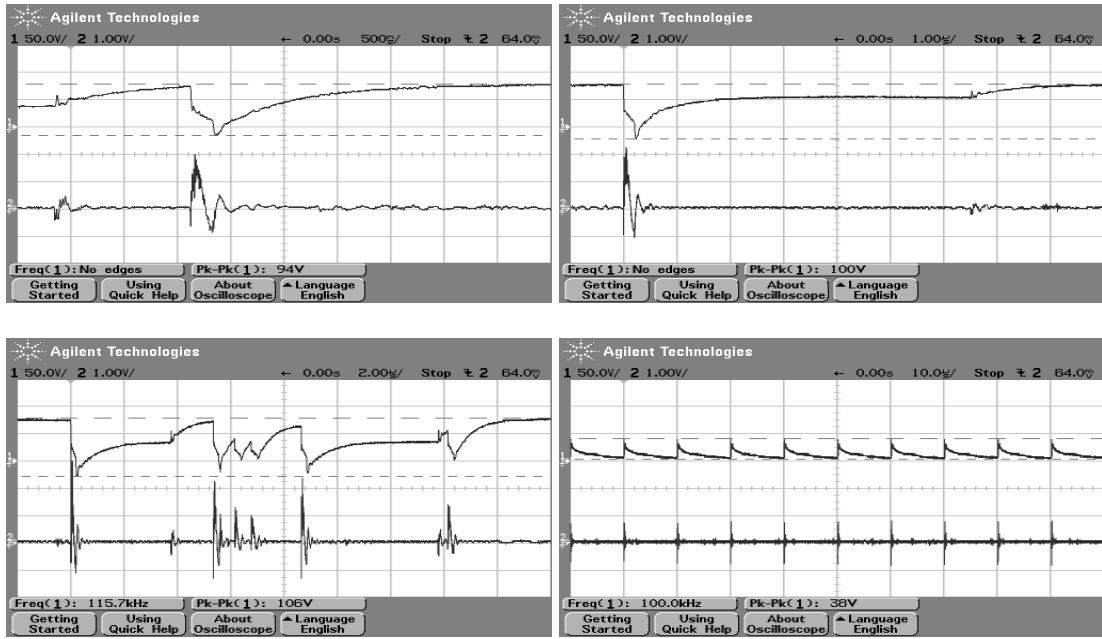


Open voltage: 60 V

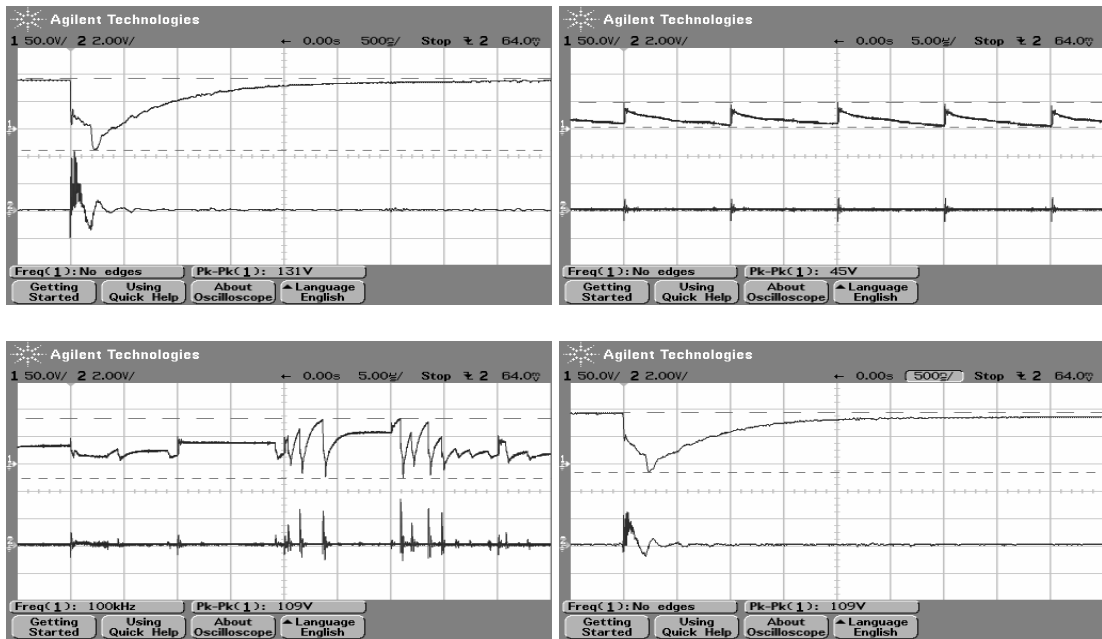


Open voltage: 70V

Figure D.2 Captured Pulse form for different open voltage values

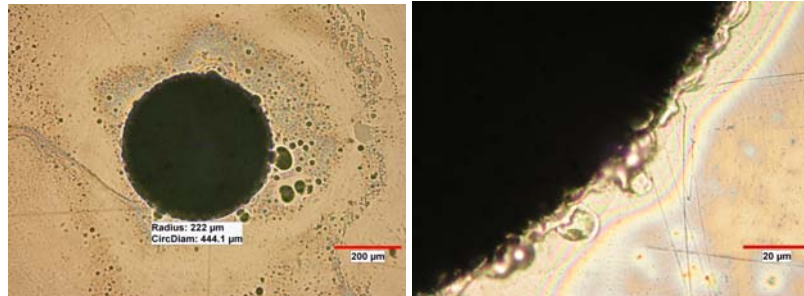


Open voltage: 80V

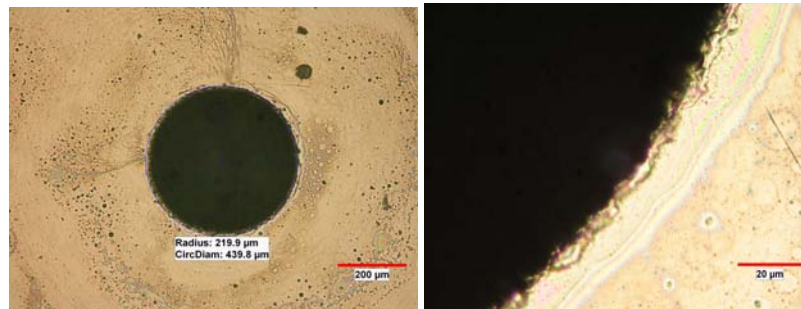


Open voltage: 90V

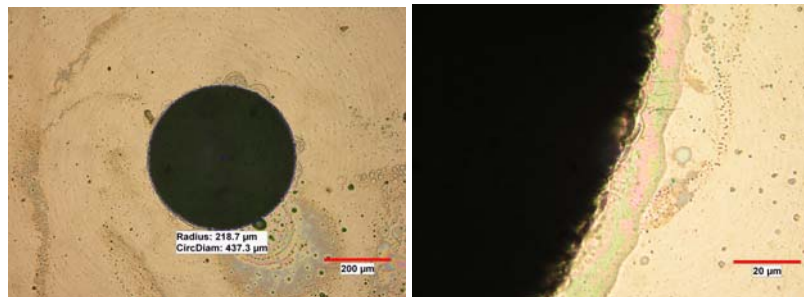
Figure D.2 (cont) Captured Pulse form for different open voltage values



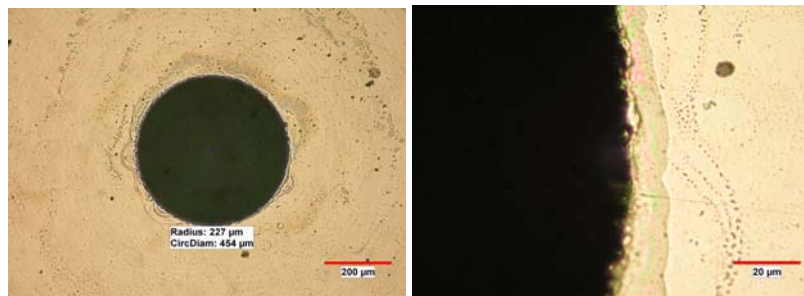
Gap voltage: 60V



Gap voltage: 80V

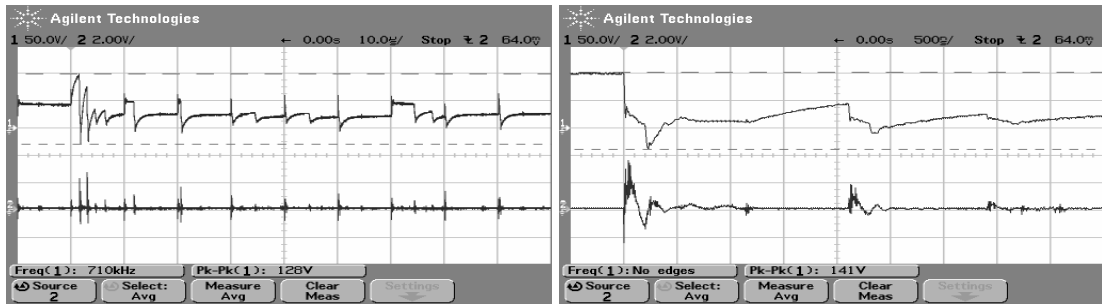
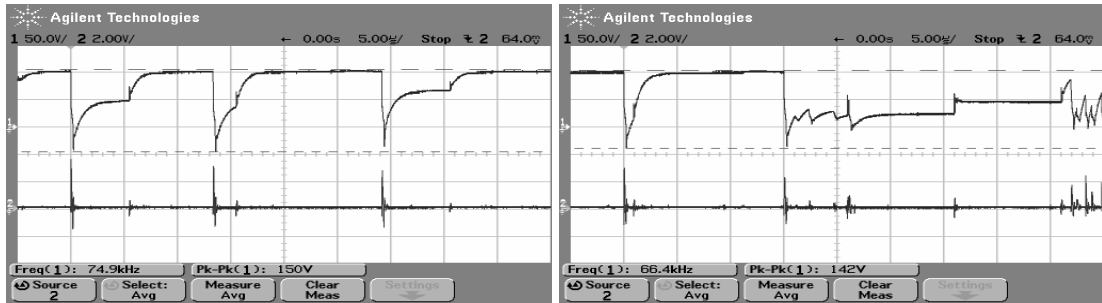


Gap voltage: 90 V

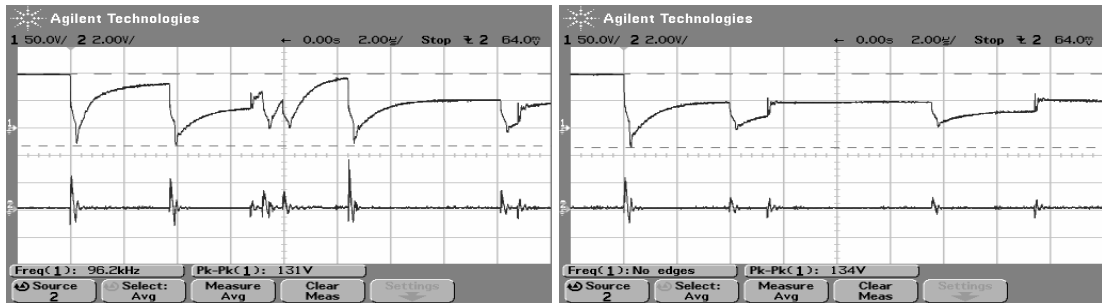
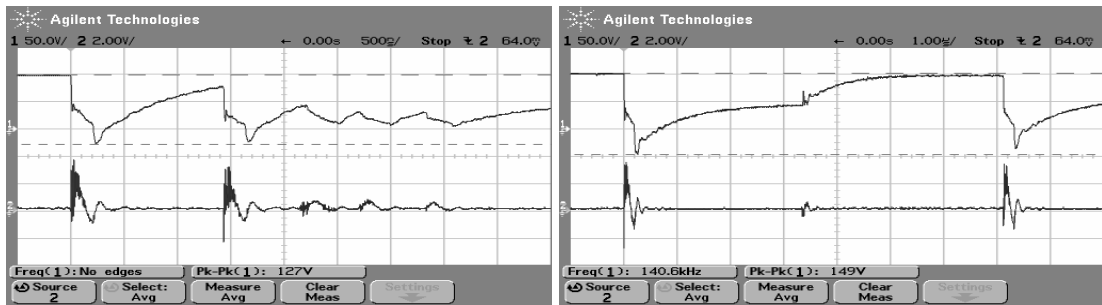


Gap voltage: 95 V

Figure D.3 Machined hole pictures from top view and 1000x magnified edge view with different gap voltage value and constant open voltage at 100V.

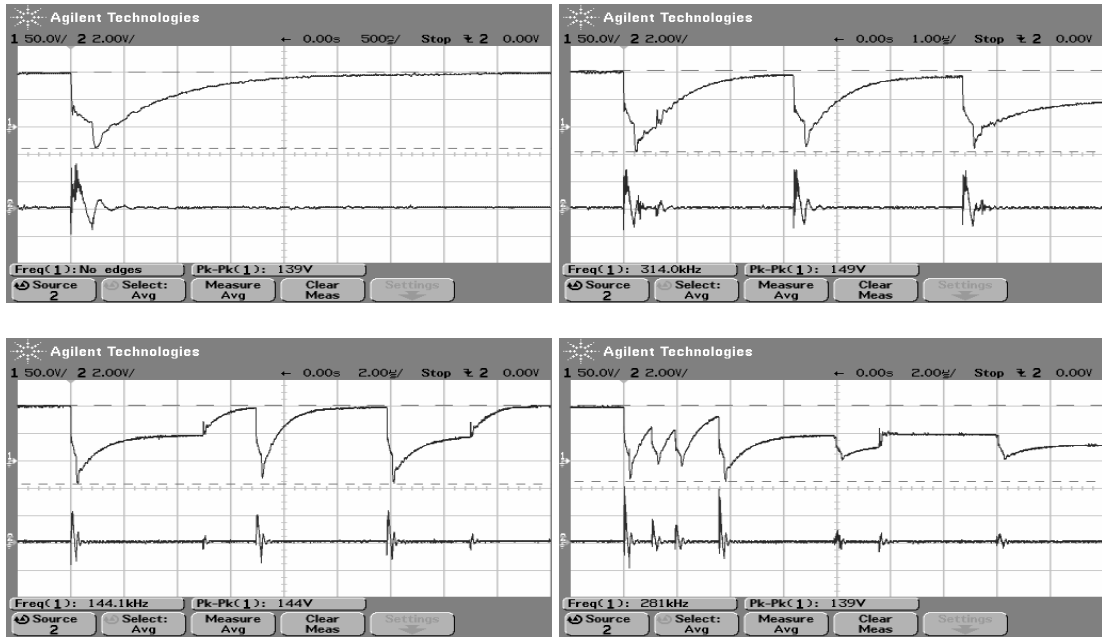


Gap voltage: 60 V

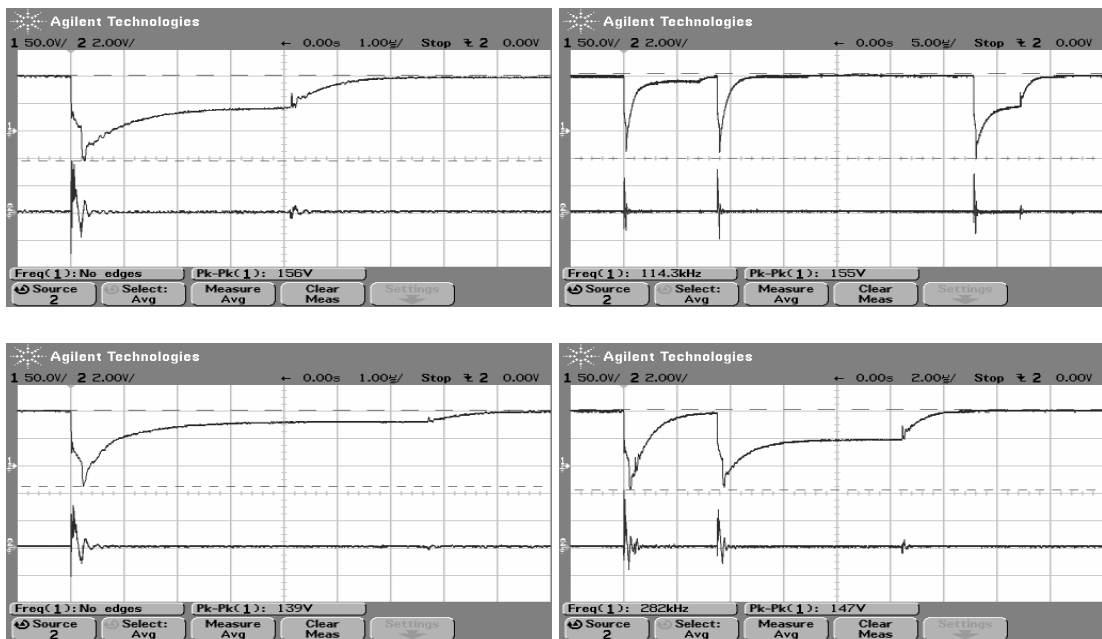


Gap voltage: 80 V

Figure D.4 Voltage and current pulse forms for different gap voltage while open voltage kept constant at 100V.



Gap voltage: 90V



Gap voltage: 95V

Figure D.4 (cont) Voltage and current pulse forms for different gap voltage while open voltage kept constant at 100V.

Table D.1 Machining results for varying gap voltage

Gap Voltage (V)	Target hole depth (mm)	Electrode removal (mm)
95	1,74	0.41
	1,79	0,44
	1,7	0,364
90	1,3047	0,129 *
	1,62	0,392
	1,5454	0,368
80	1,2029	0,371
	1,53	0,426
	1,67	0,477
60	1,659 (<i>44 min</i>)	0,539
	1,92 (<i>41min</i>)	0,638
	1,51	0,475 **

* The worn tip of electrode was not cut back sufficiently after the previous machining, some black spot (carbon) was observed over the tip of the electrode, so which results in the smaller target depth because carbon particle over the electrode decrease chance of discharge.

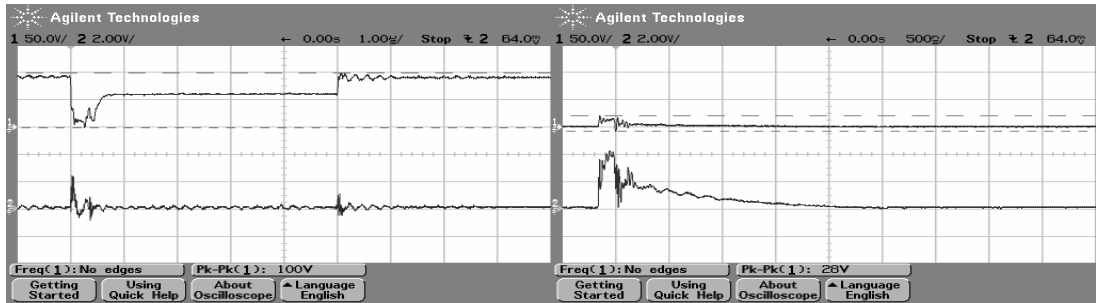
** Gap voltage is set to 75 V by accident up to 0.39mm target depth during machining

APPENDIX E

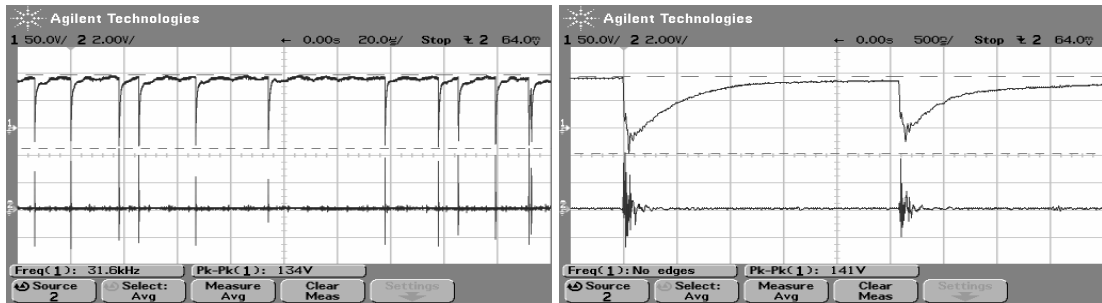
MACHINING RESULTS FOR MICRO-HOLE DRILLING WITH Ø100 µm TOOL ELECTRODE

Table E.1 Machining results by using 100 µm diameter of electrode

Mach. time (min)	Target hole depth (mm)	Hole diameter (µm)	Electrode removal (mm)	Energy parameter
15	1,5	182,00	1,3	350
15,3	1,33	179,50	0,927	350
15	0,73	180,00	0,486	350
60	0,16	160,00	0,053	114
60	0,165	162,00	0,047	105
60	2,13	159,30	0,422	14
60	1,6	162,40	0,298	14
60	2,16	174,60	0,416	14
60	2,13	174,20	0,448	14
40	1.925	168,00	0,38	14
40	1,86	156,80	0,363	14
44	1,86	157,00	0,358	14
30	1.796	167,50	0,332	14
20	1,21	163,00	0,198	14
20	1,16	156,90	0,17	14
10	0,615	145,50	0,084	14
10	0,64	154,40	0,095	14
13	0,793	140,50	0,109	14



Energy: 350



Energy: 14

Figure E.1 Pulse shapes for 100 μm diameter of electrode by using energy parameter 350 and 14.

Table E.2 Machining results with the corresponding machining parameters

Hole number	Electrode diameter (μm)	Machining time (min.)	Target depth (mm)	Electrode wear (mm)	Machining Parameters
1	400	15	3	1.299	Width:5 Freq:100 Open voltage:90 Gap:85 Energy:350 Gain: 10
2	192	8	2.5	1.35	Width:5 Freq:100 Open voltage:90 Gap:85 Energy:350 Gain: 10
4	400	14	3	1.28	Width:4 Freq:120 Open voltage:90 Gap:80 Energy:250 Gain:20
5	400	20	3	1.28	Width:4 Freq:120 Open voltage:90 Gap:80 Energy:250 Gain:20
6	400	33	3	1.266	Width:5 Freq:100 Open voltage:90 Gap:85 Energy:206 Gain:10
7	400	60	2	0.479	Width:5 Freq:100 Open voltage:90 Gap:85 Energy:105 Gain:10
8	400	52	2	0.459	Width:5 Freq:100 Open voltage:90 Gap:85 Energy:105 Gain:10
9	48	55	1.19	0.626	Width:2 Freq:120 Open voltage:80 Gap:75 Energy:14 Gain:5
10	35	50	1	0.408	Width:2 Freq:120 Open voltage:80 Gap:75 Energy:14 Gain:5
11	38	50	1.14	0.72	Width:2 Freq:120 Open voltage:80 Gap:75 Energy:14 Gain:5
12	32	100	1.06	0.4	Width:2 Freq:120 Open voltage:80 Gap:75 Energy:13 Gain:5
13	47	100	1.57	0.899	Width:2 Freq:120 Open voltage:80 Gap:75 Energy:14 Gain:5
14	43	40	0.86	0.397	Width:2 Freq:120 Open voltage:80 Gap:75 Energy:14 Gain:5
15	40	60	1.06	0.562	Width:2 Freq:120 Open voltage:80 Gap:75 Energy:14 Gain:5
16	22	50	0.84	0.125	Width:2 Freq:120 Open voltage:80 Gap:75 Energy:14 Gain:5
17	15	30	0.65	0.112	Width:2 Freq:120 Open voltage:80 Gap:75 Energy:14 Gain:5
Width μs, Frequency kHz, Open voltage V, Gap V, unit is not defined for the other parameters					

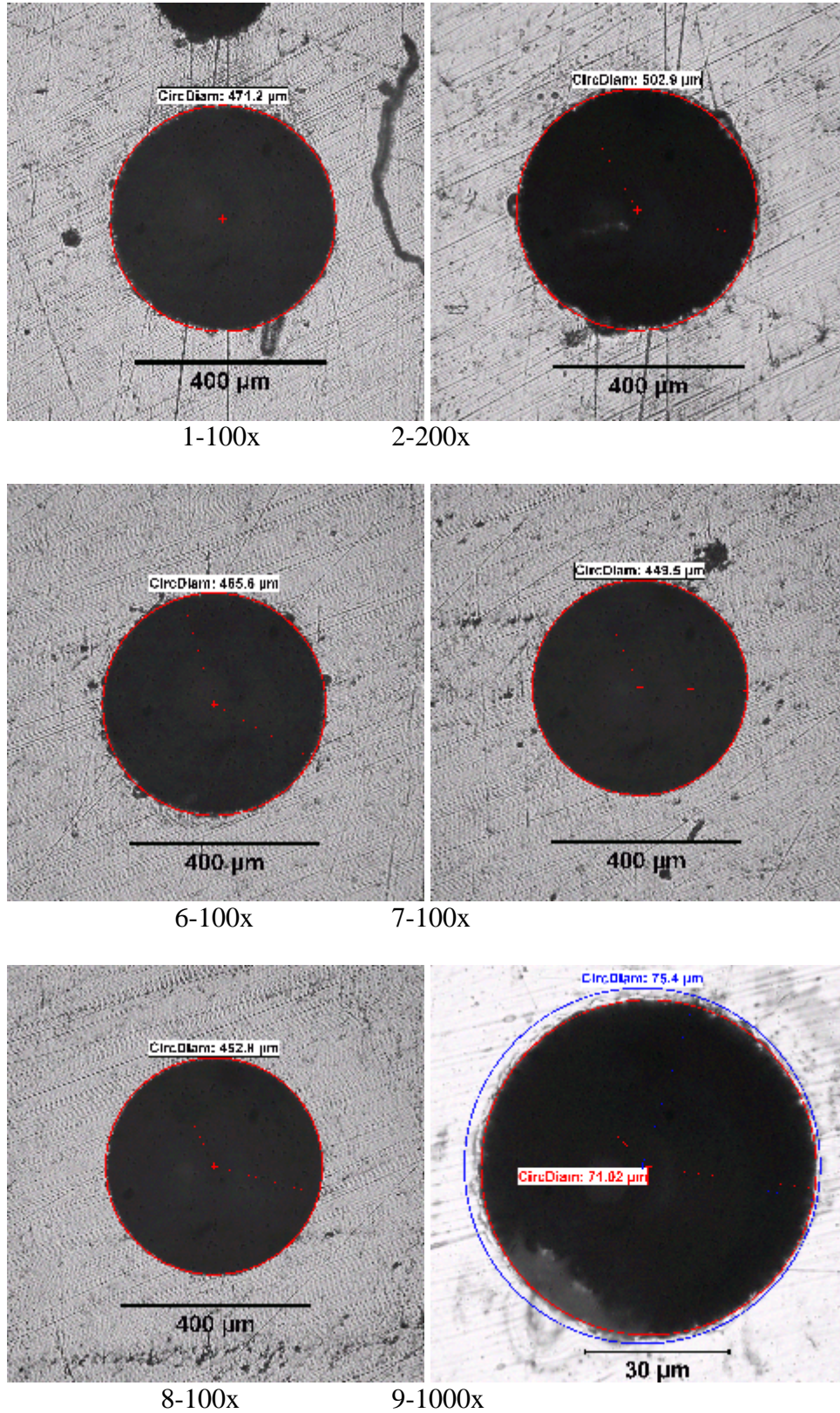


Figure E.2 Micro-hole pictures for determining circularity with the magnified view represented under each picture.

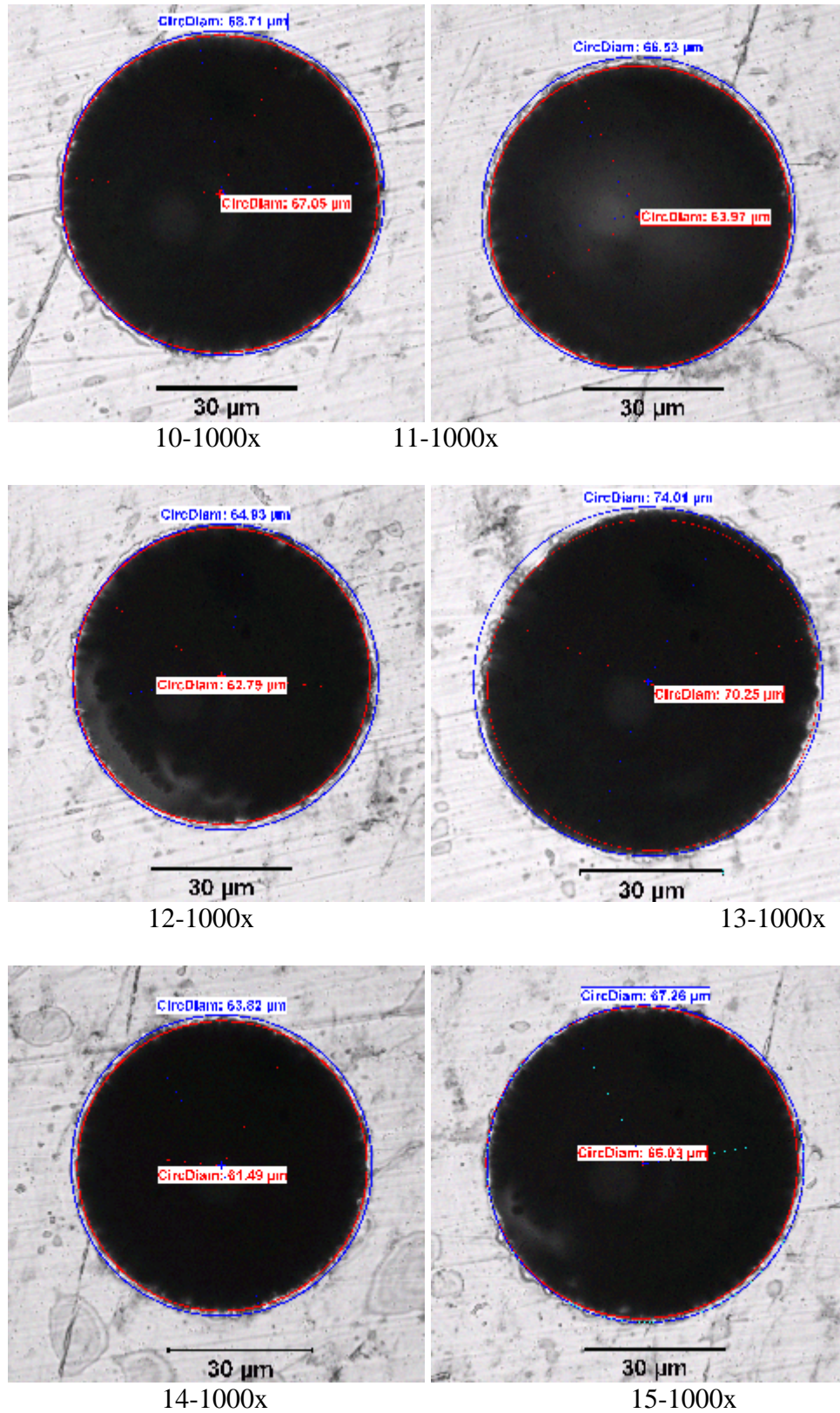


Figure E.2 (cont) Micro-hole pictures for determining circularity with the magnified view represented under each picture.

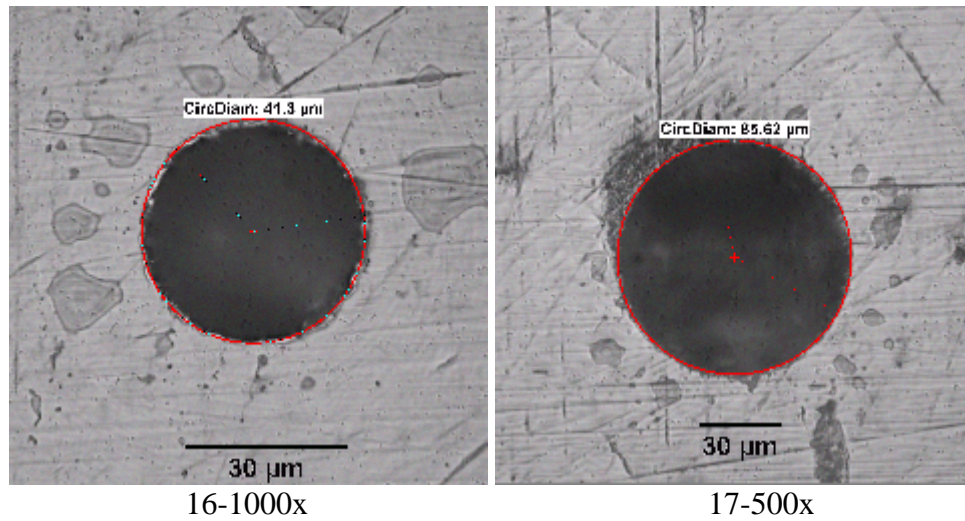


Figure E.2 (cont) Micro-hole pictures for determining circularity with the magnified view represented under each picture.

Circularity degree of the machined micro-hole are calculated by considering the most outer and the most inner diameter difference and. This gives the value of away from full circle or tendency to the elliptical shape. Table E.3 shows the circularity degree of the micro-holes with the corresponding tool electrode.

Table E.3 Circularity degree of Micro-holes

	Hole-9	Hole-10	Hole-11	Hole-12	Hole-13	Hole-14	Hole-15
Tool diameter	48	35	38	32	47	43	40
Inner diameter	71,02	67,05	63,97	62,79	70,25	61,49	66,03
Outer diameter	75,4	68,71	66,53	64,93	74,01	63,82	67,26
Circularity	2,19	0,83	1,28	1,07	1,88	1,17	0,62

*Dimensions in μm